8-2016

Simulation of flow and water quality from tile drains at the watershed and field scale

Colleen Moloney
Purdue University

Graduate School Form
30 Updated 12/26/2015

PURDUE UNIVERSITY
GRADUATE SCHOOL
Thesis/Dissertation Acceptance

This is to certify that the thesis/dissertation prepared

By Colleen Moloney

Entitled
Simulation of Flow and Water Quality from Tile Drains at the Watershed and Field Scale

For the degree of Master of Science in Agricultural and Biological Engineering

Is approved by the final examining committee:

Jane R. Frankenberger
Chair

Eileen J. Kladivko

Kevin King

Indrajeet Chaubey

To the best of my knowledge and as understood by the student in the Thesis/Dissertation Agreement, Publication Delay, and Certification Disclaimer (Graduate School Form 32), this thesis/dissertation adheres to the provisions of Purdue University's "Policy of Integrity in Research" and the use of copyright material.

Approved by Major Professor(s): Jane R. Frankenberger

Approved by: Bernard Engel 7/25/2016

Head of the Departmental Graduate Program Date

SIMULATION OF FLOW AND WATER QUALITY FROM TILE DRAINS AT THE WATERSHED AND FIELD SCALE

A Thesis

Submitted to the Faculty

of

Purdue University

by

Colleen A Moloney

In Partial Fulfillment of the

Requirements for the Degree

of

Master of Science in Agricultural and Biological Engineering

August 2016

Purdue University

West Lafayette, Indiana

To:

My parents: Carol and Tom

My siblings: Caitlin, Brian, and Matthew

and

My boyfriend: Ed

ACKNOWLEDGEMENTS

I would like to express my thanks to all the teachers, mentors, fellow students, friends and family who have helped me in many forms throughout my academic career.

First, I would like to thank my adviser Dr. Jane Frankenberger for not only helping develop my research project here, but my research technique and career. Without your support and feedback, I would not have been able to become half the researcher I am today.

I would also like to thank my committee members Drs. Indrajeet Chaubey, Kevin King, and Eileen Kladivko for the feedback on various aspects of my project and algorithm development as well as access to some amazing data sets.

To all the students and professors in both the Ecological Sciences and Engineering Interdisciplinary Graduate Program as well as the Agricultural and Biological Engineering Department. Thank you for the input on my research (even when by accident), coding advice, the coffee breaks, and especially for Margarita Club. Graduate school would not have been half as fun or rewarding without you.

TABLE OF CONTENTS

Page

Page

Page

LIST OF TABLES

Table Page

LIST OF FIGURES

Appendix Figure Page

ABSTRACT

Moloney, Colleen A. M.S.A.B.E., Purdue University, August 2016. Simulation of Flow and Water Quality from Tile Drains at the Watershed and Field Scale. Major Professor: Jane Frankenberger.

Simulation models such as the Soil and Water Assessment Tool (SWAT) have become widely used in determining the water quality impacts of various management practices. Ensuring that the algorithms accurately represent the processes simulated has become an important goal. Tile drainage is a standard practice in the Midwest, US in order to reduce risk of yield loss due to excess water. Multiple tile drainage and water table algorithms have been available in the SWAT model between the initial SWAT release and revision 638 used in this study. Testing of those algorithms is often limited. Furthermore, algorithms in the current version have not been tested using small scale measured tile discharge.

To better represent the hydrologic processes related to subsurface drainage, four modifications were made to the SWAT model subsurface hydrology routines in order to increase the physical basis of these algorithms. First, percolation through the soil profile was altered to be based on Darcy's Law and the Buckingham-Darcy Law. Second, the restrictive layer of the soil profile was redefined to be the bottom of the soil profile and an additional variable was added to control the seepage through the restrictive layer. Third, the water table height algorithm, which was based on an algorithm applicable at only one site, was redefined to be within the lowest unsaturated layer. Lastly, the lag through the tile drains, which caused an unrealistic delay under default conditions was removed and flow is delayed by only the drainage coefficient.

These changes were evaluated at the experimental tile drained field at the Southeast Purdue Agricultural Center (SEPAC). The model was developed with a single hydrologic response unit (HRU) and calibrated for both tile flow and nitrate. The modifications improved the performance of SWAT for water table and tile flow predictions, although the nitrate was more severely under-predicted.

The modifications were tested on a small watershed located in Central Ohio monitored by the USDA-ARS. Each tile output in this watershed was monitored allowing for each tile to be individually modeled and analyzed with SWAT. This watershed was also calibrated for tile flow and nitrate. Here again, the modifications showed an improvement for tile flow but a reduction in performance for nitrate. Phosphorus was also looked at but not calibrated for, and an extreme under-prediction issue was observed.

These modifications improved the physical basis or simplified the process representation in the SWAT model, and showed improvement to the tile flow model predictions. The model should be further tested and further developments, specifically for nitrogen and phosphorus, should continue.

CHAPTER 1. INTRODUCTION

1.1 Subsurface Drainage

In the Midwestern United States, tile drainage has become a standard agricultural practice in order to more quickly move water within poorly drained soils and therefore increase productivity, trafficability, and reduce yield risk. Tile drainage, which removes water from the subsurface using perforated plastic tubing (historically clay tile) (USDA-NRCS, 2001), is installed in order to move water away from crops to prevent damage. The water flowing into the drain tube is directed to a drainage ditch at the edge of the field.

The facilitation of quicker water movement out of the field alters the hydrology not only of the field but of the entire watershed the field is located within. In fact, the majority of flow in many watersheds is from tile drains. For example, Green et al. (2006) found tiles were responsible for 70% of the discharge from the Iowa River’s south fork. This alteration in hydrology has caused wetland and riparian habitat loss, leading to additional changes in watershed hydrology and nutrient cycles in the watersheds where these wetlands were originally present (Blann et al., 2009).

Artificial drainage from agricultural fields is also considered one of the major sources for downstream environmental problems (Skaggs et al., 1994). The decreased residence time of water within the soil profile and the direct and unblocked route through the tile drain to surface water causes this increase in nitrogen and phosphorus losses (Lennartz et al., 2011). These tile drains promote significant increases in nitrate losses within the field (Randall & Goss, 2008) and subsurface phosphorus losses (King et al., 2015).

1.2 Prediction of Subsurface Drain Flow

Analytical methods to predict tile flow have been developed since the early 1900s. These were primarily developed in order to determine the size and spacing of the tile drains needed to be installed in a specific field. Tile flow is often estimated using two sets of equations. The Hooghoudt equation (1940) (Equation 1.1) is a standard equation for regularly spaced tile drainage and is used in many different hydrologic models (Cooke et al., 2001).

$$q = \frac{8K_{eff}d_{te}d_{mt} + 4K_{eff}d_{mt}^2}{s_{drain}^2} \quad (1.1)$$

where q is the drainage discharge, K_{eff} is the effective saturated hydraulic conductivity for the soil profile within the water table, d_{te} is the depth from the tile drain to the equivalent restrictive layer, d_{mt} is the depth from the midpoint water table height to the tile drain, and s_{drain} is the drain spacing. It assumes an equivalent restrictive layer above the actual restrictive layer, and considers the tiles as "ditches" that start at the drain height and end at the effective restrictive layer (Ritzema, 1994). Calculations for equivalent depth of the restrictive layer were developed by Moody (1966) (Equations 1.2 & 1.3):

$$d_{te} = \frac{s_{drain}}{\frac{8}{\pi}\left(\ln\left(\frac{s_{drain}}{r_e}\right) - 1.15\right)} \quad where \quad \frac{d_{ti}}{s_{drain}} > 0.3 \quad (1.2)$$

$$d_{te} = \frac{d_{ti}}{1 + \frac{d_{ti}}{s_{drain}}\left(\frac{8}{\pi}\ln\left(\frac{d_{ti}}{r_e}\right) - 3.4\right)} \quad where \quad \frac{d_{ti}}{s_{drain}} \leq 0.3 \quad (1.3)$$

where d_{ti} is the depth from the tile drain to the actual restrictive layer and r_e is the effective tile drain radius.

For conditions where water is ponded on the surface and the water table reaches the soil surface, the Kirkham tile drainage equation (Equation 1.4) (van Schilfgaarde et al., 1957) is often used instead.

$$q = \frac{4\pi K_{eff}\left(d_{ps} + d_{st} - r_e\right)}{g s_{drain}} \quad (1.4)$$

where d_{ps} is the depth from ponded water to the soil surface, d_{st} is the depth from the soil surface to the tile drain, g is the Kirkham g-factor (Equation 1.5).

$$g = 2\ln\left(\frac{\tan\left(\frac{\pi(2d_{ti} - r_e)}{4d_{si}}\right)}{\tan\left(\frac{\pi r_e}{4d_{si}}\right)} + \sum_{m=1}^{\infty}\left(\frac{\cosh\left(\frac{\pi m s_{drain}}{2d_{si}}\right) + \cos\left(\frac{\pi r_e}{2d_{si}}\right)}{\cosh\left(\frac{\pi m s_{drain}}{2d_{si}}\right) - \cos\left(\frac{\pi r_e}{2d_{si}}\right)} \times \frac{\cosh\left(\frac{\pi m s_{drain}}{2d_{si}}\right) - \cos\left(\frac{\pi(2d_{ti} - r_e)}{2d_{si}}\right)}{\cosh\left(\frac{\pi m s_{drain}}{2d_{si}}\right) + \cos\left(\frac{\pi(2d_{ti} - r_e)}{2d_{si}}\right)}\right)\right) \quad (1.5)$$

where d_{si} is the depth from the surface to the actual restrictive layer and m is the variable used for the summation.

1.3 Computer Simulation of Drainage

Computer modeling of areas with subsurface drainage can help determine the impact of various management practices on flow and water quality in order to make decisions that can reduce subsurface nitrogen (N) and phosphorus (P) losses within the watershed. Using computer models to simulate monthly and annual drainage outputs helps determine methods to reduce the base levels of nutrient losses from tile drains. Since research has shown tile drains cause significant influence on peak rates of nutrient and sediment losses (Fausey et al., 1995), accurate simulations require daily or more frequent outputs in order to find these peaks and determine potential strategies to reduce the frequency and magnitude peak losses.

The model DRAINMOD (Skaggs, 1978) is specifically designed to simulate tile drainage and subsurface hydrology for a single drained field. DRAINMOD has been evaluated using in-field measurements for multiple drainage systems and soil types (Skaggs, 1982). Using a test field in the lower Mississippi Valley, DRAINMOD was able to better predict hydrology in wet years with a higher water table than those with less than average rainfall (Fouss et al., 1987). In order to simulate nitrogen as well as hydrology in tile drains, DRAINOMD-N was developed (Brevé et al., 1997). Wang et al. (2006) used DRAINMOD to compare the effects of drain spacing on tile flow and corn and soybean yields at a research plot in southeastern Indiana. Ale et al. (2009) used DRAINMOD to predict the benefits of a potential control drainage structure installed at a research plot in central Indiana and determined the ideal dates to raise and lower the control structure as well as found there was no significant statistical increase in surface runoff or decrease in corn yield. In contrast, Singh et al. (2007) found an increase in crop production due to controlled drainage structures in Iowa when modeling with DRAINMOD. In addition to subsurface hydrology, DRAINMOD has been found to accurately predict nitrogen losses from subsurface drainage in eastern North Carolina (Youssef et al., 2006).

While DRAINMOD is the most widely used, other models can also predict tile drainage. Rutkowski (2012) added a tile flow component in the Variable Infiltration Capacity (VIC) model, by modifying the existing subsurface algorithms using the Arno base flow curve to allow subsurface drainage based on the Hooghoudt Equation (1940) to occur at the bottom layer of the soil profile. The Root Zone Water Quality Model (RZWQM) can also predict tile drainage using the Hooghoudt equation (Ahuja et al., 2000; Singh & Kanwar, 1995).

1.4 Tile Drainage Simulations in SWAT

The Soil and Water Assessment Tool (SWAT) (Arnold et al., 1998) is a watershed scale model designed to simulate a watershed with a variety of land uses by dividing the area into hydrologic response units (HRUs) with common soil type, slope class, land use, and subbasin. Subsurface drainage algorithms have existed in SWAT since the release of SWAT2000 using a simple method based on the time to drain soil to field capacity ($TDRAIN$), and a second algorithm using the Hooghoudt and Kirkham equations was added in SWAT2005 (Table 1.1).

Table 1.1 Different tile drainage algorithms in SWAT and their approach

Algorithm	Approach
SWAT 2000 (Arnold et al., 1999)	Subsurface drainage is a function of tile depth, time to drain to field capacity, and drain tile lag
SWAT2005 (Moriasi et al., 2007)	Subsurface drainage is a function of tile spacing, depth and size using the Hooghoudt (1940) and Kirkham (van Schilfgaarde et al., 1957) Equations

Tile drainage is very dependent on the height of the water table in the Hooghoudt (Equation 1.1) and Kirkham (Equation 1.4) equations. The only variables to change from day to day are the water table height and the effective saturated hydraulic conductivity, a variable that is calculated based off the input saturated hydraulic conductivities by layer and the water table height. SWAT has gone through four main versions of water table simulation, although currently only the SWAT2005 and SWAT2012-revised algorithms are available for use (Table 1.2).

Table 1.2 Different water table depth algorithms and their approach (adopted from Moriasi et al. (2011))

Algorithm	Approach
SWAT2005 (Neitsch et al., 2002)	Water table is calculated over the entire soil profile as the ratio of excess water to maximum excess water multiplied by the air filled porosity fraction
SWAT-M (Du et al., 2005)	Water table is calculated from the entire profile based on the amount of water above field capacity compared to saturation
SWAT2012 (Moriasi et al., 2009)	Change in water table is a function of change in soil water and water table factor (calibration parameter)
SWAT2012-revised (Moriasi et al., 2011)	Change in water table is a function of change in soil water and water table factor calculated by soil properties of the layer

Since the implementation of tile drainage algorithms, SWAT has been used to simulate many watersheds containing subsurface drainage systems. Sui and Frankenberger (2008) found that monthly tile flow and nitrate losses from the SWAT2005 tile drainage routine were within acceptable ranges in a small Indiana watershed. The two different tile drainage algorithms were compared by Rahman et al. (2011), who found in the Upper Red River North Basin (in North Dakota and Minnesota) the SWAT2000 and SWAT2005 tile drain algorithms both performed similarly (R^2 = 0.58 and 0.60 respectively), but neither predicted the influence of snowfall within acceptable accuracy. In a study to determine the effectiveness of the SWAT2005 tile algorithms located at the Salt Fork Watershed in Iowa, Moriasi et al. (2012) found predicted watershed streamflow performance at the monthly (NSE = 0.85) and daily (NSE = 0.76) time scales acceptable including very good percent bias values for calibration (-2.3%) and validation (2.5%). Moriasi et al. (2013a) also looked at flow and nitrogen output at the tile on a monthly time step in a watershed to find driving factors regarding nitrogen loss in tiles and determined the deeper the drain, the less nitrate left through the drain using the University of Minnesota’s Agricultural Experiment Station near Waseca Minnesota. A later study looked at monthly flow and nitrate output from tiles using the SWAT2005 tile equations and found the new algorithms could perform acceptably at those scales (Moriasi et al., 2013b). Rahman et al. (2014) used the SWAT2000 algorithms to simulate tile flow at the Red River of the North Basin and found when applied to a single field the algorithms showed 37% of the water yield on average consisted of tile drainage, an acceptable proportion per previous studies and, when applied to the entire basin, an increase in drained lands would cause streamflow peaks to become more normalized. Boles et al. (2015) implemented the SWAT2005 tile drainage routine on a small Indiana watershed to determine the effectiveness of the new algorithms along with the most sensitive variables at the stream outlet and found that the curve number required a 25% decrease in tile drained land to successfully predict tile flow, and the depth to restrictive layer, lateral saturated conductivity, and static maximum depressional storage all needed significant calibration for the SWAT2005 subroutines. Bauwe et al. (2016) tested the effect of using the Curve Number vs Green Ampt infiltration algorithms on the same tile drained watershed in northeastern Germany and determined that both infiltration methods led to acceptable results for daily (NSE = 0.50 & 0.45 and PBIAS = 13.2% & 21.4%, respectively) and monthly (NSE = 0.57 & 0.50 and PBIAS = -7.5% & -23.3%, respectively) catchment stream as well as daily (NSE = 0.35 & 0.33 and PBIAS =

9.1% & 16.4%, respectively) and monthly (NSE = 0.47 & 0.42 and PBIAS = -9.1% & -16.4%, respectively) watershed tile flow obtained by projecting a small catchment to approximate the total flow from tiles in the watershed.

Golmohammadi et al. (2016) developed a new version of the SWAT2005 algorithms that fully integrates DRAINMOD subsurface flow calculations, which they called SWATDRAIN, including additional site specific input requirements and found this new version better predicted daily and monthly water table depth and tile drainage flow. While SWATDRAIN does improve simulation of subsurface hydrology in SWAT, the additional inputs include soil water characteristic data such as water table, volume drained, and upward flux relationships that are difficult to apply to large scales that SWAT is often used for.

While many of these studies show improvement for the current algorithms available in SWAT, they do not address several shortcomings within the model's subsurface flow calculations.

1.5 Objectives

The overall goal of this research study is to improve SWAT's ability to accurately predict daily tile drainage outputs in Midwestern tile drained lands from a field to a small watershed scale. The specific research objectives were:

1. Implement new subroutines in the SWAT model for soil water balance and evaluate model simulations of a tiled field in Eastern Indiana.
2. Compare the original to the improved version of SWAT by simulating a small tile-drained watershed in Central Ohio.

1.6 Thesis Organization

This thesis contains four chapters. Chapter 1 provides a background on the subsurface drainage practice and its prediction, the different computer models that predict subsurface drainage, and specifically the history of how the SWAT model predicts tile drainage. Chapters 2 and 3 are written as journal articles and describe the methods and results for the research objectives. Chapter 2 addresses Objective 1, presenting the improvements made to the SWAT model and initial results on a single field. SWAT model outputs are compared to both measured data and previous DRAINMOD simulations. Chapter 3 addresses Objective 2, applying the altered SWAT model on a larger scale in a watershed containing tiled and untiled lands. Chapter

4 contains the research study's conclusions and significant findings as well as recommendations for future studies and improvements.

1.7 Bibliography

Ahuja, L. R., Johnsen, K. E., & Rojas, K. W. (2000). Water and chemical transport in soil matrix and macropores. In L. R. Ahuja (Ed.), *Root Zone Water Quality Model: Modelling management effects on water quality and crop production*. Highlands Ranch, CO: Water Resources Publisher.

Ale, S., Bowling, L. C., Brouder, S. M., Frankenberger, J. R., & Youssef, M. A. (2009). Simulated effect of drainage water management operational strategy on hydrology and crop yield for Drummer soil in the Midwestern United States. *Agricultural Water Management*, *96*(4), 653–665.

Arnold, J. G., Gassman, P. W., King, K. W., Saleh, A., & Sunday, U. (1999). *Validation of the subsurface tile flow component in the SWAT model*. *ASAE Paper No. 992138*. St. Joseph, MI: ASAE.

Arnold, J. G., Srinivasan, R., Muttiah, R. S., & Williams, J. R. (1998). Large Area Hydrologic Modeling and Assessment Part 1: Model Development. *Journal of the American Water Resources Association*, *34*(1), 73–89.

Bauwe, A., Kahle, P., & Lennartz, B. (2016). Hydrologic evaluation of the curve number and Green and Ampt infiltration methods by applying Hooghoudt and Kirkham tile drain equations using SWAT. *Journal of Hydrology*, *537*, 311–321.

Blann, K. L., Anderson, J. L., Sands, G. R., & Vondracek, B. (2009). Effects of Agricultural Drainage on Aquatic Ecosystems: A Review. *Critical Reviews in Environmental Science and Technology*, *39*(11), 909–1001.

Boles, C. M. W., Frankenberger, J. R., & Moriasi, D. N. (2015). Tile Drainage Simulation in SWAT2012: Parameterization and Evaluation in an Indiana Watershed. *Transactions of the ASABE*, *58*(5), 1201–1213.

Bottcher, A. B., Monke, E. J., & Huggins, L. F. (1981). Nutrient and Sediment Loadings from a Subsurface Drainage System. *Transactions of the ASABE*, *24*(5), 1221–1226.

Brevé, M. A., Skaggs, R. W., Parsons, J. E., & Gilliam, J. W. (1997). DRAINMOD-N, a nitrogen model for artificially drained soils. *Transactions of the ASAE*, *40*(4), 1067–1075.

Cooke, R. A., Badiger, S., & García, A. M. (2001). Drainage equations for random and irregular tile drainage systems. *Agricultural Water Management*, *48*, 207–224.

Du, B., Arnold, J. G., Saleh, A., & Jaynes, D. B. (2005). Development and application of SWAT to landscapes with tiles and potholes. *Transactions of the ASAE*, *48*(3), 1121–1133.

Fausey, N. R., Brown, L. C., Belcher, H. W., & Kanwar, R. S. (1995). Drainage and Water Quality in Great Lakes and Cornbelt States. *Journal of Irrigation and Drainage Engineering*, *121*(4), 283–288.

Fouss, J. L., Bengtson, R. L., & Carter, C. E. (1987). Simulating Subsurface Drainage in the Lower Mississippi Valley with DRAINMOD. *Transactions of the ASAE*, *30*(6), 1679–1688.

Golmohammadi, G., Prasher, S. O., Madani, A., Rudra, R. P., & Youssef, M. A. (2016). SWATDRAIN, a new model to simulate the hydrology of agricultural Lands, model development and evaluation. *Biosystems Engineering*, *141*, 31–47.

Green, C. H., Tomer, M. D., Di Luzio, M., & Arnold, J. G. (2006). Hydrologic Evaluation of the Soil and Water Assessment Tool for a Large Tile-Drained Watershed in Iowa. *Transactions of the ASABE*, *49*(2), 413–422.

Hooghoudt, S. B. (1940). Bijdragen tot de kennis van eenige natuurkundige grootheden van den grond. No. 7. Algemeene beschouwing van het probleem van de detailontwatering en de infiltratie door middel van parallel loopende drains, greppels, slooten en kanalen. *Verslagen van Landbouwkundige Onderzoekingen*, *46*(14), 515–707.

King, K. W., Williams, M. R., Macrae, M. L., Fausey, N. R., Frankenberger, J. R., Smith, D. R., Kleinman, P. J. A., Brown, L. C. (2015). Phosphorus Transport in Agricultural Subsurface Drainage: A Review. *Journal of Environmental Quality*, *44*(2), 467.

Lennartz, B., Janssen, M., & Tiemeyer, B. (2011). Effects of Agricultural Drainage on Water Regime and Solute Transport at Different Spatial Scales. In M. K. Shukla (Ed.), *Soil Hydrology, Land Use and Agriculture: Measurement and Modelling* (pp. 266–290). Oxfordshire, England: CAB International Publishing.

Moody, W. T. (1966). Nonlinear Differential Equation of Drain Spacing. *Journal of the Irrigation and Drainage Division*, *92*(IR 2), 1–9.

Moriasi, D. N., Arnold, J. G., & Green, C. H. (2007). Incorporation of Hooghoudt and Kirkham Tile Drain Equations into SWAT2005. In *4th Annual Interational SWAT Conference* (pp. 139–147).

Moriasi, D. N., Arnold, J. G., Vazquez-Amabile, G. G., & Engel, B. A. (2011). Shallow Water Table Depth Algorithm in SWAT: Recent Develpoments. *Transactions of the ASABE*, *54*(5), 1705–1711.

Moriasi, D. N., Arnold, J. G., Vazquez-Amabile, G. G., Engel, B. A., & Rossi, C. G. (2009). Incorporation of a new shallow water table depth algorithm into SWAT2005. *Transactions of the ASABE*, *52*(3), 771–784.

Moriasi, D. N., Gowda, P. H., Arnold, J. G., Mulla, D. J., Ale, S., & Steiner, J. L. (2013a). Modeling the impact of nitrogen fertilizer application and tile drain configuration on nitrate leaching using SWAT. *Agricultural Water Management*, *130*, 36–43.

Moriasi, D. N., Gowda, P. H., Arnold, J. G., Mulla, D. J., Ale, S., Steiner, J. L., & Tomer, M. D. (2013b). Evaluation of the Hooghoudt and Kirkham Tile Drain Equations in the Soil and Water Assessment Tool to Simulate Tile Flow and Nitrate-Nitrogen. *Journal of Environmental Quality*, *42*(6), 1699.

Moriasi, D. N., Rossi, C. G., Arnold, J. G., & Tomer, M. D. (2012). Evaluating hydrology of the Soil and Water Assessment Tool (SWAT) with new tile drain equations. *Journal of Soil and Water Conservation*, *67*(6), 513–524.

Neitsch, S. L., Arnold, J. G., Kiniry, J. R., Williams, J. R., & King, K. W. (2002). *Soil and Water Assessment Tool Theoretical Documentation, Version 2000*. College Station, TX.

Rahman, M. M., Lin, Z., Jia, X., Steele, D. D., & DeSutter, T. M. (2014). Impact of Subsurface Drainage on Stream Flows in the Red River of the North Basin. *Journal of Hydrology*, *511*, 474–483.

Rahman, M. M., Lin, Z., & Moriasi, D. N. (2011). Applying SWAT for impact analysis of tile drainage on streamflow in a snow dominated watershed. Paper number 1110866. In *ASABE Annual International Meeting* (pp. 4934–4947). Louisville, KY.

Randall, G. W., & Goss, M. J. (2008). Nitrate Losses to Surface Water Through Subsurface, Tile Drainage. In J. L. Hatfield & R. F. Follett (Eds.), *Nitrogen in the Environment* (2nd ed., pp. 145–175). Oxford, UK: Elsevier.

Ritzema, H. P. (1994). Subsurface Flow to Drains. In *Drainage principles and applications* (2nd ed., pp. 263–304). Wageningen; Netherlands: International Institute for Land Reclamation and Improvement.

Rutkowski, S. (2012). *Role of Climate Variability on Subsurface Drainage and Streamflow in Agricultural Watersheds* (Master's Thesis). Purdue University.

Singh, P., & Kanwar, R. S. (1995). Modification of RZQM for Simulating Subsurface Drainage by Adding a Tile Flow Component. *Transactions of the ASAE*, *38*(2), 489–498.

Singh, R., Helmers, M. J., Crumpton, W. G., & Lemke, D. W. (2007). Predicting effects of drainage water management in Iowa's subsurface drained landscapes. *Agricultural Water Management*, *92*(3), 162–170.

Skaggs, R. W. (1978). *A water management model for shallow water table soils*. *Water Resources Research Institute of the University of North Carolina* (Vol. 134).

Skaggs, R. W. (1982). Field Evaluation of a Water Management Simulation Model. *Transactions of the ASAE*, *25*(3), 666–674.

Skaggs, R. W., Brevé, M. A., & Gilliam, J. W. (1994). Hydrologic and water quality impacts of agricultural drainage. *Critical Reviews in Environmental Science and Technology*, *24*(1), 1–32.

Sui, Y., & Frankenberger, J. R. (2008). Nitrate Loss From Subsurface Drains in an Agricultural Watershed Using SWAT2005. *Transactions of the ASABE*, *51*(4), 1263–1272.

USDA-NRCS. (2001). Water Management (Drainage). In *Part 650 Engineering Field Handbook National Engineering Handbook*.

van Schilfgaarde, J., Engelund, F., Kirkham, D., Peterson, D. F., & Maasland, M. (1957). Theory of Land Drainage. In J. N. Luthin (Ed.), *Drainage of Agricultural Lands* (pp. 79–285).

Wang, X., Mosley, C. T., Frankenberger, J. R., & Kladivko, E. J. (2006). Subsurface drain flow and crop yield predictions for different drain spacings using DRAINMOD. *Agricultural Water Management*, *79*, 113–136.

Youssef, M. A., Skaggs, R. W., Chescheir, G. M., & Gilliam, J. W. (2006). Field Evaluation of a Model for Predicting Nitrogen Losses from Drained Lands. *Journal of Environmental Quality*, *35*(6), 2026–2042.

CHAPTER 2. IMPROVEMENT OF SUBSURFACE HYDROLOGY SUBROUTINES IN SWAT AND EVALUATION OF SIMULATIONS ON A TILED FIELD

2.1 Introduction

Tile drain systems are commonplace in the Midwestern United Sates as a way to control water flow in agricultural fields where little slope and poorly drained soils cause increased risk of crop damage from excess water. These tile systems have important hydrologic impacts at both field and watershed scales. For example, in Iowa, Green et al. (2006) found that tile drainage was responsible for 70% of the total discharge at the watershed outlet. King et al. (2015) found similar results in a small watershed in Ohio where 28% of precipitation was recovered as tile flow and 47% of mean monthly stream flow came from the tiles. Using the SWAT Model, Boles et al. (2015) found tile drains contributed to 32.1% of the total stream discharge annually at a watershed in Indiana.

Field scale models such as DRAINMOD (Skaggs, 1978; Wang et al., 2006) have been widely used to predict drain flow. DRAINMOD-N (Youssef et al., 2006) also predicts nutrient losses from subsurface drainage from specific fields. While modeling at a field level is valuable for developing and evaluating field-scale management strategies to reduce subsurface nutrient losses, being able to accurately simulate tile drain outputs using a watershed scale model such as SWAT can evaluate strategies on a larger scale and not just a single field.

In order to develop and test modifications to the SWAT water table and tile drain algorithms, long term drain flow data are needed. An experimental drainage field at the Southeast Purdue Agricultural Center (SEPAC) has been monitored since 1984 (Kladivko et al., 1991, 1999, 2004, 2005; Larney et al., 1988, 1989). It has also been modeled using DRAINMOD (Wang et al., 2006) providing a useful comparison of algorithms and performance.

Data available for the six monitored tiles at SEPAC includes: yield, management strategies including planting, harvest, tillage, fertilizer, and pesticide applications, water quantity and quality, and weather including temperature and precipitation (Kladivko et al., 1991, 1999, 2004, 2005; Larney et al., 1989). The rich data available at this site as well as the published studies create an excellent test dataset for model simulations.

The objective of this chapter was to improve SWAT's ability to model tile drainage at a daily scale using physically-based relationships that can apply at all locations rather than site-specific empirical relationships. These changes will be useful in determining the sources of flow within a watershed and if peak flow from a drain can alter the hydrology and water quality of a water network.

2.2 SWAT Improvements

Changes were made to four components: soil percolation, restrictive layer definition, water table depth, and tile drain delay. Line numbers provided in this report refer to SWAT2012 rev. 638 (not publicly released, from here on referred to as SWAT). This revision of SWAT was provided by the developers in order to add on tile nitrate load to the output.sub file.

2.2.1 Percolation through the Soil Profile

Percolation is defined in SWAT as the downward movement of water through the soil profile. The "excess water," which is defined as the water stored above field capacity, moves down through the profile at a rate based on soil properties, such as hydraulic conductivity, and the volume of water within the profile. Once water percolates to the bottom of the profile, if the bottom layer is above saturation, the water that does not seep below the soil profile begins to pool. Then starting at the bottom layer, SWAT redistributes the water above saturation back up to the layer above for each layer until there no layer holds water above saturation. For SWAT, the downward movement is in the percmicro.f subroutine and the upward movement is in the sat_excess.f subroutine.

Current Algorithm: A defined proportion of a layer's excess water ($SW_{ly,excess}$) is allowed to percolate through the soil profile at a rate (travel time) determined by the layer's excess water and saturated conductivity using an S curve equation (Equations 2.1-2.5).

$$w_{perc,ly} = SW_{ly,excess} \times \left(1 - e^{-\frac{24\,hrs}{TT_{perc}}}\right) \quad when \quad SW_{ly,excess} > 0 \qquad 2.1$$

$$w_{perc,ly} = 0 \quad when \quad SW_{ly,excess} \leq 0 \qquad 2.2$$

$$SW_{ly,excess} = SW_{ly} - FC_{ly} \qquad 2.3$$

$$TT_{perc} = \frac{SAT_{ly} - FC_{ly}}{K_{sat}} \quad when \quad \frac{SAT_{ly} - FC_{ly}}{K_{sat}} > 2 \qquad 2.4$$

$$TT_{perc} = 2\ hr \quad when \quad \frac{SAT_{ly} - FC_{ly}}{K_{sat}} \leq 2 \qquad 2.5$$

where the subscript ly is used to reference soil layers in the profile, $w_{perc,ly}$ is the percolation from layer ly to the layer below for the day [mm H_2O], $SW_{ly,excess}$ is the amount of soil water above field capacity in the layer [mm H_2O], TT_{perc} is the percolation travel time for the layer [hr], SAT_{ly} is the amount of water stored in the layer at saturation less wilting point [mm H_2O], FC_{ly} is the amount of soil water stored in the layer at field capacity less wilting point [mm H_2O], K_{sat} is the saturated hydraulic conductivity for the soil layer [mm/hr], and SW_{ly} is the amount of soil water stored in the layer less wilting point [mm H_2O]. These calculations are in the percmicro.f subroutine (Appendix A.11.1).

The SWAT Theoretical Documentation (Neitsch et al., 2011) does not give a source for these equations. With this method, the water content of the layer does not have any influence on TT_{perc} and therefore no effect on daily percolation. In most instances, TT_{perc} was found to be 2 hours meaning that every layer would drain to field capacity in a day. The Theoretical Documentation states that "SWAT directly simulates saturated flow only" (Neitsch et al., 2011, pg 150) while Equations 2.1-2.5 show SWAT models do simulation flow from anywhere between field capacity and saturation.

Algorithm Modification: For the SWAT modification developed in this study, an alternative method to Equations 2.1-2.5 based on Darcy's Law (Darcy, 1856) and the Buckingham-Darcy Law (Buckingham, 1907) was added to provide a physically-based method. The hydraulic conductivity is calculated based off the water content at the start of the day and is assumed to be constant throughout the day. If the soil layer starts the day at saturation, Darcy's Law is used (Equation 2.6).

$$w_{perc,ly} = K_{sat} \times 24hr \qquad 2.6$$

For soil layers that start the day less than saturation, the Buckingham-Darcy Law is used (Equation 2.7)

$$w_{perc,ly} = \frac{SW_{ly}}{depth_{ly}} K_{\theta} \times 24hr \qquad 2.7$$

where $depth_{ly}$ is the depth of the layer [mm] and K_{θ} is the hydraulic conductivity for the layer at water content θ [mm/hr], which is calculated using the Brooks and Corey Equations (Brooks & Corey, 1964) (Equations 2.8-2.9).

$$K_\theta = K_{sat}\left(\frac{\theta_{ly} - \theta_{r,ly}}{\phi_{ly} - \theta_{r,ly}}\right)^n \qquad 2.8$$

$$n = 3 + \frac{2}{\lambda_{ly}} \qquad 2.9$$

where θ_{ly} is the volumetric water content for the layer [mm^3/mm^3], $\theta_{r,ly}$ is the residual volumetric water content for the layer [mm^3/mm^3], ϕ_{ly} is the soil porosity for the layer [mm^3/mm^3], and λ_{ly} is the pore size index for the layer. To estimate the residual water content and pore size index in this method, the equations Rawls & Brakensiek (1985) developed for $\theta_{r,ly}$ (Equation 2.10) and λ_{ly} (Equation 2.11) are used.

$$\begin{aligned}\theta_{r,ly} = &-0.0182482 + 0.00087269S_{ly} + 0.00513488C_{ly} + 0.02939286\phi_{ly} \\ &- 0.00015395C_{ly}^2 - 0.0010827S\phi_{ly} - 0.00018233C_{ly}^2\phi_{ly}^2 \\ &+ 0.00030703C_{ly}^2\phi_{ly} - 0.0023584\phi_{ly}^2C_{ly}\end{aligned} \qquad 2.10$$

$$\begin{aligned}\ln(\lambda_{ly}) = &-0.7842831 + 0.0177544S_{ly} - 1.062498\phi_{ly} - 0.00005304S_{ly}^2 \\ &- 0.00273493C_{ly}^2 + 1.11134946\phi_{ly}^2 - 0.03088295S\phi_{ly} \\ &+ 0.00026587S_{ly}^2\phi_{ly}^2 - 0.00610522C_{ly}^2\phi_{ly}^2 \\ &- 0.00000235S_{ly}^2C_{ly} + 0.00798746C_{ly}^2\phi_{ly} \\ &- 0.00674491\phi_{ly}^2C_{ly}\end{aligned} \qquad 2.11$$

where S_{ly} is the proportion of sand in the layer and C_{ly} is the proportion of clay in the soil layer.

This algorithm alteration causes less water to seep through the soil layer for almost the entire range of water storage, as shown in Figure 2.1 for the fourth layer (970-1200 mm depth) in the soil profile at SEPAC ($K_{sat} = 4.68 mm/hr$, $C_{ly} = 21\%$, $S_{ly} = 19\%$, $BD = 1.70 g/cc$ (BD is bulk density, used in porosity calculations)).

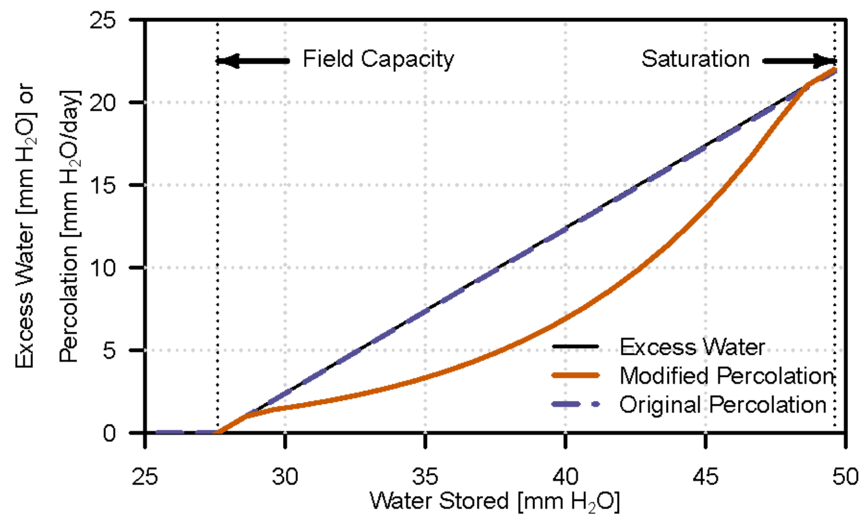

Figure 2.1 Comparison of the Percolation Algorithms using data from the bottom layer of the actual soil profile at SEPAC

The original algorithm allows 99% of the excess water to percolate each day, causing the lines to almost coincide for the entire plot. For water storage levels just above field capacity (27.6 mm H_2O) and just below saturation (49.6 mm H_2O) in the layer shown, the Buckingham Darcy Equation predicts more percolation than excess water (i.e., water above field capacity). Therefore, all excess water percolates.

2.2.2 Definition and Use of the Restrictive Layer Depth

Restrictive layers are found in the poorly drained soils throughout the Midwestern United States (Winters & Simonson, 1951). Wet periods, like those experienced from early fall to spring, are caused by the shallow depth of restrictive layers in the Midwest. Percolation is limited by the low saturated hydraulic conductivity of this layer.

Current Algorithm: The depth from the bottom of the soil profile to the restrictive layer (DEP_IMP) is the only variable used in determining the proportion of percolation that ends up seeping through the bottom of the profile. This algorithm is described in the Theoretical Documentation to only affect HRUs with a perched water table, but is actually in effect for all HRUs in the model (Neitsch et al., 2011). Sui & Frankenberger (2008) first observed that although not clearly documented, this variable controls both the depth and seepage through the restrictive layer (Equations 2.12-2.14).

$$w_{perc,btm} = w_{perc,btm,orig} \times \frac{d_{diff}}{d_{diff} + e^{8.833-2.598 d_{diff}}} \quad when \quad d_{diff} \geq 0 \qquad 2.12$$

$$w_{perc,btm} = 0 \quad when \quad d_{diff} < 0 \qquad 2.13$$

$$d_{diff} = z_{nly} - DEP\_IMP \qquad 2.14$$

where $w_{perc,btm}$ is the percolation past the bottom of the soil profile (i.e. seepage) [mm H_2O], $w_{perc,btm,orig}$ is the original calculation for percolation through the bottom layer via the percolation algorithm ($w_{perc,ly}$) [mm H_2O], and d_{diff} is the distance downward from the bottom of the soil profile (z_{nly}) to the restrictive layer (DEP_IMP) [m]. This calculation at the bottom of the profile is the only point within all of SWAT where the restrictive layer influences water movement through the profile (Figure 2.2). This calculation is performed in the subroutine percmicro.f (Appendix A.11.2).

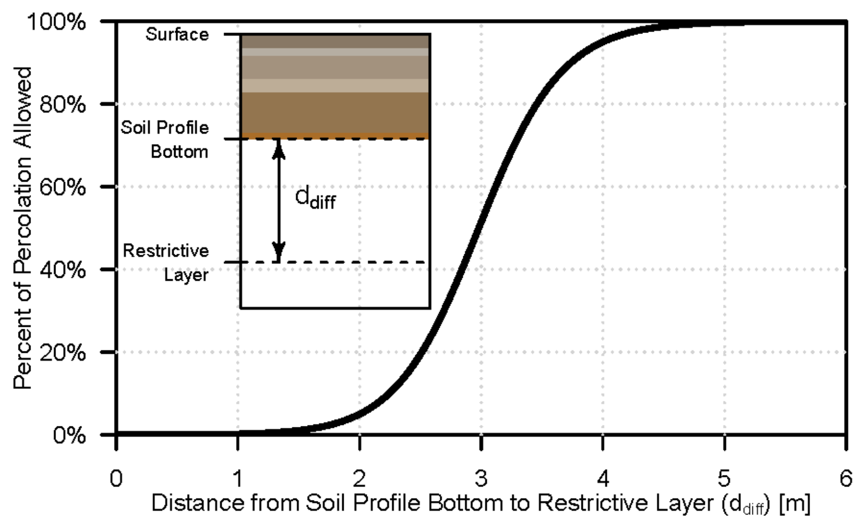

Figure 2.2 Percent of percolation that becomes seepage through the restrictive layer in the original SWAT algorithm, based off the distance downward from the bottom of the soil profile to the restrictive layer

Using the restrictive layer depth in this manner makes the input a calibration input and negates the physical meaning. This definition would not be as much a concern but the restrictive layer depth is also used in the tile drainage calculation as a physical input. These two uses create a dual meaning where the restrictive layer depth is a physical parameter that needs to be accurate to the actual soil profile, but is also a calibrated parameter to approximate seepage past the bottom of the profile.

Algorithm Modification: Two changes were made to remove the dual nature of the restrictive layer and add physical basis to how the model uses the restrictive layer. First, the hydraulic conductivity of the restrictive layer ($KSAT\_IMP$) was added as an additional HRU input. Seepage through the restrictive layer ($w_{perc,btm}$) is calculated as percolation (as described in the previous section), but is then limited to the restrictive layer hydraulic conductivity (Equations 2.15-2.16).

$$w_{perc,btm} = w_{perc,btm,orig} \quad when \quad w_{perc,btm,orig} \leq KSAT\_IMP \qquad 2.15$$

$$w_{perc,btm} = KSAT\_IMP \times 24hr \quad when \quad w_{perc,btm,orig} > KSAT\_IMP \qquad 2.16$$

where $KSAT\_IMP$ is the saturated hydraulic conductivity of the restrictive layer [mm/hr]. This new algorithm has a physical basis instead of using an approximated empirical formula (Figure 2.3).

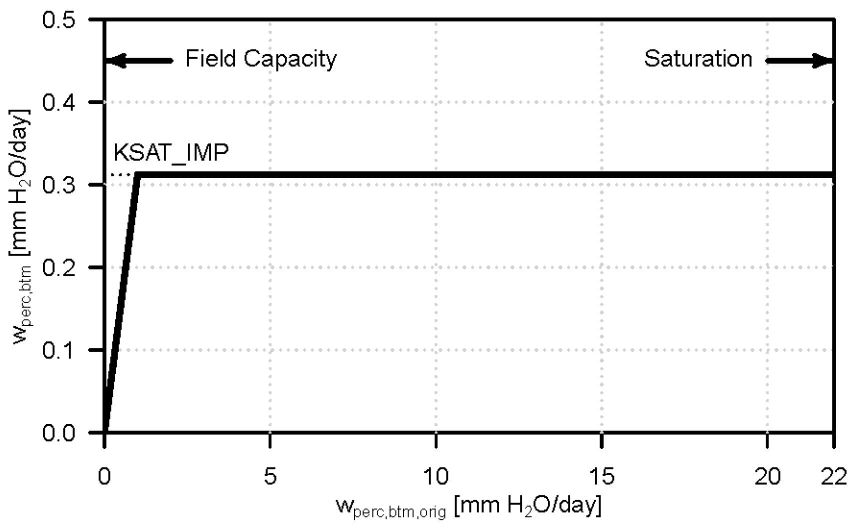

Figure 2.3 Seepage using the calculated percolation through the bottom layer limited by the restrictive layer saturated hydraulic conductivity

Second, when the restrictive layer is within the soil profile, instead of cutting off all seepage to the vadose zone as described in Neitsch et al. (2011), the restrictive layer is assumed to be at the bottom of the soil profile and seepage occurs at the restrictive layer, and when the restrictive layer is below the bottom of the soil profile seepage occurs at the bottom of the profile as SWAT does currently (Figure 2.4).

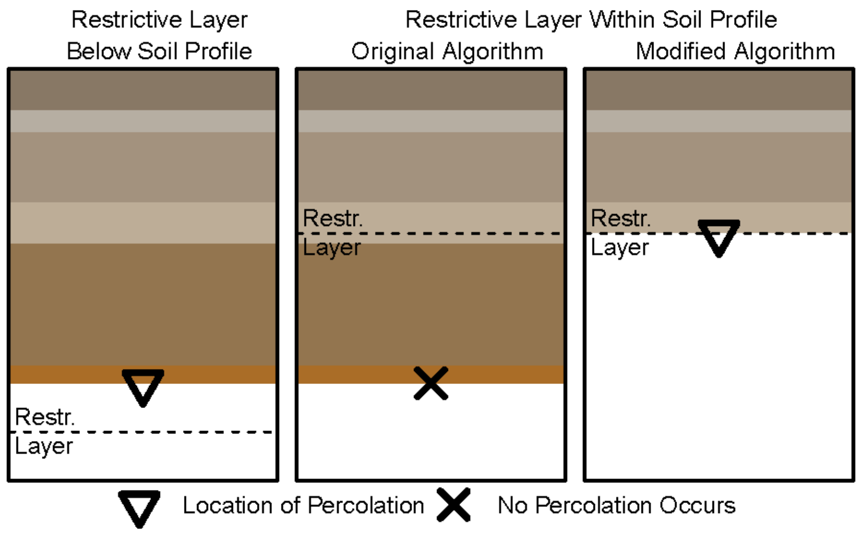

Figure 2.4 Restrictive Layer's Effect on Seepage when within and below the profile for both original and modified algorithm

2.2.3 Water Table Depth

Water table is the primary variable when determining tile drainage using equations such as the Hooghoudt (1940). When the water table is below the tile drain, no flow can occur. The magnitude of the tile flow is based on how high the water table is above the tile drains, and therefore calculating water table depth is critical for accurate drain flow predictions. In SWAT, there are two algorithms available to calculate water table. These algorithms are signified by a flag IWTDN, which defaults to 0, and the alternative algorithm is only used when the flag is changed to 1.

Current Default Algorithm (IWTDN = 0): The theoretical documentation in SWAT indicates a relationship of the soil water balance over the whole profile without splitting into layers to determine water table (Equation 2.17) (Neitsch et al., 2011).

$$h_{wtbl} = \frac{SW - FC}{(POR - FC) \times (1 - \phi_{air})} \times DEP\_IMP \qquad 2.17$$

where h_{wtbl} is the water table height above the restrictive layer [mm], SW is the water stored in the soil profile on that day minus the wilting point [mm H_2O], FC is the water stored in the soil profile at field capacity minus the wilting point [mm H_2O], POR is the porosity of the soil profile [mm], ϕ_{air} is the air-filled porosity of the soil profile expressed as a fraction and defined to be 0.5 in the subroutine, and DEP_IMP is the depth of the restrictive layer from the soil surface [mm].

Equation 2.17 is all that is described in the SWAT Theoretical Documentation (Neitsch et al., 2011). However in the code (subroutine percmain.f) there are additional equations (Equations 2.18-2.22).

$$h_{wtbl} = DEP\_IMP \times xx \tag{2.18}$$

$$xx = \frac{SW - FC}{yy - FC} \quad where \quad \frac{SW - FC}{yy - FC} \leq 1 \tag{2.19}$$

$$xx = 1 \quad where \quad \frac{SW - FC}{yy - FC} > 1 \tag{2.20}$$

$$yy = POR \times \phi_{air} \quad where \quad POR \times \phi_{air} \geq 1.1 \times FC \tag{2.21}$$

$$yy = 1.1 \times FC \quad where \quad POR \times \phi_{air} < 1.1 \times FC \tag{2.22}$$

where xx and yy are substitution placeholders for the algorithm.

These approximations are likely inappropriate in many soils. To determine how frequently the approximation was used vs. the original equation, typical values for various texture classes were obtained from Maidment (1993) and the relationship shown in Equation 2.21 was calculated. In fine textured soils such as silt loam and silty clay loam, the variable, yy is always defined as $1.1 \times FC$ (Table 2.1). Using this definition, $xx = 1$ whenever $SW > 1.1 \times FC$ causing h_{wtbl} to be defined as the surface. This calculation is in the percmain.f subroutine (Appendix A.10.1).

Table 2.1 Texture Class Conditions for Current SWAT Water Table Algorithms (Texture Class POR and FC from Maidment (1993))

Texture Class	POR*	FC*	$POR \times \phi_{air} \geq 1.1 \times FC$ (original equation used)
Sand	0.404	0.058	X
Loamy Sand	0.382	0.070	X
Sandy Loam	0.358	0.112	X
Loam	0.346	0.153	X
Silt Loam	0.368	0.197	
Sandy Clay Loam	0.250	0.107	X
Clay Loam	0.267	0.121	X
Silty Clay Loam	0.263	0.158	
Sandy Clay	0.191	0.100	
Silty Clay	0.229	0.137	
Clay	0.203	0.124	

* Porosity (i.e. saturation) and Field Capacity values have wilting point subtracted, as this is what the SWAT algorithms use

Current Alternative Algorithm (IWTDN = 1): Moriasi et al. (2011) updated SWAT with a new algorithm to calculate water table based on change in water storage between days (Equation 2.23).

$$\Delta h_{wtbl} = \sum_{ly=1}^{nly} vwt_{ly} \times \Delta SW_{ly} \qquad 2.23$$

where Δh_{wtbl} is the change in depth from the surface to the water table for the day [mm], nly is the number of layers in the soil profile, vwt_{ly} is the variable water table factor for the layer, and ΔSW_{ly} is the change in soil water from the previous day for the layer [mm]. These equations are in the percmain.f subroutine (Appendix A.10.1).

Variable water table factor (vwt_{ly}) was based on a calibrated polynomial equation for the variable water table factor from Moriasi et al. (2011) using data from a study in the Muscatatuck River basin, IN (Equation 2.24).

$$vwt_{ly} = 786.84\phi_{ly}^2 - 171.14\phi_{ly} + 14.864 \qquad 2.24$$

However, in the SWAT soil_phys.f subroutine (Appendix A.8), the equation for the variable water table factor contained different constants (Equations 2.25-2.26).

$$vwt_{ly} = 437.13\phi_{drain,ly}^2 - 95.08\phi_{drain,ly} + 8.257 \qquad 2.25$$

$$\phi_{drain,ly} = \phi_{ly} - \theta_{fc,ly} \qquad 2.26$$

where $\theta_{fc,ly}$ is the volumetric water content at field capacity [mm^3/mm^3] and $\phi_{drain,ly}$ is the drainable soil porosity [mm^3/mm^3]. While the method developed by Moriasi et al. (2011) showed an improvement from the original method at the site where the equations were developed, there has been no published testing on the accuracy of the water table output outside of the initial alterations.

The variable water table factor was developed from a single site, which limits its applicability to other sites. Moriasi et al. (2011) stated that this new method should be checked using other more diverse sites. The improved results from this equation are not necessarily accurate for different soils and locations. The inconsistency between the publications on the alteration and the actual subroutines also raises cause for concern.

Algorithm Modification: Water table algorithms were changed to use soil water properties at the end of the day to determine water table to a similar algorithm as SWAT-M (Du et al., 2005), a modification not currently available in SWAT. The algorithm identifies the lowest layer in which soil water is less than 95% of saturation as the layer where the water table is located (denoted wly). The water table height within the layer is calculated as a proportion of the depth of the layer and the ratio between the water greater than field capacity and the water to saturation from field capacity and then added to the height of the layer (Equations 2.27-2.28).

$$h_{wtbl} = \left(DEP\_IMP - z_{wly}\right) + h_{wtbl,wly} \qquad 2.27$$

$$h_{wtbl,wly} = depth_{wly}\left(\frac{SW_{wly} - FC_{wly}}{SAT_{wly} - FC_{wly}}\right) \qquad 2.28$$

where z_{wly} is the depth of the bottom of the layer from the soil surface and $h_{wtbl,wly}$ is the height of the water table from the bottom of the identified layer [mm] (Figure 2.5). While this approach does not follow a theoretical approach such as Brooks and Corey (1964), it has more physical basis than the Moriasi et al. (2011) version, and does not require intensive calculations and should at least place the water table in the correct layer.

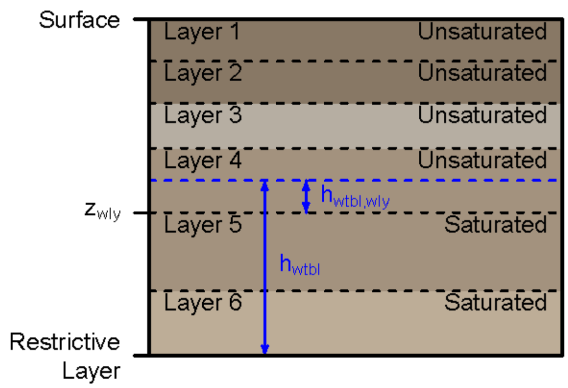

Figure 2.5 Diagram depicting the new water table algorithm where $wly = Layer\ 4$

2.2.4 Tile Drain Flow Lag

Current Algorithm: In addition to limiting tile flow to the drainage coefficient, SWAT also implements a time delay after this limit is used (Equations 2.29-2.31).

$$tile_{wtr,avail} = tile_{wtr,orig} + tile_{wtr,leftover} \qquad 2.29$$

$$tile_{wtr} = tile_{wtr,avail} \times TT_{lag} \qquad 2.30$$

$$tile_{wtr,leftover} = tile_{wtr,avail} - tile_{wtr} \qquad 2.31$$

where $tile_{wtr,avail}$ is the available drainage discharge for the day [mm/day], $tile_{wtr,orig}$ is the calculated drainage discharge for the day [mm/day], $tile_{wtr,leftover}$ is the drainage discharge delayed from the previous day [mm/day], $tile_{wtr}$ is the new drainage discharge for the day [mm/day], and TT_{lag} is tile drainage travel time. These calculations are performed in the subroutine substor.f (lines 67, 71, 86, 90, & 101). The tile time delay represents the proportion of drainage discharge allowed to flow from the HRU that day (Equation 2.32).

$$TT_{lag} = 1 - e^{-\frac{24hrs}{GDRAIN}} \qquad 2.32$$

where $GDRAIN$ is the drain tile lag time [hr]. If the user does not input a value for TT_{lag}, the variable is defaulted at 96 hr giving a TT_{lag} of 0.221 (Figure 2.6). The time delay factor is calculated in both schedule_ops.f and hydroinit.f (Appendix A.9).

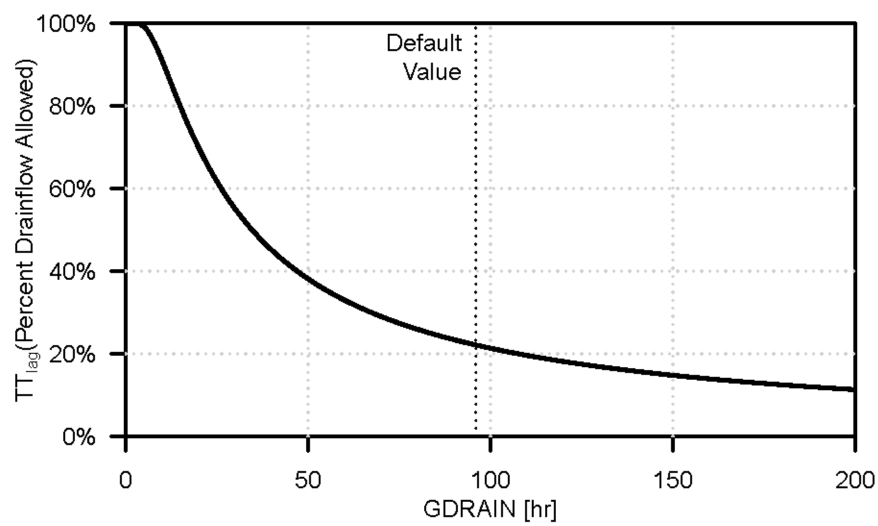

Figure 2.6 Tile drainage lag based off the drain tile lag time

Algorithm Modification: Flow through tile drains is very fast, once the water reaches the drain, which is calculated using the Hooghoudt and Kirkham equations. The only potential cause of delay once in the drain is due to limitations in the size of the drain, which is calculated using the drainage coefficient. In SWAT, if $GDRAIN$ is set to 0 by the user the default value is used instead, which is 96 hours. Because of the likelihood that the user will set $GDRAIN$ to 0 or the default, the use of $GDRAIN$ was removed from SWAT and TT_{lag} was defined to be one, effectively removing this additional delay. The removal of the tile drain lag leads to better prediction of tile drainage peak magnitude and the drainage event lasts a shorter amount of time (Figure 2.7).

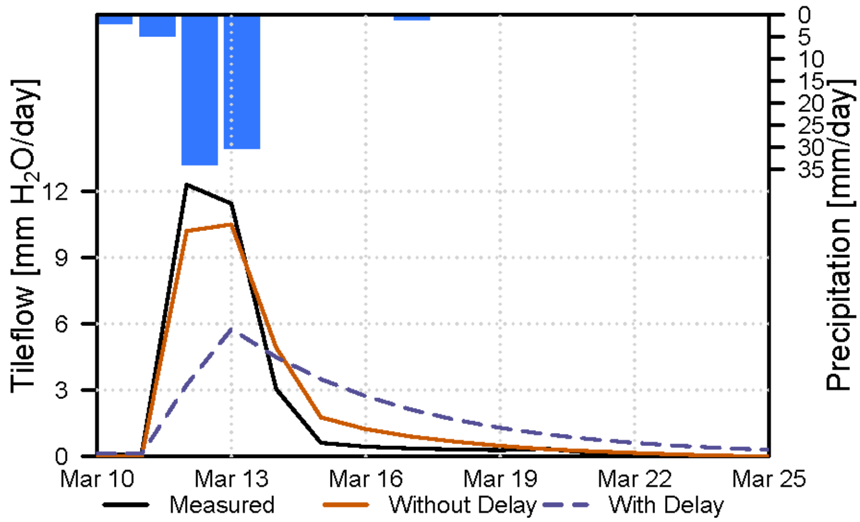

Figure 2.7 Example tile drainage output with and without delay algorithm

2.2.5 Subroutines Altered for Changes

In order to implement these changes, a number of additions to the SWAT source code had to be made (Table 2.2).

Table 2.2 Alterations to the SWAT Model by Subroutine

Subroutine Name	Description of Changes
allocate_parms.f	Allocation of dimensioned variables: bc_lam(:,:), bc_thr(:,:), ksat_imp(:), sol_exw(:,:), sol_sep(:,:), sol_ule(:,:)
hruday.f90	Write additional HRU output files: soil_phys.out
hydroinit.f	If ITDRN = 2: Remove tile delay
modparm.f	Addition of new variables: bc_lam(:,:), bc_thr(:,:), iimp, iwdn, iwsl, ksat_imp(:), sol_exw(:,:), sol_sep(:,:), sol_ule(:,:)
percmain.f	Assign sol_sep(:,:) and sol_ule(:,:) to 0 at start of day Assign sol_exw(:,:) from sw_excess If IWTDN = 2: Addition of new water table algorithm
percmicro.f	If IWDN = 1: New percolation algorithm If IIMP = 1: New seepage algorithm Assign sol_sep(:,:) from sepday
readbsn.f	Add in reading IIMP AND IWDN from basins.bsn
readfile.f	Add in reading IWSL from file.cio: Open soil_phys.out If IWSL = 1: Open sepday.out, satexcess.out, ulexcess.out
readhru.f	Add in reading ksat_imp(:,:) from *.hru files
readsol.f	If IIMP = 1: New soil profile algorithm
sat_excess.f	Assign sol_ule(:,:) from ulexcess
schedule_ops.f	If IDRN = 2: Remove tile delay
soil_phys.f	Calculate Brooks-Corey Parameters
writed.f	If IWSL = 1: write sepday.out, satexcess.out, ulexcess.out
zero2.f	Set new variables to 0 before values read in or calculated

A total of six new variables were added into SWAT (Table 2.3).

Table 2.3 Additional SWAT Variables

New Variable	Definition
bc_lam(:,:)	Brooks Corey Pore Size Index
bc_thr(:,:)	Books Corey Residual volumetric water content [mm^3/mm^3]
ksat_imp(:)	Saturated hydraulic conductivity of the restrictive layer [mm/hr]
sol_exw(:,:)	Excess water in the soil layer for the day [mm H_2O]
sol_sep(:,:)	Downward water movement in the soil layer for the day [mm H_2O]
sol_ule(:,:)	Upward water movement in the soil layer for the day [mm H_2O]

In addition to the four algorithm changes discussed above, additional output files were created in order to better assess the code output (Table 2.4).

Table 2.4 Additional Output File Names and Descriptions

Output Name	Description
soil_phys.out	Flag Required: No Outputs: depth, field capacity, saturation, and beta coefficient for each layer in the profile and the entire profile
sepday.out	Flag Required: Yes (IWSL = 1) Outputs: amount of excess water at the beginning of the day for each soil layer in the profile
satexcess.out	Flag Required: Yes (IWSL = 1) Outputs: amount of water percolating down to the next layer for each layer in the profile (seepage for bottom layer)
ulexcess.out	Flag Required: Yes (IWSL = 1) Outputs: amount of water moving above the layer for each layer in the soil profile

All modified code is provided in Appendix A.

2.3 Application to a Drained Indiana Field

2.3.1 Description of Study Site

The Southeast Purdue Agricultural Center (SEPAC) was used as a single tile model for the study (Figure 2.8) (Kladivko et al., 1991, 1999). The drainage site consists of 3.3 ha in Jennings County, IN (85°32’23” W, 39°1’30” N). The topography is flat with elevation ranging from 238 m to 239 m, and slopes between 0% and 1.5%. The site consists entirely of Cobbsfork silt loam (MUKEY: 633185). This soil was formerly called Clermont, which is the name used in previously published papers, but the name was changed by the NRCS in the 1990 Soil Survey.

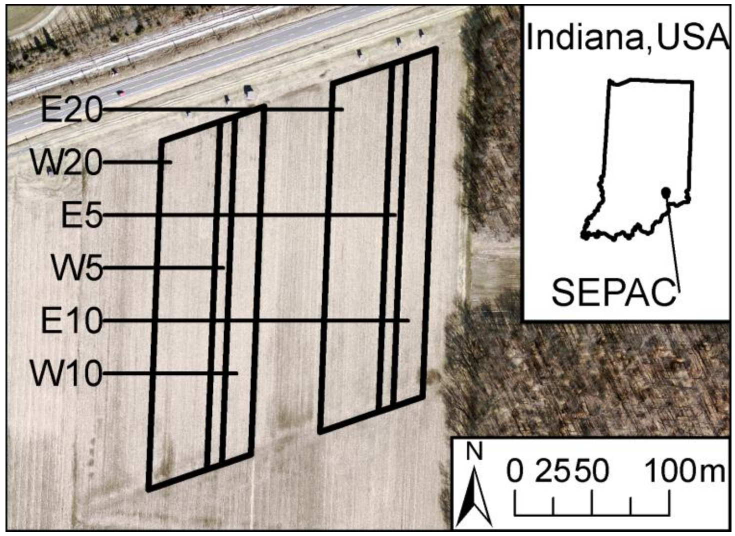

Figure 2.8 SEPAC Drainage Field Location

The drainage system has east (E) and west (W) replicates of 5, 10, and 20 m spacings totaling six 225 m drains (E5, E10, E20, W5, W10, and W20). The east and west plots are separated by an unmonitored 40 m spacing. Drain flow and Nitrate-N have been monitored since 1986 by Kladivko et al. (1991, 1999). In this study data from 1986 to 2000 were used, which are the same years used by Wang et al. (2006) in a modeling study using DRAINMOD.

2.3.2 Model Set Up

The SWAT model was initially set up using the ArcSWAT 2012.10_2.15 with ArcGIS 10.2.2. Once the input tables were written, ArcSWAT was not used and all changes were performed manually or using R scripts.

Each tile was considered separately and treated as its own watershed with a single subbasin containing a single hydrologic response unit (HRU). To do this, each tile was manually delineated in ArcSWAT. Because ArcSWAT requires two subbasins to accept the model, a “dummy” subbasin was added to the north side of the field where the tiles drained into a main so each tile drained into a single subbasin. Stream pathways were manually delineated from each subbasin to where the main is located solely to ensure SWAT runs properly. Since only the tile outlets were monitored the exact stream delineation was not a concern.

Before any manual changes, models for W20, W10, and W5 were separated out individually from the eastern fields. The channel file (chan.deg) in each model was changed to only refer to the channel (i.e., tile outlet) of the subbasin each site was. The routing file (fig.fig) also was rewritten for each model so only the single subbasin routes to the single stream.

SWAT was set up to run for 22 years, 1980-2001, for the W20, W10, and W5 models where the first five years (1980-1984) were used as a "warm up" period using the management data from 1985.

2.3.2.1 Management Practices

Management practices, which were the same for the entire field, are shown in Table 2.5. Corn was planted after spring chisel till from 1984 to 1993. Starting in 1994, a corn-soybean rotation was implemented with a winter wheat cover crop after each corn year and tillage only in the spring before corn planting. Management practices were determined using Larney et al. (1989), Kladivko et al. (2004, 2005), Negm et al. (2014), and Wang et al. (2006). For the model, no herbicide data was considered. Tillage was listed as the day before planting starting in 1987 (Kladivko et al., 2005). Harvest dates were based off the middle date in ranges given by Kladivko et al. (2005). Wang et al. (2006) stated the winter wheat cover crop was killed via herbicide approximately a week before soybean planting. Dates of operations from 1994-2001 were approximated using the 1985-1993 rotation. Harvest dates for all soybean years were based off the mean harvest date reported for Indiana by the USDA National Agricultural Statistics Service (1997). The management practices were added to the management file in the SWAT model by considering all 22 years as a single rotation.

Table 2.5 Management Practices for SEPAC Field Site

Date	Operation	Date	Operation	Date	Operation
1985		**1990**		**1995 (cont.)**	
4/19	NH_3: 285 kg N/ha	5/27	NH_3: 228 kg N/ha	10/6	Harvest
4/20	Tillage, Chisel	5/29	Tillage, Chisel	10/13	Plant, Wheat
4/22	18-5-0: 8 kg N/ha	5/30	19-7-0: 28 kg N/ha	**1996**	
4/22	Plant, Corn	5/30	Plant, Corn	4/25	Kill, Wheat
9/24	Harvest	10/29	Harvest	4/28	Plant, Soybean
1986		**1991**		10/12	Harvest
4/27	NH_3: 285 kg N/ha	4/28	NH_3: 228 kg N/ha	**1997**	
4/14	Tillage, Chisel	4/30	Tillage, Chisel	5/4	NH_3: 177 kg N/ha
4/30	18-5-0: 21 kg N/ha	5/1	19-7-0: 28 kg N/ha	5/7	19-7-0: 28 kg N/ha
4/30	Plant, Corn	5/1	Plant, Corn	5/7	Plant, Corn
9/26	Harvest	9/20	Harvest	10/6	Harvest
1987		**1992**		10/13	Plant, Wheat
4/25	NH_3: 285 kg N/ha	5/2	NH_3: 228 kg N/ha	**1998**	
4/27	Tillage, Chisel	5/4	Tillage, Chisel	4/25	Kill, Wheat
4/28	18-5-0: 22 kg N/ha	5/5	19-7-0: 28 kg N/ha	4/28	Plant, Soybean
4/28	Plant, Corn	5/5	Plant, Corn	10/12	Harvest
9/16	Harvest	10/5	Harvest	**1999**	
1988		**1993**		5/4	NH_3: 177 kg N/ha
4/29	NH_3: 285 kg N/ha	5/7	NH_3: 228 kg N/ha	5/7	19-7-0: 28 kg N/ha
5/1	Tillage, Chisel	5/9	Tillage, Chisel	5/7	Plant, Corn
5/2	18-5-0: 11 kg N/ha	5/10	19-7-0: 28 kg N/ha	10/6	Harvest
5/2	Plant, Corn	5/10	Plant, Corn	10/13	Plant, Wheat
10/6	Harvest	10/13	Harvest	**2000**	
1989		**1994**		4/25	Kill, Wheat
5/15	NH_3: 228 kg N/ha	4/28	Plant, Soybean	10/12	Plant, Soybean
5/17	Tillage, Chisel	10/12	Harvest	8/26	Harvest
5/18	18-5-0: 20 kg N/ha	**1995**		**2001**	
5/18	Plant, Corn	5/4	NH_3: 200 kg N/ha	5/4	NH_3: 177 kg N/ha
10/18	Harvest	5/7	19-7-0: 28 kg N/ha	5/7	19-7-0: 28 kg N/ha
		5/7	Plant, Corn	4/28	Plant, Corn
				8/26	Harvest

2.3.2.2 Geospatial Input Data

The National Elevation Dataset (Gesch, 2007; Gesch et al., 2002) and SSURGO Database (USDA-NRCS Soil Survey Staff, 2014) were used for elevation and soil data (Table 2.6), respectively. While measured soil data was available for the site, many of the properties required for SWAT to successfully run were not available and so the SSURGO data was used for all inputted soil properties. The same file used for watershed delineation was also used as the land use input as the entire model was agricultural-row crops (AGGR).

Table 2.6 Soil Properties of Cobbsfork Silt Loam

Depth [mm]	K_{sat} [mm/hr]	AWC [mm/mm] *	POR [mm/mm] **
0-300	33.01	0.21	0.38
300-460	33.01	0.22	0.35
460-970	27.94	0.18	0.29
970-1270	4.68	0.12	0.22
1270-2160	1.48	0.07	0.21
2160-2290	1.48	0.07	0.19

** FC is calculated in SWAT as AWC (Available Water Content) plus a calculated WP (wilting point)*

***POR is calculated within SWAT and is not an input*

2.3.2.3 Weather Data

The precipitation and temperature data prepared by Wang et al. (2006) was used in this study. This data included onsite measurements when available and North Vernon's rainfall gage when it was not. The hourly data required by DRAINMOD was aggregated by day, as SWAT uses daily precipitation data.

2.3.2.4 Drainage Parameters

Drainage parameters from field measurements by Larney et al. (1988) and the previous DRAINMOD study by Wang et al. (2006) were added to the model (Table 2.7).

Table 2.7 Drainage Subroutine Parameters

Variable	Description	Input File	Value
DEP_IMP	Depth from surface to restrictive layer	*.hru	1200 mm
DDRAIN	Depth from surface to tile drains	*.mgt	750 mm
RE	Effective radius	*.sdr	11 mm
SSTMAXD	Maximum surface storage	*.sdr	10 mm
DRAIN_CO	Drainage coefficient	*.sdr	20 mm/day
KSAT_IMP	Saturated hydraulic conductivity of restrictive layer	*.hru	0.013 mm/hr
SDRAIN	Tile drain spacing (value is dependent on the tile sites)	*.sdr	5000, 10,000, or 20,000 mm

2.3.3 Model Calibration Approach

Six parameters were calibrated: two for tile flow (Table 2.8) and four for nitrate loads through the tiles (Table 2.9). These parameters were selected for calibration because of the model sensitivity and because they could not be directly measured. Calibration years were 1988-1989, the same years as the previous DRAINMOD study (Wang et al., 2006) in order to more appropriately compare results. Original and Modified SWAT were calibrated separately for tile flow and tile nitrate in order to ensure the best performance for both sets of subroutines.

Table 2.8 Parameters Used in Tile Flow Calibration

Parameter	Definition	Input File	Range
CN2	SCS Curve Number (CN II)	*.mgt	-30 – 10% (by 5%)
LATKSATF	Multiplication factor to determine saturated hydraulic conductivity from soil layer properties	*.sdr	1 – 10 (by 1)

Table 2.9 Parameters Used in Tile Nitrate Calibration

Parameter	Definition	Input File	Range
NPERCO	Nitrate percolation coefficient	*.bsn	0.01 & 0.25 – 1 (by 0.25)
SDNCO	Denitrification threshold water content	*.bsn	0.25 – 2 (by 0.25) & 1.1
CDN	Denitrification exponential rate coefficient	*.bsn	0 – 3 (by 0.5)
CMN	Rate factor for humus mineralization of active organic nutrients	*.bsn	0.0001 & 0.0005 – 0.003 (by 0.0005)

Two different measures were used when calibrating, the Nash-Sutcliffe Efficiency (NSE, Equation 2.33) (Nash & Sutcliffe, 1970) and Percent Bias (PBIAS, Equation 2.34)

$$NSE = 1 - \frac{\sum_{i=1}^{n}(O_i - P_i)^2}{\sum_{i=1}^{n}(O_i - \bar{O})^2} \qquad 2.33$$

$$PBIAS = \frac{\sum_{i=1}^{n} P_i - \sum_{i=1}^{n} O_i}{\sum_{i=1}^{n} O_i} \qquad 2.34$$

where n is the number of days in the simulation, O_i is the observed value at day i, P_i is the predicted (or modeled) value at day i, and $\bar{O}$ is the arithmetic mean of the observed values. The interpretation of these statistics is found in Table 2.10. The closer the NSE is to 1 and the closer PBIAS is to 0 the better the model performs.

Table 2.10 Interpretation of Statistical Measures

Statistic	Range	Interpretation
Nash-Sutcliffe Efficiency	$NSE < 0$	The predicted values are not as accurate as the average of the observed values
	$NSE = 0$	The predicted values are just as accurate as the average of the observed values
	$0 < NSE < 1$	The predicted values are more accurate than the average of the observed values
	$NSE = 1$	The predicted values are a perfect predictor of the observed values
Percent Bias	$PBIAS < 0$	The predicted values are biased to be lower than the observed values
	$PBIAS = 0$	The predicted values are not biased compared to the observed values
	$0 < PBIAS$	The predicted values are biased to be higher than the observed values

In order to ensure every combination of inputs was used, an R-Script was developed to change the inputs accordingly, run SWAT, calculate the NSE and PBIAS, and then write out the statistics to a common table.

The final combination of variables for tile flow was decided by using Equation 2.35 to combine PBIAS and NSE into a single value and selecting the lowest value of the results for each subbasin.

$$|PBIAS| + (1 - NSE) \times 100 \tag{2.35}$$

To weight the PBIAS value more for the tile nitrate calibrations, Equation 2.36 was used to combine PBIAS and NSE into a single value and selecting the lowest value of the results for each subbasin.

$$|PBIAS| + (1 - NSE) \times 10 \tag{2.36}$$

These equations were developed for this study in order to create a multi-objective calibration within the semi-automated method used within R.

2.4 Results

For the Results section, revision 638 of SWAT using the Moriasi water table and tile drainage algorithms is referred to as the original SWAT and the version of SWAT including all four of the above described changes is referred to as the modified SWAT.

2.4.1 Hydrology

2.4.1.1 Tile Flow Calibration Results

Calibration (1988-1989) and validation (1985-1987 & 1990-2000) were performed for both the original and modified SWAT (Table 2.11). Curve number reduction was less than expected in a tile drainage simulation for the original SWAT and was at the expected reduction for the modified SWAT. The W10 and W5 calibrations for modified SWAT both ended on the maximum curve number reduction. Due to this, it is possible a further reduction of curve number could lead to a better result. For the original SWAT calibration at W20, LATKSATF had no effect for the values 5-10 and so the lowest value was used. The W10 and W5 both required very little LATKSATF increase for both versions of SWAT, an unexpected result.

Table 2.11 Tile Flow Calibration Values Parameters for both versions of SWAT

Model	Version	CN	LATKSATF
All	Uncalibrated Value		1
W20	Original SWAT	-5%	5
	Modified SWAT	-20%	4
W10	Original SWAT	-10%	2
	Modified SWAT	-30%	2
W5	Original SWAT	-15%	1
	Modified SWAT	-30%	1

The final NSE values were lower than what is normally considered as satisfactory for a monthly time step (Moriasi et al., 2007), but assessments done here were at a daily scale allowing for a larger margin of error (Table 2.12). On average, the PBIAS values performed better for the modified SWAT, although both versions of the model produced very good results. The modified SWAT had better NSE values for calibration, but worse for validation. The three models performed similarly although there were performance differences. On average across both versions of SWAT, W20 performed best overall and W5 performed the worst.

Table 2.12 Tile flow calibration and validation statistics for both versions of SWAT

Model	Version	Time Period	NSE	PBIAS
W20	Original SWAT	Calibration (1988-1989)	0.35	-1.5%
		Validation (1985-1987 & 1990-2000)	-0.02	2.6%
	Modified SWAT	Calibration (1988-1989)	0.38	-2.1%
		Validation (1985-1987 & 1990-2000)	0.07	3.7%
W10	Original SWAT	Calibration (1988-1989)	0.47	-7.3%
		Validation (1985-1987 & 1990-2000)	0.20	10.5%
	Modified SWAT	Calibration (1988-1989)	0.52	-4.8%
		Validation (1985-1987 & 1990-2000)	-0.01	17.6%
W5	Original SWAT	Calibration (1988-1989)	0.41	-4.6%
		Validation (1985-1987 & 1990-2000)	0.11	18.7%
	Modified SWAT	Calibration (1988-1989)	0.43	-17.2%
		Validation (1985-1987 & 1990-2000)	-0.31	4.3%

2.4.1.2 W20 Water Table

The water table was lowered considerably with the new algorithms (Figure 2.9). While this is still not a good representation of the measured water table, the modified SWAT predicts the time water table crosses from above to below the drains at the end of the season (May) and when it rises above the drains at the start of the season (December) similar to DRAINMOD where the original SWAT output never predicts water table lowering to below the tile drains. This is a primary function for the water table as drainage occurs only when the water table is above the drains. Similar issues with the water table staying right above the drain location have been noted at this site when it was modeled with VIC (Rutkowski, 2012).

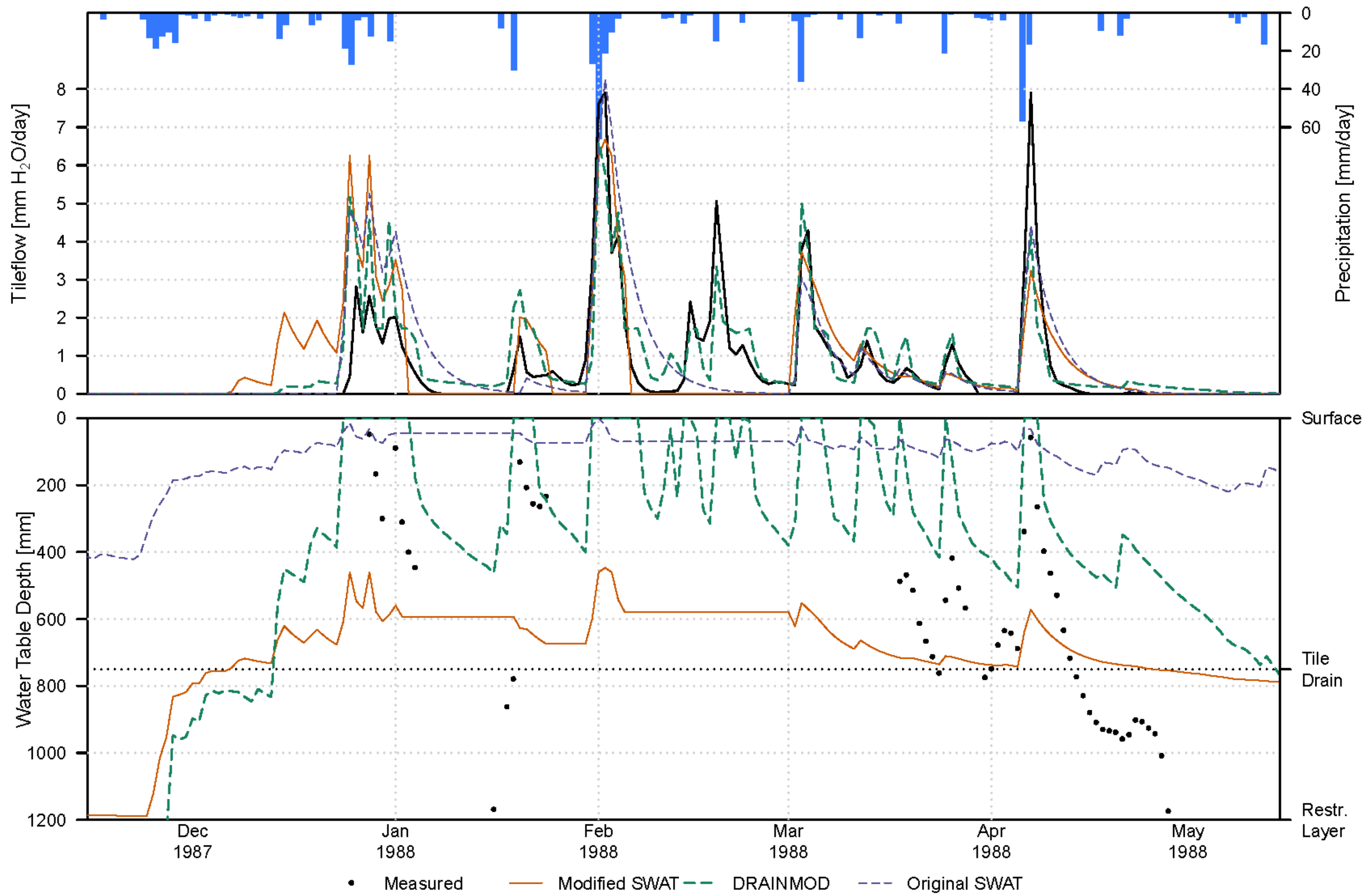

Figure 2.9 Predicted and Observed Water Table and Tile Flow from W20

The water table algorithms still need significant work in the SWAT model to get to a level of performance similar to DRAINMOD. The modified algorithms should have predicted the water table to within a layer of where it was measured and this did not occur. The extreme under-predictions for the modified SWAT are caused due to an incorrect soil water balance. Water is not held in the profile long enough to raise the storage to saturation, even with the slower movement due to Darcy's and the Buckingham-Darcy based algorithms.

2.4.1.3 W20, W10, and W5 Tile Flow

The eastern tiles were not modeled due to issues found in the previous DRAINMOD study (Wang et al., 2006) and belief the forested area to the east of the field caused alterations in subsurface hydrology.

The variation not only in calibration results, but the performance for the calibration and validation periods for the three different spacings emphasize the importance of drain spacing for drain flow prediction. The addition of more physically based equations caused modified SWAT to catch more tile drainage peaks (example: late-January) that the original SWAT did not predict (Figure 2.10). Tile flow in modified SWAT did not have extended lags as the original SWAT modeled (example: early-January, early-February, and early-April). The modified SWAT not only predicted the duration of the drainage event more accurately, but also the magnitude of the peak drain flow better (example: early-February, early-April). The modified SWAT also predicted short time periods with frequent peaks more accurately than the original SWAT (example: late-December).

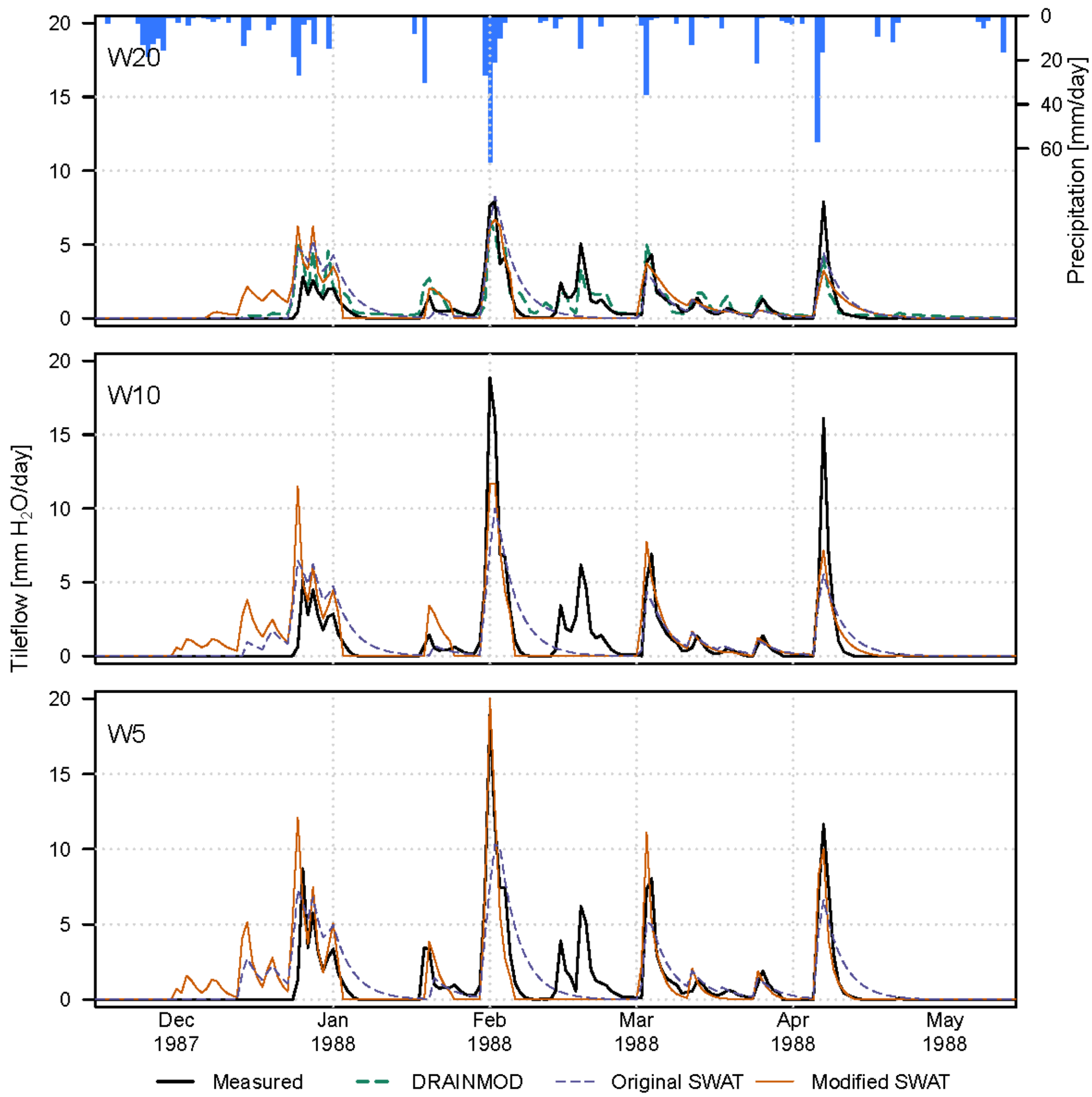

Figure 2.10 Predicted and Observed Tile Flow from W20, W10, and W5

W5 had the worst overall statistical performance of all three tile spacings, this was also found in the DRAINMOD study (Wang, et al., 2006). While the bias for all three spacings was very small for most of the calibration period, the drainage season from January to July of 1989 had the most under-prediction (Figure 2.11). A source of this larger bias could be due to W5's location in between W10 and W20 additional flow that is unaccounted for could flow in from other plots.

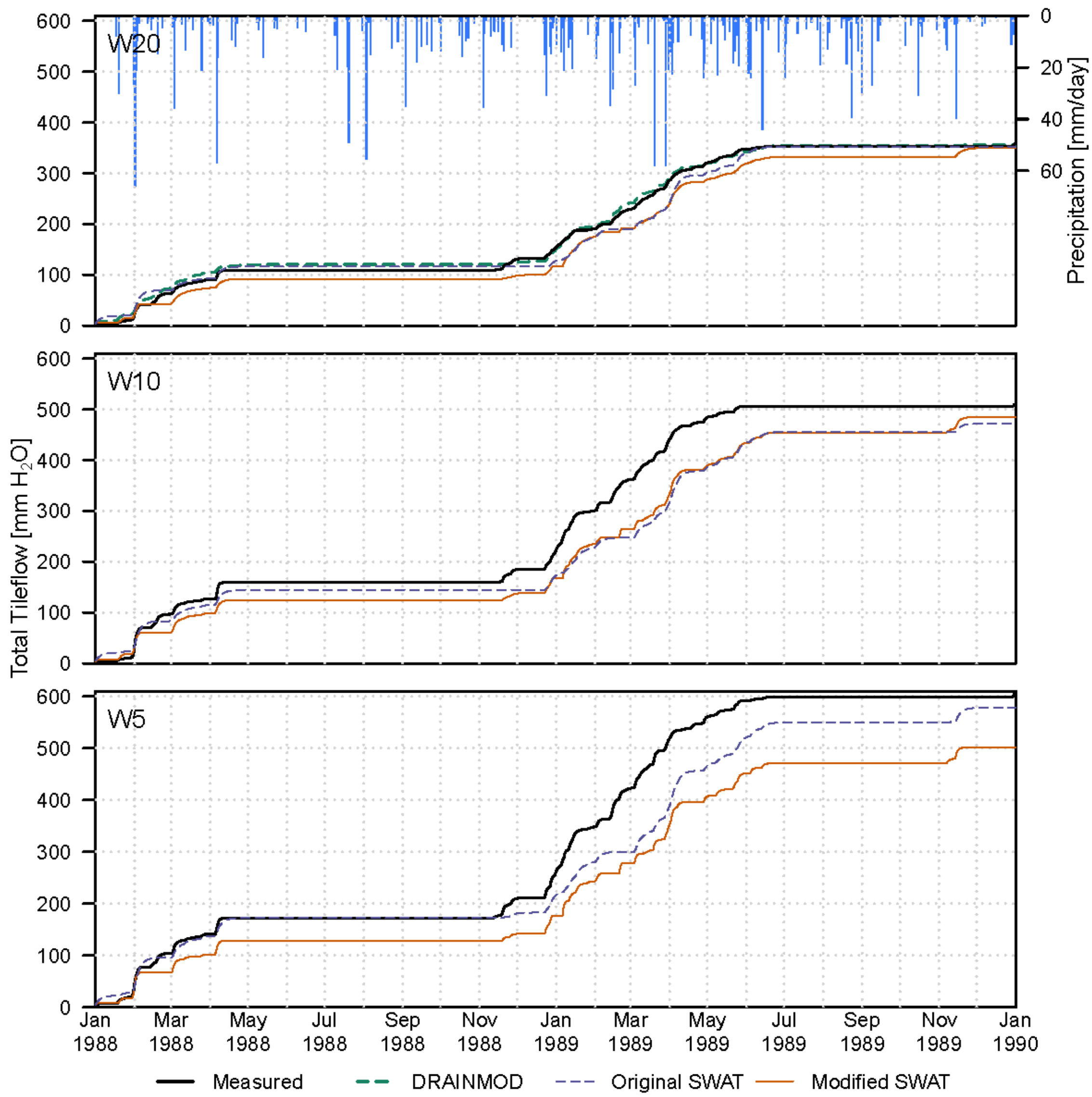

Figure 2.11 Cumulative Predicted and Observed Tile Flow from W20, W10, and W5 during the calibration period

The performance for the single tile flow models were satisfactory. The spacings, while effecting the patterns of tile flow, did not cause a large reduction in SWAT performance although more over-predictions occurred as the tile spacings reduced in size. The results did show an improvement in tile drainage event predictions statistically and visually for modified SWAT. The addition of these physically based algorithms added more sensitivity to the drainage curves allowing for steeper declines after peak flow. The bias was very good throughout the study but, the end of the drainage season showed more under-predictions than the beginning of the season. This was caused by SWAT frequently predicting tile flow too early in year and simulating events that were not observed in the field.

2.4.1.4 W20 Tile Flow compared to DRAINMOD study

Wang, et al. (2006) reported evaluation statistics separately for the years with on-site rainfall (1985-1990 and 1997). These data allowed for more accurate predictions and when compared to performance by SWAT, DRAINMOD performed much better than both versions of SWAT and neither the modified nor original SWAT were clearly better performers on average (Table 2.13).

Table 2.13 W20 daily performance statistics for years with on-site rainfall data

	DRAINMOD		Original SWAT		Modified SWAT	
Year	NSE	PBIAS	NSE	PBIAS	NSE	PBIAS
1985	0.61	-23.7%	-0.01	26.0%	0.28	14.6%
1986	0.68	-20.9%	0.48	14.2%	0.31	19.6%
1987	0.64	2.9%	0.33	-12.7%	0.02	-1.5%
1988*	0.75	-2.7%	0.51	-16.5%	0.62	-23.1%
1989*	0.79	1.4%	0.15	9.7%	0.10	13.4%
1990	0.56	-19.3%	0.23	11.1%	0.47	-0.9%
1997	0.28	-17.6%	0.33	-49.6%	0.33	-51.6%

** Calibration years for tile flow*

Despite using the same Hooghoudt and Kirkham tile drainage equations in DRAINMOD and SWAT, vast differences are seen in the overall statistics as well as those separated by year. DRAINMOD calculates water table based on the wet and dry zones in the profile and the volume of air in the profile. The soil water characteristic data including the water table-volume drained relationship is an input in DRAINMOD as well. SWAT does not require as detailed data for inputs as it is a larger scale model, and so cannot calculate water table in this manner. These two different water table calculation approaches are the driving force behind the different tile flow results between DRAINMOD and SWAT.

2.4.2 Tile Nitrate

2.4.2.1 Calibration Results

For this study, the nitrate data was limited to 1989-1999. Due to this only the second year of the original two years of calibration for tile flow was used when calibrating nitrate (1989) and the remaining years were used for validation (1990-1999), and calibration was performed for both versions of SWAT again to ensure the best performance of both could be compared (Table 2.14).

Table 2.14 Tile Nitrate Calibration Values Parameters for both versions of SWAT

Model	Version	NPERCO	SDNCO
All	Uncalibrated Value	0.2	1.1
W20	Original SWAT	0.01	1.1
	Modified SWAT	0.01	1.5
W10	Original SWAT	0.01	1.1
	Modified SWAT	0.01	1.5
W5	Original SWAT	0.01	1.1
	Modified SWAT	0.01	1.5

CMN and CDN were not sensitive for both versions of SWAT and so the default values were used. NPERCO had the same calibration value throughout, an expected result as the nitrogen algorithms were not altered in this study. Each version of SWAT consistently used the same SDNCO value for each model. This is due to SDNCO's definition to be a percent of field capacity which would change between these two model versions. Although the best performance had very similar parameters for each model and version, the performance for the modified SWAT was extremely poor when compared to the original SWAT (Table 2.15)

Table 2.15 Nitrate calibration and validation statistics for both versions of SWAT

Model	Version	Time Period	NSE	PBIAS
W20	Original SWAT	Calibration (1989)	0.25	-34.2%
		Validation (1990-1999)	-0.20	-29.5%
	Modified SWAT	Calibration (1989)	-0.07	-85.8%
		Validation (1990-1999)	-0.02	-82.4%
W10	Original SWAT	Calibration (1989)	0.08	-13.3%
		Validation (1990-1999)	-0.27	5.4%
	Modified SWAT	Calibration (1989)	-0.04	-80.3%
		Validation (1990-1999)	-0.09	-69.2%
W5	Original SWAT	Calibration (1989)	-0.11	-6.4%
		Validation (1990-1999)	-0.10	-5.4%
	Modified SWAT	Calibration (1989)	-0.06	-75.1%
		Validation (1990-1999)	-0.10	-67.6%

The only NSE value over 0 was for the original SWAT calibration period in W20. The NSE values were extremely similar for the other calibration and validation sets. The modified SWAT regularly had at least a doubled PBIAS under-prediction.

2.4.2.2 W20, W10, and W5 Tile Nitrate

The alterations of the tile drainage subroutines reduced the performance of the nitrate tile outputs by reducing the amount of nitrate predicted. The original and modified SWAT routines both under-predicted and even missed many peaks (Figure 2.12). At the peak nitrate loads, the modified SWAT under-predicted the nitrate peak loads much more than the original SWAT (example: early-February and early-April). Both versions of SWAT showed high peaks shortly after fertilization application (example: late-May and June).

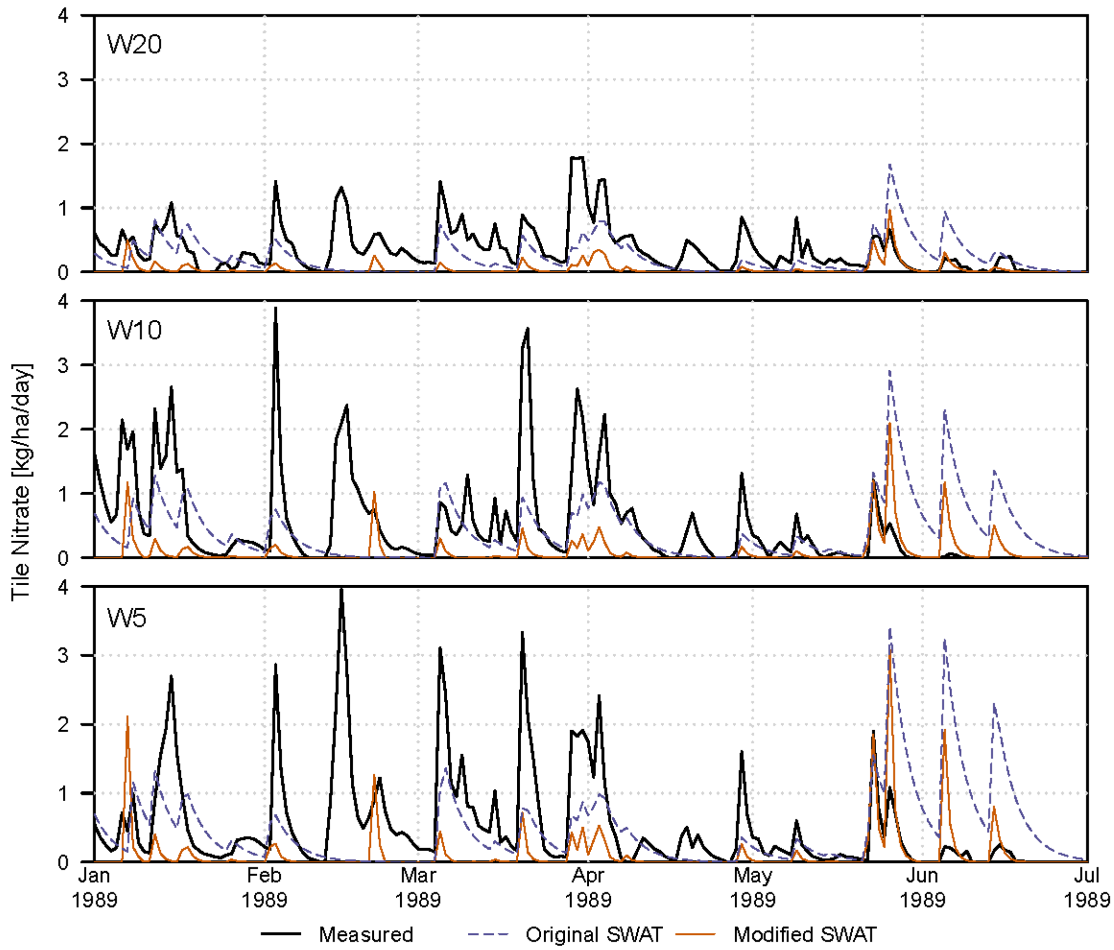

Figure 2.12 Predicted and Observed Tile Nitrate Load from W20, W10, and W5

SWAT's poor nitrate response is primarily a function of concentration. The concentration in the measured samples ranged from 0 to over 100 mg/l, while predicted contractions ranged from 0 to 93 mg/l in the original SWAT and 0 to 49 mg/l in the modified SWAT. Both versions of SWAT showed high peaks shortly after fertilizer application (example:

late-May and June). The over estimation and too quick depletion of nitrogen after rainfall events has been observed previously (Hu et al., 2007). This quick release of nitrogen post application may be caused by how SWAT treats nitrogen in the soil. Denitrification occurs based on a calibration based exponential function using denitrification rate coefficient (CDN), the nutrient cycling temperature factor, nutrient cycling water factor, organic carbon, and threshold water content for denitrification (SDNCO). Three of these five factors can be altered by the user (CDN, SDNCO, and organic carbon). The temperature nutrient cycling factor is also based off an exponential fitted curve using only the soil layer's temperature as an input variable, and the water nutrient cycling factor is based off the current water content in the layer and field capacity. The combination of these fitted parameters and exponential equations creates a relationship where a slight change in temperature can double the amount of nitrogen that is denitrified if the water balance is high enough.

2.4.3 Yield Comparison

While no alterations were made to the crop growth algorithms, there was a concern the alterations of the soil profile, by cutting off the depth at the restrictive layer could potentially have a negative effect on yield predictions. SWAT consistently over-predicted corn yield and under-predicted soybean yield across both versions and all tile spacings when compared to the measured yield (Table 2.16). When modified and original SWAT to each other on average, the corn yields varied by 0.03 Mg/ha and the soybean yields varied by 0.02 Mg/ha.

Table 2.16 Measured and SWAT simulated Yield for Corn and Soybean (units: Mg/ha)

Model	Version	Corn	Soybean
W20	Measured	9.35	3.93
	Original SWAT	10.49	2.39
	Modified SWAT	10.68	2.39
W10	Measured	9.36	3.77
	Original SWAT	12.01	2.39
	Modified SWAT	11.50	2.44
W5	Measured	9.38	3.93
	Original SWAT	11.07	2.39
	Modified SWAT	11.48	2.39

These small variations in yield between SWAT models is most likely caused by the alterations in soil water balance. The crop growth is effected by nitrogen only when the crop experiences nitrogen stress, something that did not happen for either version of SWAT. Despite the poor nitrate predictions from the tiles, SWAT still is able to predict corn yield within 20% on average although soybean yield is under-predicted by 40% on average for the three years of data. The tile drainage volume and drainage pattern do not matter significantly to SWAT yield predictions, as long as the plant available water is within acceptable ranges (i.e. no drought stress or water-logged stress). This small yield change is one of the potential unintended consequences of the modifications made to improve subsurface hydrology.

2.5 Conclusion

The modified SWAT algorithms provide a more physically based approach to calculate tile drainage and removes the empirical basis for the previous versions, although more work is needed. Correctly predicting the water table and soil water processes is critical for realistic simulation of tile drain flow. Most previous studies have predicted flow at the outlet, and did not look at individual tiles, let alone water table. Percolation through the soil profile was redefined based on Darcy's and the Buckingham-Darcy Law instead of an empirical S-Curve. The restrictive layer depth (DEP_IMP) was redefined to be a physical parameter so that the actual depth can be used and seepage was rewritten to be based off percolation and limited by a user-supplied conductivity (KSAT_IMP) instead of being based on another S-Curve. The water table was redefined as an approximate proportion instead of a change calculated by the change in stored water and another calibrated parameter. Tile flow is no longer delayed using an S-Curve defined by a coefficient based off the calibration parameter GDRAIN, but is only limited by the physical parameter drainage coefficient (DRAIN_CO).

Fifteen subroutines had to be modified to achieve these changes. The modified version of SWAT improved the prediction of daily tile flow, as it successfully predicted more peaks and did not underestimate the smaller peaks compared with the original SWAT. The overall shape of the drainage events also improved with the addition of more physically based equations. The modified SWAT did reduce nitrate performance by causing more under-predictions and missing peaks due to the changes in tile flow as well as a reduction in nitrate concentration in the flow due to the soil water balance changes.

2.6 Bibliography

Boles, C. M. W., Frankenberger, J. R., & Moriasi, D. N. (2015). Tile Drainage Simulation in SWAT2012: Parameterization and Evaluation in an Indiana Watershed. *Transactions of the ASABE*, *58*(5), 1201–1213.

Brooks, R. H., & Corey, A. T. (1964). Hydraulic properties of porous media. *Hydrology Papers No. 3*.

Buckingham, E. (1907). *Studies on the movement of soil moisture*. *Bull. 38*. Washington, DC.

Darcy, H. (1856). De`termination des lois d'e` coulement de l'eau a` travers le sable. In *Les Fontaines Publiques de la Ville de Dijon* (pp. 590–594). Victor Dalmont, Paris.

Du, B., Arnold, J. G., Saleh, A., & Jaynes, D. B. (2005). Development and application of SWAT to landscapes with tiles and potholes. *Transactions of the ASAE*, *48*(3), 1121–1133.

Gesch, D. B. (2007). The National Elevation Dataset. In *Digital Elevation Model Technologies and Applications: The DEM User's Manual* (2nd ed., pp. 99–118). Bethesda, Maryland: American Society for Photogrammetry and Remote Sensing.

Gesch, D. B., Oimoen, M., Greenlee, S., Nelson, C., Steuck, M., & Tyler, D. (2002). The National Elevation Dataset: Photogrammetric Engineering and Remote Sensing.

Green, C. H., Tomer, M. D., Di Luzio, M., & Arnold, J. G. (2006). Hdrologic Evaluation of the Soil and Water Assessment Tool for a Large Tile-Drained Watershed in Iowa. *Transactions of the ASABE*, *49*(2), 413–422.

Hooghoudt, S. B. (1940). Bijdragen tot de kennis van eenige natuurkundige grootheden van den grond. No. 7. Algemeene beschouwing van het probleem van de detailontwatering en de infiltratie door middel van parallel loopende drains, greppels, slooten en kanalen. *Verslagen van Landbouwkundige Onderzoekingen*, *46*(14), 515–707.

Hu, X., McIsaac, G. F., David, M. B., & Louwers, C. A. L. (2007). Modeling Riverine Nitrate Export from an East-Central Illinois Watershed Using SWAT. *Journal of Environmental Quality*, 36(4), 996–1005.

Kladivko, E. J., Frankenberger, J. R., Jaynes, D. B., Meek, D. W., Jenkinson, B. J., & Fausey, N. R. (2004). Nitrate leaching to subsurface drains as affected by drain spacing and changes in crop production system. *Journal of Environmental Quality*, *33*(5), 1803–1813.

Kladivko, E. J., Grochulska, J., Turco, R. F., van Scoyoc, G. E., & Eigel, J. D. (1999). Pesticide and Nitrate Transport into Subsurface Tile Drains of Different Spacings. *Journal of Environmental Quality*, *28*(3), 997.

Kladivko, E. J., van Scoyoc, G. E., Monke, E. J., Oates, K. M., & Pask, W. (1991). Pesticide and nutrient movement into subsurface tile drains on a silt loam soil in Indiana. *Journal of Environmental Quality*, *20*, 264–270.

Kladivko, E. J., Willoughby, G. L., & Santini, J. B. (2005). Corn Growth and Yield Response to Subsurface Drain Spacing on Clermont Silt Loam Soil. *Agronomy Journal*, *97*(5), 1419.

Larney, F. J., Kladivko, E. J., & Monke, E. J. (1988). Subsurface Drain Spacing Effects on Soil Moisture Regime of Clermont Silt Loam. *Transactions of the ASAE*, 1128–1134.

Moriasi, D. N., Arnold, J. G., Vazquez-Amabile, G. G., & Engel, B. A. (2011). Shallow Water Table Depth Algorithm in SWAT: Recent Develpoments. *Transactions of the ASABE*, *54*(5), 1705–1711.

Nash, J. E., & Sutcliffe, J. V. (1970). River Flow Forecasting Through Conceptual Models Part I - A Discussion of Principles. *Journal of Hydrology*, *10*, 282–290.

Negm, L. M., Youssef, M. A., Skaggs, R. W., Chescheir, G. M., & Kladivko, E. J. (2014). DRAINMOD-DSSAT Simulation of the Hydrology , Nitrogen Dynamics , and Plant Growth of a Drained Corn Field in Indiana. *Journal of Irrigation and Drainage Engineering*, *140*, 1–12.

Larney, F. J., Kladivko, E. J., Monke, E. J., & Mannering, J. V. (1989). Corn Growth and Yield Behavior with Distance from Subsurface Drains in Drier-Than-Normal Growing Seasons. *Transactions of the ASAE*, *32*(2), 579–587.

Maidment, D. R. (1993). *Handbook of Hydrology*. New York, NY: McGraw-Hill, Inc.

Moriasi, D. N., Arnold, J. G., Van Liew, M. W., Binger, R. L., Harmel, R. D., & Veith, T. L. (2007). Model evaluation guidelines for systematic quantification of accuracy in watershed simulations. *Transactions of the ASABE*, *50*(3), 885–900.

Neitsch, S. L., Arnold, J. G., Kiniry, J. R., & Williams, J. R. (2011). *Soil & Water Assessment Tool Theoretical Documentation*. College Station, TX: Texas Water Resources Institute.

Rawls, W. J., & Brakensiek, D. L. (1985). Prediction of Soil Water Properties for Hydrologic Modeling. In E. B. Jones & T. J. Ward (Eds.), *Watershed Management in the Eighties* (pp. 293–299). Denver, CO: American Society of Civil Engineers.

Rutkowski, S. (2012). *Role of Climate Variability on Subsurface Drainage and Streamflow in Agricultural Watersheds*. Purdue University.

Skaggs, R. W. (1978). *A water management model for shallow water table soils*. *Water Resources Research Institute of the University of North Carolina* (Vol. 134).

Sui, Y., & Frankenberger, J. R. (2008). Nitrate Loss From Subsurface Drains in an Agricultural Watershed Using Swat2005. *Transactions of the ASABE*, *51*(4), 1263–1272.

USDA National Agricultural Statistics Service. (1997). Usual Planting and Harvesting Dates for U.S. Field Crops. In *Agricultural Handbook Number 628* (pp. 23–24).

USDA-NRCS Soil Survey Staff. (2014). Soil Survey Geographic (SSURGO) Database. Retrieved September 15, 2014, from http://sdmdataaccess.nrcs.usda.gov/

Wang, X., Mosley, C. T., Frankenberger, J. R., & Kladivko, E. J. (2006). Subsurface drain flow and crop yield predictions for different drain spacings using DRAINMOD. *Agricultural Water Management*, *79*, 113–136.

Winters, E., & Simonson, R. W. (1951). The Subsoil. In *Advances In Agronomy* (Vol. 3, pp. 1–92).

Youssef, M. A., Skaggs, R. W., Chescheir, G. M., & Gilliam, J. W. (2006). Field Evaluation of a Model for Predicting Nitrogen Losses from Drained Lands. *Journal of Environmental Quality*, *35*(6), 2026–2042.

CHAPTER 3. EVALUATION OF SWAT MODEL SIMULATIONS OF FLOW AND NUTRIENTS FROM TILE DRAINS IN A SMALL WATERSHED IN OHIO

3.1 Introduction

In order to manage water within poorly-drained agricultural fields, subsurface tile drains are a standard practice. This practice has become so widely used that it has been found to control 40-70% of flow leaving the watershed in Iowa (Green et al., 2006) and Ohio (King et al., 2014). As a result, tile drain flow is also a major source of nutrient losses that cause downstream environmental problems (Skaggs et al., 1994). Simulation models are needed to predict these losses and assess solutions.

One watershed-scale model that simulates subsurface drainage outflow is the Soil and Water Assessment Tool (SWAT) (Arnold et al., 1998). The model divides watersheds into hydrologic response units (HRUs) with common soil type, land use, slope class, and subbasin, and tile drainage can be simulated in each or a subset of every HRU in the watershed modeled.

As explained in Chapter 2, four changes have been made to SWAT in order to improve current tile drainage simulations and add more physical basis to the algorithms. First, the restrictive layer usage was changed to remove the dependence of seepage to the aquifer on the restrictive layer depth by adding the hydraulic conductivity of the restrictive layer as a new input. Also, the soil profile depth was limited to the depth of the restrictive layer as water that goes past the restrictive layer is not considered in the water table balance. Second, percolation through the soil profile was modified to calculate a flow rate based on Darcy's and the Buckingham-Darcy laws instead of an algorithm allowing a set percentage of excess water through the profile independent of the current soil-water balance. Third, the water table depth algorithm was simplified, placing the water table within the lowest unsaturated layer rather than the complex, site-specific equation based on change in water storage of each layer for each day as developed by Moriasi et al (2007a). Fourth, the tile drainage delay based on the calibration parameter GDRAIN was removed, as the drainage coefficient limits the drainage each day. In this chapter, SWAT version 638 is referred to as “original” and the version with these four modifications is referred to as “modified”.

USDA-ARS has monitored a small watershed in central Ohio since 2005, which provides an opportunity to test the algorithms. The watershed, denoted as “Watershed B”, measures 3.8 km^2 in area and is located within the Upper Big Walnut Creek Watershed (Figure 3.1). Monitoring at the watershed outlet and six tile drain outlets was designed to assess watershed conservation practices (King et al., 2008), and data have been published in a series of papers (King et al., 2008, 2014, 2015, 2016; Williams et al., 2015a, 2015b).

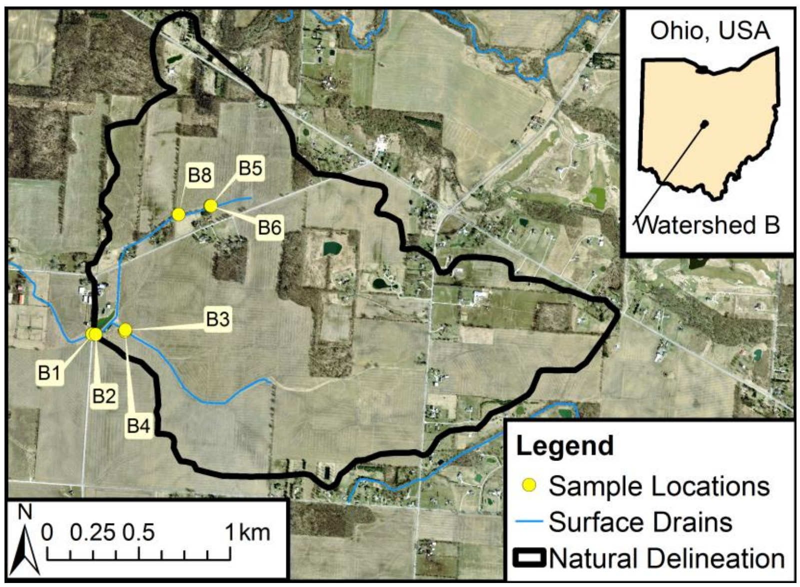

Figure 3.1 Watershed B Location and Sampling Spots

Seven years of monitoring data have quantified the importance of tile drains in watershed hydrology in this watershed. Tile drains contribute 47% of streamflow (King et al., 2014), 56% of the nitrogen (Williams et al., 2015a), and 40% of the total phosphorus losses (King et al., 2015). This rich dataset, including detailed data at all active tile drain outlets plus the watershed outlet, provides a unique opportunity to test tile drain and watershed SWAT outputs.

The objective of this chapter is to simulate each drain tile as well as the entire Watershed B using SWAT, in order to (1) compare outputs from the original SWAT to the modified version developed in Chapter 2, (2) understand the sensitivity of the new algorithms in simulating tile drainage, and (3) gain greater insight into SWAT simulation of tile drains.

3.2 Site Description and Model Set Up

The part of the Midwestern United States where Watershed B is located has a humid climate with hot summers allowing for 160 growing days from late April to mid-October (King et al., 2015). The 30-year precipitation average (1981-2010) is 993 mm/yr with most snow occurring from December to March (NOAA National Climatic Data Center, 2015).

Elevation in Watershed B varies from 313 to 330 m with an average slope of 1.49%. The two major soil types are Bennington silt loam (54%) and Pewamo silty clay loam (45%). The land use is 71% agriculture, 24% farmstead or residential, and 5% woodland. The agricultural area is dominated by corn-soybean rotations, and approximately 89% is systematically tile drained as described below. Two surface drains flow through Watershed B, providing a connection with the six tile outlets within the watershed.

The watershed was monitored at seven locations from 2005 to 2012 (Figure 3.1). Daily values provided by the USDA-ARS and used in this study are: flow, NO_3-N, soluble reactive phosphorus, and total phosphorus. A detailed description of the instrumentation, sampling techniques, and other water quality parameters measured can be found in King et al. (2015).

3.2.1 Watershed Discretization

ArcSWAT 2012.10_2.15 within ArcGIS 10.2.2 was used to initially set up the model. In order to evaluate the tile drain outflow, each tile drained area was modeled as a separate subbasin. A delineation of this watershed based only on topography was provided by the USDA-ARS and encompasses 3.8 km^2. However, the tile drainage pattern within fields can change flow direction and therefore a more precise determination was made of the area flowing into each drain outlet as described below, and a predefined watershed delineation was used with each tiled outlet as a subbasin.

The field area draining into each tile outlet was estimated using a combination of sources, including maps provided by King et al. (2016), aerial imagery, 14 historical tile map plans (one of which is shown as an example in Figure 3.2), the location of the main drains obtained from the Delaware County Ohio Soil and Water Conservation District, and an area estimation based on total flow (Table 3.1). The locations for which tiles maps are available are shown in Figure 3.3. The area estimation based on total flow was determined by taking the average of annual flow of each subbasin and multiplying it by a known ratio of flow to area to approximate the area contributing to the subbasin area (“Flow based estimation” column in

Table 3.1). This known ratio was calculated by dividing the previously published delineations of watersheds B2, B4, and B8 by their average annual flow and taking the average of the three subbasins to approximate the area per flow. Outlets B3 and B6 were more uncertain and the following paragraphs describe how the delineations were finalized.

- B3 is the largest and contains the most uncertainty in its delineation. The easternmost tile map shows tiles possibly going to a different main, the diagonal ditch just south of the watershed, but the field was still all considered to drain into B3 since the main still could travel to the ditch within the watershed and there was no tile maps or other data to definitively say otherwise. For the southwest section, the original watershed delineation was used as the field boundary since the tile drain map available shows tiles draining south as well as north towards B3.
- B6 includes a main that goes underneath the road north of the region to allow it to drain to the sampling site north of the road (King, personal communication). The tile map includes area south of that field which is no longer agricultural land and so not included in the tile maps. The southern end of the tile map in the area appears to drain south but aerial imagery shows a consistent drain system, which could mean the tile drain map, is out of date. The central area in between the two southern regions that do drain into B6 might have been previously agricultural and therefore tiled but with no tile maps this cannot be confirmed and so was not included.

Even with the effort invested in this analysis, there are likely errors. If all areas had similar hydrologic behavior, the total annual flow should be proportional to area. This was not the case for Watershed B where large variation was seen between the flow estimations and the delineations by King et al. (2015) as well as the final delineation in this study. The tile map plans may not have been accurate as changes are known to occur during installation. These changes could be the direction of the drain itself, the direction of flow, etc. Even with exact final drainage maps, determining the subsurface hydrology would not be perfect as many other factors can effect subsurface hydrology.

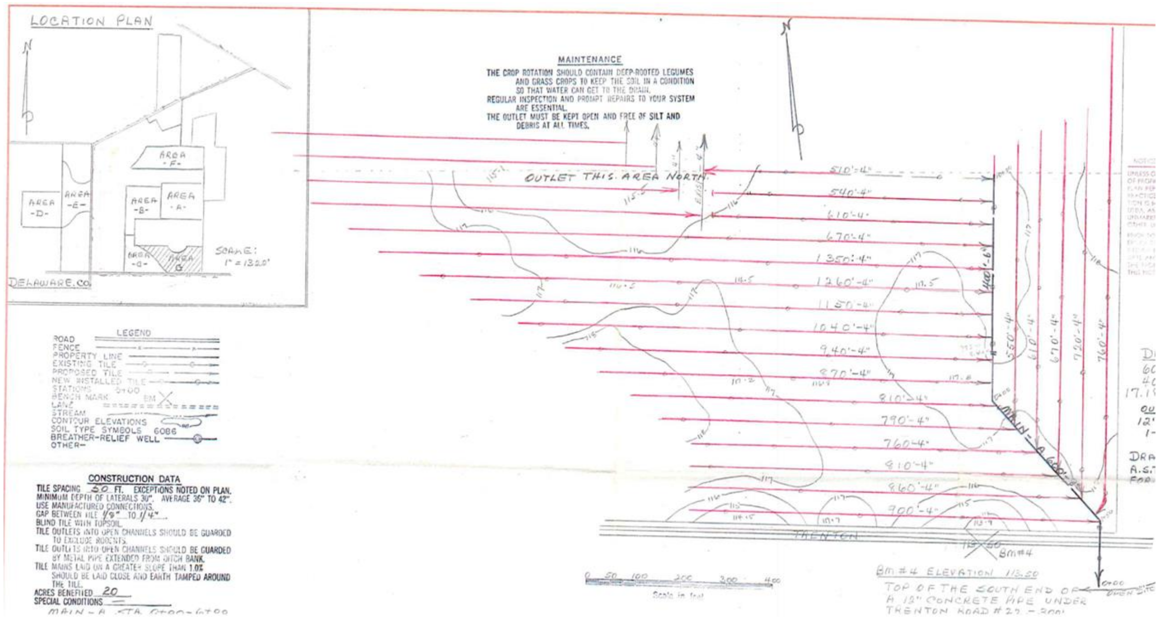

Figure 3.2 Example Historical Tile Drain Map, which provided information used in determining tile flow direction

Table 3.1 Tiled field subbasin areas and source data

Outlet	Sources	Subwatershed Area Estimation: [ha]		
		King et al. (2015)	Flow Based Estimation	Final Area Delineated
B2	King et al. (2016), Orthoimagery	14	9	14
B3	Orthoimagery, Tile Maps (9)	212	146	161
B4	King et al. (2016), Orthoimagery, Tile Maps (1)	15	11	15
B5	Orthoimagery, Tile Maps (2)	22	41	24
B6	Orthoimagery, Tile Maps (3)	49	34	34
B8	King et al. (2016), Orthoimagery, Tile Maps (1)	7	12	9

After the additional area surrounding the watershed that drained into the watershed was added, the estimated watershed area increased to 4.1 km^2 from the 3.8 km^2 topography-based delineation. The tile-drained subbasins comprise 2.6 km^2 of the total watershed, leaving 1.5 km^2 of area in the watershed undrained (Figure 3.3).

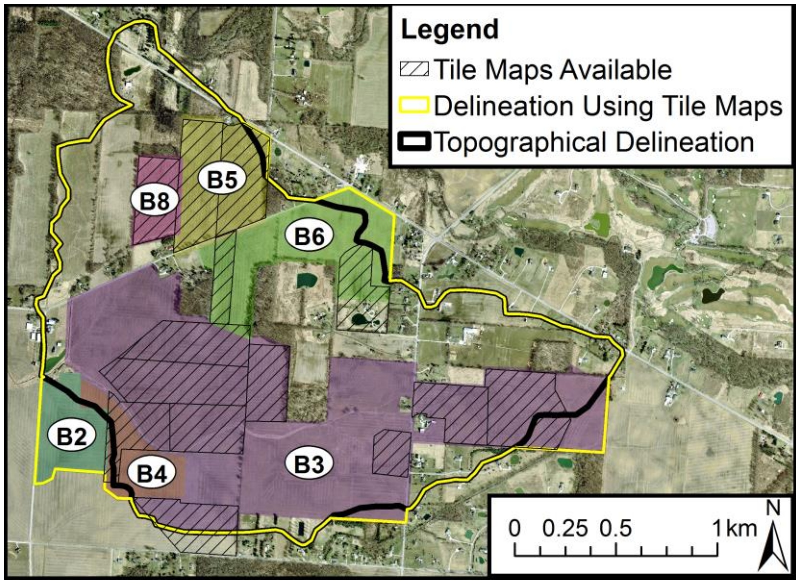

Figure 3.3 Subbasins for each tile drain outlet (colored areas), watershed delineations, and area with available tile maps

3.2.2 Management Practices

A single set of management practices were used for each subbasin, even though multiple fields were within some of the subbasins. Management practices were determined using data from King et al. (2015, 2016) and a management database provided by the USDA-ARS for the watershed. Management data was only collected 2003-2008, so for the additional years the same crop rotation was continued from the years with data. Dates were approximated for all management practices done in those years, including planting, harvest, fertilizer, and tillage when applicable.

Fertilizer data was converted to elemental rates in order to compare the rates when producers used different fertilizer types. Because SWAT does not treat mineral fertilizer types differently, converting all rates to their elemental rates did not alter model performance. To simulate manure addition for which the nutrient content was available, a new entry was made to the fertilizer database with 90% of N in the organic form, and all of the inorganic form (10% of total) as ammonia, following the proportions provided by (Kellogg & Moffitt, 2011). The tillage practice post-chicken manure application was simulated as shallow chisel, based on information provided in King et al. (2015). No pesticide applications were simulated. Management for each subwatershed was determined as follows:

- B2 and B4 were combined by King et al. (2016) to a single management strategy and are also listed as the same tract number according to the database and so were simulated with the same management strategy. The management for 2004-2012 was listed explicitly in King et al. (2016) and was used exactly.
- B3 includes seven different fields with management data for the years 2003-2009, which were consolidated to a single management scheme. In order to determine the primary crop for each year of the simulation, a weighted average by field area was used. Management was based on an area weighted average of fields that planted that crop. In 2004, one field listed a chicken manure application twice in a single month, this was considered an error and the average date was used for the whole outlet calculations.
- B5 and B8 are part of the same field, according to tract numbers, and were modeled with the same management practices. King et al. (2016) included management practices and rotations from 2004 to 2012 for B8. This rotation was used for both of these fields.
- B6 had four fields within its boundaries which were then consolidated to a single management strategy. One of the smaller fields had only a single year of data and so was not used when determining rotation. The same weighted average method was used to determine outlet B6's strategy as was used for outlet B3. For the chicken manure application in late 2006, only half the actual rate was simulated as approximately half the field data indicated a manure application occurred.

The resulting management operation schedules are shown in Table 3.2.

Table 3.2 Management strategies used for agricultural areas in the SWAT model, combining individual fields in the subbasin where appropriate

		B2 & B4		B3		B5 & B8		B6	
2005	Tillage			4/16	Minimum*				
	Plant	5/7	Soybean	4/16	Corn	5/7	Soybean	5/4	Soybean
	Fertilizer			4/18	23.5 N				
					32.2 P				
	Fertilizer			6/7	153.1 N				
	Harvest	10/5		10/25		10/5		10/2	
2006	Tillage	4/30	Chisel			5/11	Chisel	4/30	Finisher**
	Fertilizer	5/1	32.1 N	3/28	20.2 N	5/11	82.1 N	4/30	32.6 N
			48.7 P		22.5 P		48.7 P		48.4 P
	Plant	5/1	Corn	4/29	Soybean	5/11	Corn	4/30	Corn
	Fertilizer	6/20	167.3 N			6/12	167.3 N	6/20	167.4 N
	Manure							10/16	228.0 N
									58.7 P
	Tillage							10/17	Chisel
	Harvest	10/27		10/10		11/10		11/10	
2007	Fertilizer			4/16	20.2 N				
					22.5 P				
	Plant	5/9	Soybean	5/6	Soybean	5/7	Soybean	5/9	Soybean
	Harvest	10/10		10/1		10/2		10/10	
	Manure	10/16	456.1 N			10/5	456.1 N		
			117.4 P				117.4 P		
	Tillage	10/17	Chisel			10/6	Chisel		
2008	Tillage					4/21	Chisel	5/1	Finisher
	Fertilizer			4/14	20.2 N	4/21	46.7 N	5/1	46.6 N
					22.5 P		19.5 P		19.4 P
	Plant	5/7	Soybean	5/4	Soybean	4/21	Corn	5/1	Corn
	Fertilizer					6/4	167.3 N	6/7	167.4 N
	Harvest	10/2		10/5		9/29		10/6	
2009	Tillage	5/17	Chisel						
	Fertilizer	5/18	32.1 N	4/19	20.2 N				
			48.7 P		22.5 P				
	Plant	5/18	Corn	5/13	Soybean	5/26	Soybean	5/26	Soybean
	Harvest	11/2		10/27		10/19		10/19	

Table 3.2 continued.

		B2 & B4		**B3**		**B5 & B8**		**B6**	
2010	Tillage			4/30	Minimum*	4/30	Chisel		
	Fertilizer			4/30	23.5 N	4/30	64.4 N		
					32.2 P		34.1 P		
	Plant	5/10	Soybean	4/30	Corn	4/30	Corn	5/10	Soybean
	Harvest	10/4		10/11		10/11		10/4	
2011	Tillage	6/5	Chisel						
	Fertilizer	6/6	32.1 N						
			48.7 P						
	Plant	6/6	Corn	6/6	Soybean	6/6	Soybean	6/6	Soybean
	Harvest	11/11		11/5		11/5		11/5	
2012	Tillage			5/12	Minimum*	5/12	Chisel		
	Fertilizer			5/12	23.5 N	5/12	64.4 N		
					32.2 P		34.1 P		
	Plant	5/14	Soybean	5/12	Corn	5/12	Corn	5/14	Soybean
	Harvest	10/15		11/8		11/8		10/15	

Note: Fertilizer and Manure units in terms of kg / ha
** Minimum tillage simulated as “Generic Conservation Tillage” in SWAT*
*** Finisher tillage simulated as “Soil Finisher” in SWAT*

For the untiled agricultural fields, a rotation of planting, auto-fertilization, and harvest was simulated each year. Auto-fertilization is a process created in SWAT that applies nitrogen when the plant reaches a nitrogen stress threshold. This automatic management strategy was considered acceptable as the untiled areas were not the main target of this study and were not calibrated. This approach should lead to comparable error from untiled areas for both versions of SWAT when analyzing the total stream flow, nitrate, and phosphorus results.

3.2.3 Geospatial Input Data

All data were projected in North American Datum 1983 State Plane Ohio North FIPS 341 Feet. Five main geospatial inputs are used in SWAT: elevation, subbasin delineation (when automatic delineation by ArcSWAT is not used), stream pathway, land use, and soil type.

The 3-m resolution National Elevation Dataset (Gesch, 2007; Gesch et al., 2002) was used. The 2.5-ft resolution Ohio Statewide Imagery Program I (OSIP-I) (Ohio Geographically Referenced Information Program, 2006) was also examined as it had a higher resolution and was more recent, but calculated slopes were unrealistically high within the watershed.

For watershed streams, a GIS dataset called “Historical County Drainage” provided by the Delaware Soil and Water Conservation District (2009) was used, which included both surface and subsurface drainage. All surface, or “open” streams were initially selected, but after a visit to the watershed, it appeared that the “stream” upstream from the sampling sites shown by the county drainage map was more like a grassed waterway, and the stream layer was clipped to reflect the in-person observation. Because each subbasin requires a stream in SWAT, small “streams” were manually added to connect each sampling sites to the stream.

Land use followed a file provided by the USDA-ARS indicating three classes: wooded, urban, and agriculture. The additional area added by the tile fields, as well as untiled agricultural land were added onto the agricultural land and simulated as Agricultural Land-Row Crops. The farmstead and residential area was simulated as Residential-Low Density, and the wooded area was simulated as Forest-Deciduous.

SSURGO 2.0 data was used for the soil input (USDA-NRCS Soil Survey Staff, 2014). Three soil series containing a total of four different soils are within watershed B, ranging from very poorly drained to a small percentage of moderately well drained with varying soil properties (Table 3.3).

Table 3.3 Drainage parameters for soils in Watershed B (data aquired from USDA-NRCS Soil Survey Staff (2014))

Soil Series	Drainage Class	Texture	Permeability	MUKEY	Area [km^2]
Bennington	Somewhat poorly drained	Silt loam	Slow	172038 172039	2.1 0.15
Centerburg	Moderately well drained	Silt loam	Moderately slow	172044	0.04
Pewamo	Very poorly drained	Silty clay loam	Moderately slow	172077	1.82

3.2.4 Weather Data

Precipitation data was monitored on site by the USDA-ARS from 2005 to 2012 (King et al., 2008). Precipitation for a five year warm-up period, and temperature data for the entire duration, were from the Climate Forecast System (Saha et al., 2014) and acquired using the SWAT Global Weather Data website (http://globalweather.tamu.edu/). Relative humidity, solar radiation, and wind speed were simulated using SWAT from the WGEN_US_First Order Monthly Weather Database in the ArcSWAT interface.

3.2.5 Tile Drain Parameters

For the original SWAT, the SWAT2005 drainage routine was selected by setting ITDRN to 1, and the SWAT2012-revised water table routines was by setting IWTDN to 1. Tile drainage specific parameters shown in Table 3.4 were also added prior to calibration In addition the restrictive layer depth for the untiled areas was set at 3,000 mm as recommended by Boles et al. (2015). Tile drain depth and spacing were based on site specific values from King et al. (2015), while effective radius was determined from Skaggs (1980) using the 0.2 m field tile diameter reported by King et al. (2015). The maximum surface storage was estimated to be 10 mm.

Table 3.4 Drainage Subroutine Parameters

Variable	Description	Input File	Value
DDRAIN	Depth from surface to tile drains	*.mgt	900 mm
SDRAIN	Spacing between tile drains	*.sdr	15000 mm
RE	Effective radius	*.sdr	5 mm
SSTMAXD	Maximum surface storage	*.sdr	10 mm
DRAIN_CO	Drainage coefficient	*.sdr	10 mm/day

3.2.6 Model Simulations

In ArcSWAT, the pre-defined watershed option was used in order to supply SWAT with subbasin and stream files as an alternative to using the automatic delineation more frequently used when setting up the SWAT model. Hydrologic response units (HRUs) were defined with only one slope class and a 1% threshold for soil and land use. The model was run for thirteen years (2000-2012) including five years of warm up (2000-2004) before reaching years with output. Tile flow was calibrated 2005-2008 and validated 2009-2012. Due to the nitrate management availability, nitrate was calibrated 2005-2006 and validated 2007-2008. Phosphorus was assessed only during 2005-2008 as well. Once the input tables were written and management practices added, all changes were done manually or using R scripts.

3.3 Model Calibration and Parameter Sensitivity

Calibration was kept to a minimum (four hydrology and three nitrogen parameters) to focus on the effect of the modified algorithms rather than curve fitting. The sensitivity of the modified algorithms to these seven parameters was explored graphically.

3.3.1 Parameter Choice and Range

Four parameters related to tile drain flow were calibrated (Table 3.5). Curve number was reduced up to 50%. This level of reduction, although greater than in many other papers, is reasonable because tile drains, which have been documented to provide 47% of streamflow in this watershed (King et al., 2014) can only discharge water that has infiltrated. Curve number as a method for limiting infiltration is different than the original curve number conceptualization, which was developed to predict "direct runoff" or streamflow at a watershed scale, which may include channel runoff, surface runoff, and subsurface flow (Garen & Moore, 2005). To predict the observed tile drain flow, a much lower curve number was needed. The range for DEP_IMP was based on estimates by King (personal communication). KSAT_IMP was used as a calibration parameter only for modified SWAT, as the parameter does not exist in the original subroutines. While many studies vary LATKSATF between 1 and 4, a larger range was used to capture the drain flow patterns observed. Because the Kirkham equation was almost never used due to the water table rarely rising to the surface, a high lateral saturated conductivity was needed to capture the quick drain flow response in the measured data.

Table 3.5 Parameters Used in Tile Flow Calibration

Parameter	Definition	Input File	Range
CN2	SCS Curve Number (CN II)	*.mgt	-50 - +0% (by 5%)
DEP_IMP	Depth from surface to restrictive layer	*.hru	1500 - 2000 mm (by 100 mm)
KSAT_IMP	Hydraulic Conductivity of the restrictive layer (Modified SWAT only)	*.hru	0, 0.1, 0.25, 0.5, & 1 mm/hr
LATKSATF	Multiplication factor to determine saturated hydraulic conductivity from soil layer properties (unitless)	*.sdr	1 – 10 (by 1)

After tile drain flow was calibrated, the model was calibrated for tile nitrate using the same data collected by King et al. Initially, NPERCO, SDNCO, CDN, and CMN were used as calibration parameters (Table 3.6). Little change resulted from altering CMN (humus mineralization rate factor) leading to it being dropped from final calibration and the default 0.0003 value to be used.

Table 3.6 Parameters Used in Tile Nitrate Calibration

Parameter	Definition	Input File	Range
NPERCO	Nitrate Percolation Coefficient	*.bsn	0.01, 0.05 – 1.00 (by 0.05)
SDNCO	Denitrification Threshold Water Content	*.bsn	0.5 – 2 (by 0.1)
CDN	Denitrification Exponential Rate Coefficient	*.bsn	0 – 3 (by 0.25)

3.3.2 Performance Criteria

The model was calibrated for tile flow and nitrate using data collected by King et al. (2008) in 2005-2008 and evaluated using two different measures, the Nash-Sutcliffe Efficiency (NSE) and Percent Bias (PBIAS) as described in Chapter 2.

For both tile flow and nitrate calibration, the original and modified SWAT subroutines were calibrated separately so to compare best performance for both versions of the model.

Calibration calculations were completed for each subbasin individually for tile flow, allowing for each subbasin to have a unique combination of flow parameters. However, all three nitrate calibration parameters were basin-wide parameters and therefore only one combination could be used for all subbasins. Because of this restriction, calibration was completed based on total stream nitrate at the watershed outlet. No calibrations were performed on the untiled subbasin since the total basin outflow was modeled reasonably without further calibration.

The final combination of variables was decided by using Equation 3.1 to combine PBIAS and NSE into a single value and selecting the lowest value of the results for each subbasin.

$$|PBIAS| + (1 - NSE) \times 100 \qquad 3.1$$

This equation, previously used in Chapter 2, was created as a part of this study to have a multi-objective calibration within the R-script used. The calibration script for the Ohio site tile flow calculated the statistic for all 6 tile flow outlets simultaneously for all combination of tile flow calibration parameters. The calibration script for nitrate calculated the statistical results for the stream outlet nitrate loads only for all combination of the nitrate calibration parameters.

3.3.3 Parameter Sensitivity

3.3.3.1 Tile Drainage Parameters

Sensitivity curves were created for CN, LATKSATF, DEP_IMP, and KSAT_IMP. For each parameter, the three others were varied with one high and one low value (i.e. for the CN sensitivity curves LATKSATF, DEP_IMP, and KSAT_IMP were varied) to total eight combinations of the three other parameters over the full range of the variable in which sensitivity was being tested. Each variable's high and low values are listed in **Error! Reference source not found.**.

Table 3.7 Low and high parameter values used in tile flow sensitivity curves

	CN (%)	LATKSATF	DEP_IMP (mm)	KSAT_IMP (mm/hr)
Low value	-50	1	1500	0.1
High value	0	10	2000	1

Each curve was analyzed visually based on the slope of the curves, the location of peaks in the curve (if any), and the influence of the other parameters. Due to the qualitative nature of this analysis, the possibility of falsely identifying a parameter as sensitive or not significant. The curves shown in Figure 3.4 through Figure 3.7 show the results for subbasin B2 only. The other subbasin sensitivity curves can be found in Appendix C. The NSE plots are limited to NSE = 0 on the y-axis as when NSE is less than 0 the average of observed is considered a more reliable predictor than the model itself.

For CN, the two sets of four lines in the NSE sensitivity plot are clearly grouped by the LATKSATF values (Figure 3.4) with the low LATKSATF value (in orange) performing worse overall. The low LATKSATF consistently has a lower PBIAS than the high LATKSATF curve with the same DEP_IMP and KSAT_IMP. The high LATKSATF and high KSAT_IMP value curves both have the highest NSE at the largest CN reduction, but the curve shape varies with the deeper DEP_IMP value curve almost immediately decreasing in performance and the shallower DEP_IMP value rising until a 10% CN reduction. The high slopes in almost all of these curves show the significant dependence tile flow has on CN as it is the primary variable in splitting surface runoff and percolation.

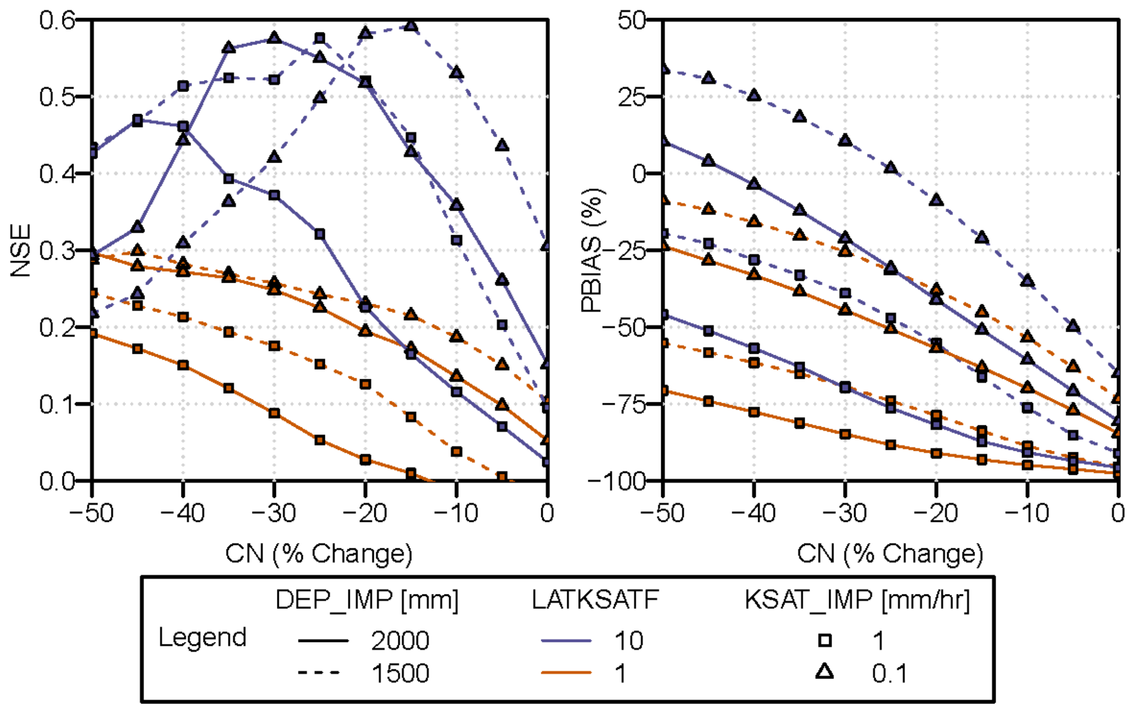

Figure 3.4 Sensitivity Curves for CN using the modified SWAT in subbasin B2

For LATKSATF, the best NSE performance are the curves with the high CN reduction (Figure 3.5). All four of these curves have similar shape and peak between a LATKSATF four and five. The curves without any CN reduction performed better with a low KSAT_IMP value. The curve with no CN reduction, the deeper DEP_IMP value, and the high KSAT_IMP value only reached an NSE value above zero when the LATKSATF was higher than six. Only two curves reached a 0% PBIAS out of the eight total, the curves with the high CN reduction and a low KSAT_IMP value. The curves with no CN reduction always under-predicted by 70% or greater. The LATKASTF values showed a higher slope, and therefore higher sensitivity with the greater CN reduction. As CN drives the amount of water percolating in the soil profile and LATKSATF drives how fast water moves once it is the soil profile, this inter-dependence is expected. When more water is in the profile (i.e. a larger CN reduction), LATKSATF has a larger effect on tile flow performance.

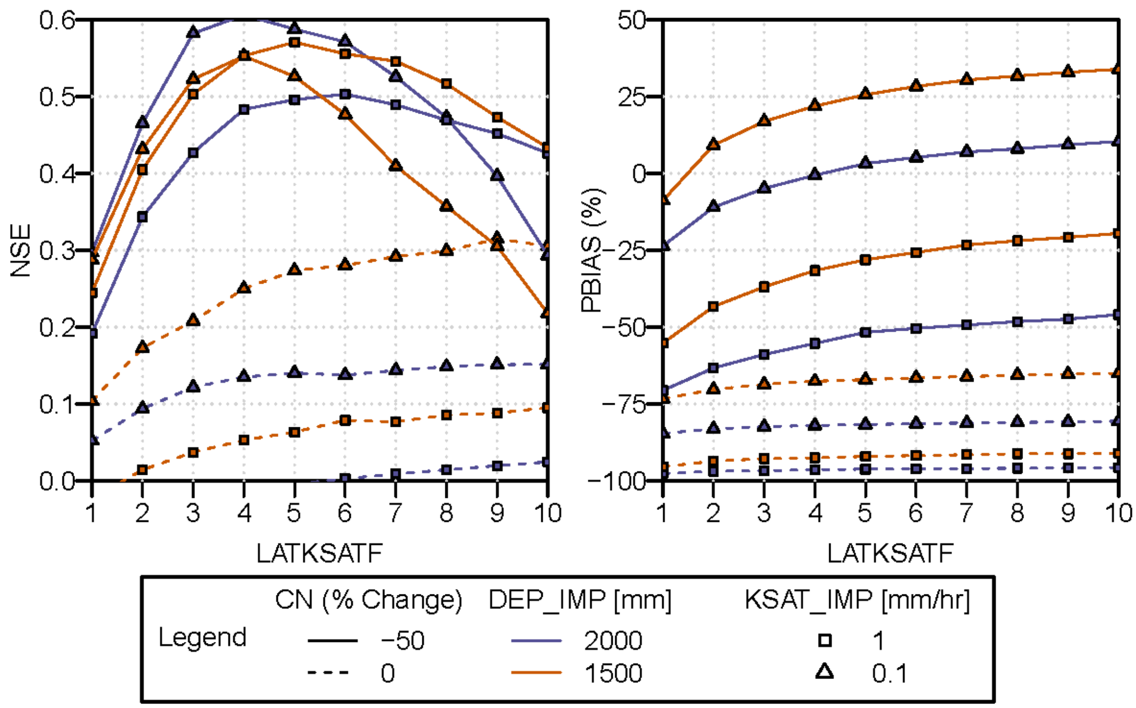

Figure 3.5 Sensitivity Curves for LATKSATF using the modified SWAT in subbasin B2

For both the PBIAS and NSE sensitivity curves for DEP_IMP, the best performance was for the curve with the high CN reduction and high LATKSATF value (Figure 3.6). Due to the little slope is seen in the DEP_IMP sensitivity curves, it was concluded the DEP_IMP variable was not very sensitive to the calibration performed in Ohio.

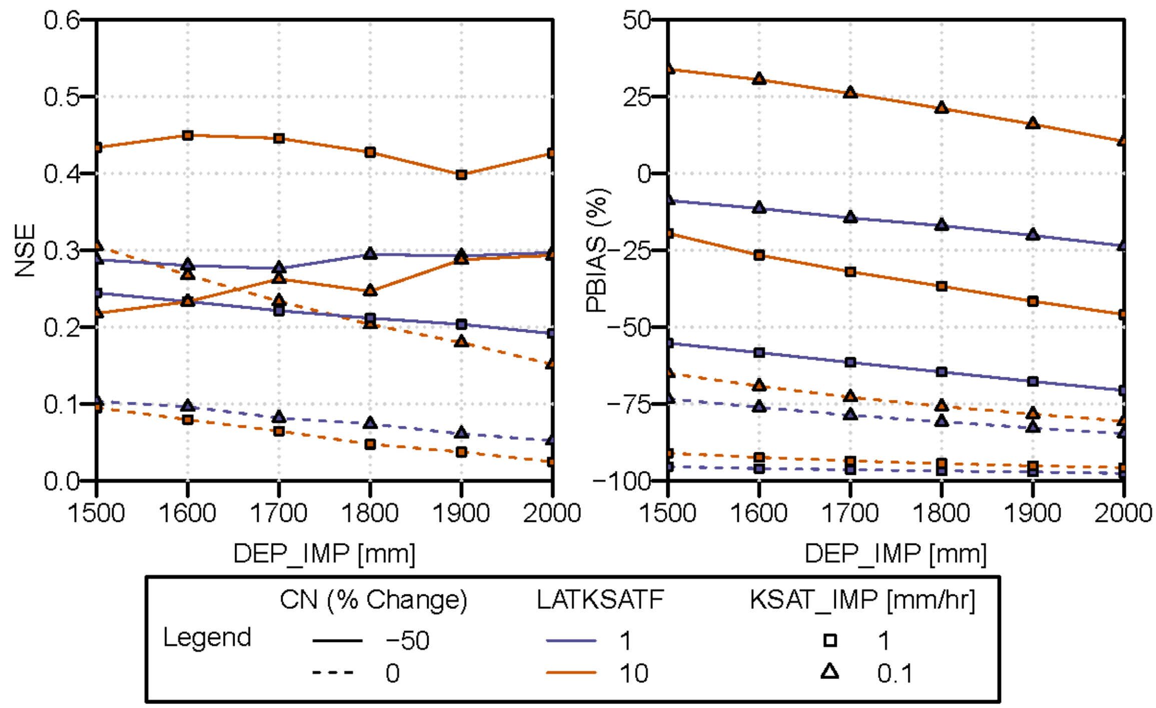

Figure 3.6 Sensitivity Curves for DEP_IMP using the modified SWAT in subbasin B2

The KSAT_IMP NSE curves showed the extreme dependence KSAT_IMP also has on LATKSATF and CN although the two variables did not appear to have a large dependence on KSAT_IMP (Figure 3.7). Two KSAT_IMP NSE curves have a constant increase as KSAT_IMP increases are the greater CN reduction and high LATKSATF value curves. These two curves are also the two that have a PBIAS greater than 0% (indicating an over-estimation of tile flow) at any KSAT_IMP value. The high LATKSATF value and greater CN reduction curves show almost no sensitivity for NSE (i.e. little slope). All curves with no CN reduction had a downwards slope as KSAT_IMP increased. The PBIAS sensitivity is grouped by the CN reduction. The greater CN reduction has the lower PBIAS magnitude and greatest slope. The curves with no CN reduction constantly under-predict by at least 50% and have very little slope. The performance increase by only two of the sensitivity curves is due to the water balance caused by the interactions of LATKSATF and CN. The greater CN reduction and high LATKSATF value have the highest water content in the soil profile and so an increase in seepage rate past the bottom of the soil profile should reasonably help the tile flow predictions. The greater CN reduction in the PBIAS image also show that KSAT_IMP has more effect when there is more water and water movement in the soil profile.

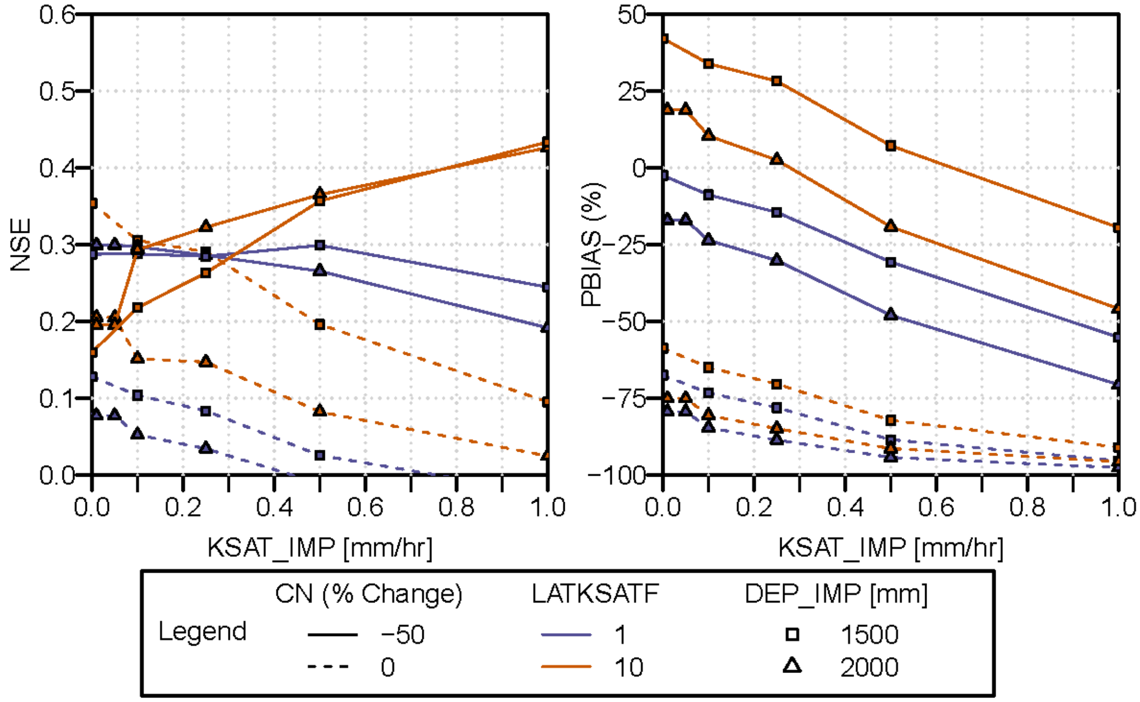

Figure 3.7 Sensitivity Curves for KSAT_IMP using the modified SWAT in subbasin B2

Overall, the CN and LATKSATF values had the most sensitivity and also showed extreme dependence on each other. KSAT_IMP, the variable added in the modified SWAT, also showed some sensitivity, but it was dependent on CN and LATKSATF if there was any sensitivity at all. DEP_IMP surprisingly had little sensitivity in this model. A larger more robust study on the sensitivity of these variables will assist in evaluating the effect of these variables.

3.3.3.2 Nitrate Parameters

Similar to tile flow, sensitivity curves for NPERCO, SDNCO, and CDN were created based on the nitrate load at the watershed outlet. For each variable, the two other parameters were varied with one high, one middle, and one low value to total nine combinations, one more combination than the tile flow curves. The same visual assessment was made for these curves as was for tile flow, including the same risks in a qualitative and not quantitative approach.

Each variable's high, middle, and low values are listed in Table 3.8. The curves shown in Figure 3.8 through Figure 3.10 show the results for the streamflow output. The subbasin sensitivity curves based on tile flow nitrate loads can be found in Appendix C. Due to the worse performance for stream nitrate, the NSE plots are limited to NSE = -0.25 on the y-axis instead of NSE = 0 as was the limit for tile flow.

Table 3.8 Low and high parameter values used in nitrate sensitivity curves

	SDNCO	CDN	NPERCO
Low value	0.5	0	0.01
Middle Value	1.1	1.5	0.45
High value	2	2.25	0.95

The SDNCO sensitivity showed an extreme response between 0.9 and 1.1 (Figure 3.8). Denitrification is key process, and SDNCO sets the threshold moisture content as percent of field capacity above which this process takes place. At levels below about 0.9, performance is poor from too much denitrification and insufficient nitrate remaining. While all curves were similarly shaped and sloped, SDNCO had visible groups of lines based on the NPERCO value. The group with the highest PBIAS was the highest NPERCO value, followed by the middle then the lowest NPERCO values. The NSE curves where less clear with the low NPERCO value performing best at low SDNCO values and the high NPERCO value performing best at the high SDNCO values. These curves show that SDNCO is most likely the main driving factor when addressing nitrate loads.

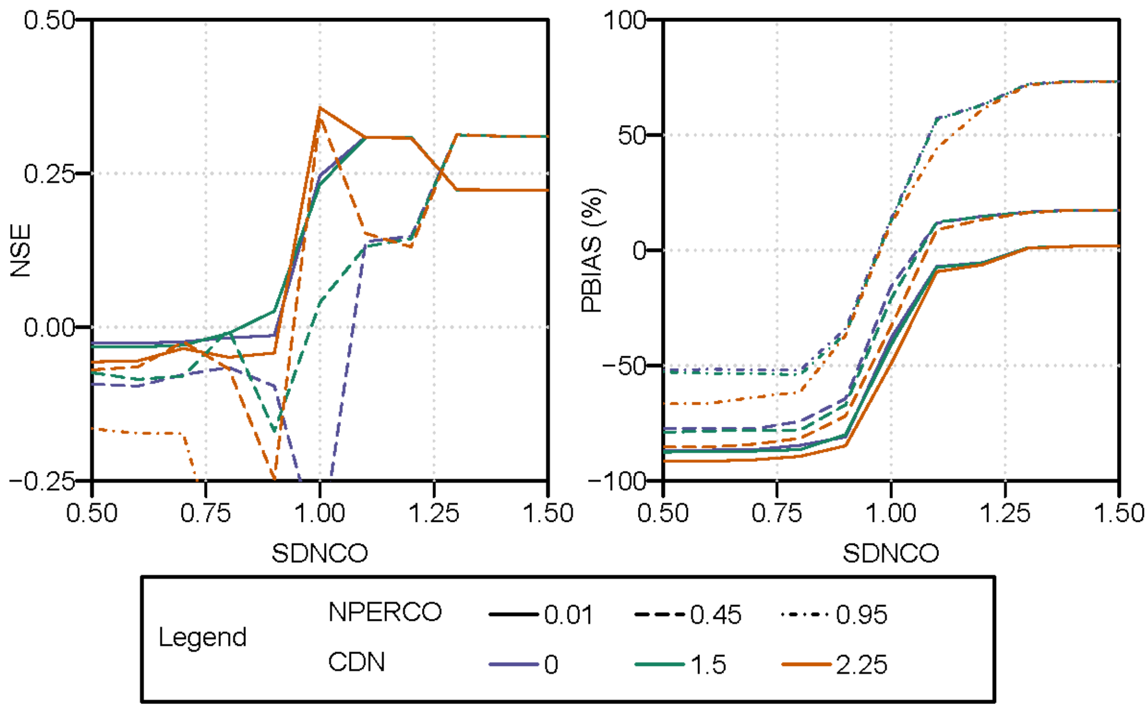

Figure 3.8 Sensitivity Curves for SDNCO using the modified SWAT streamflow

CDN showed the least sensitivity (i.e. the smallest slope overall) out of the three nitrate calibration parameters (Figure 3.9). The lowest SDNCO curves all performed worst for both NSE and PBIAS. These curves also showed a large increase in PBIAS at CDN = 0.25 but a decrease in NSE at CDN = 0.5. The middle and high SDNCO values performed similarly overall, but with reducing sensitivity. The high SDNCO had no sensitivity to CDN at all. As SDNCO is the threshold limit for denitrification to occur and CDN is only used in the denitrification simulations, a threshold that never allows denitrification to occur (in this case, the high SDNCO value only) would remove any dependence on CDN. The middle SDNCO value showed the same high sensitivity around CDN = 0.5 for the NSE curves, but, unlike the low SDNCO curve, an increase in performance was shown. The high NPERCO values had the highest PBIAS (over 50% consistently), but have such a low NSE that the curves are not visible in the NSE graph except the curve with a low SDNCO once CDN exceeded 2.0. This varying curve patterns emphasizes CDN’s dependence on SDNCO and NPERCO, but the little slopes for most of the CDN range shows the little sensitivity CDN has.

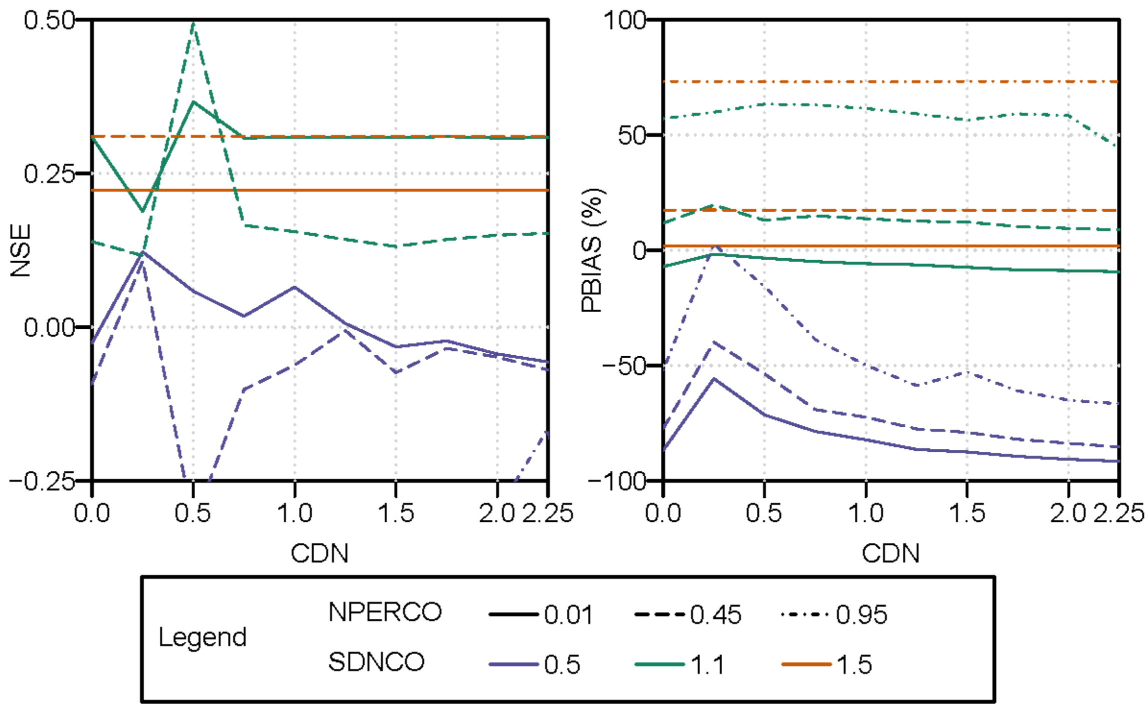

Figure 3.9 Sensitivity Curves for CDN using the modified SWAT streamflow

NPERCO had similar curve shapes and slopes for all of PBIAS, a slow increase in bias throughout the entire range of NPERCO values (Figure 3.10). For NSE, the curves were again grouped by SDNCO. All curves had similar shape, but the sudden decrease in NSE occurs at different NPERCO values. This further emphasizes the dependence NPERCO has on SDNCO. The high SDNCO curves had the most dramatic drop off between NPERCO = 0.6 and 0.7. The middle SDNCO value had a two-step drop off, a small drop between NPERCO = 0.3 and 0.4 as well as a large drop off between NPERCO = 0. 5 and 0.6. The low SDNCO had a less steep drop off starting at NPERCO = 0.5.

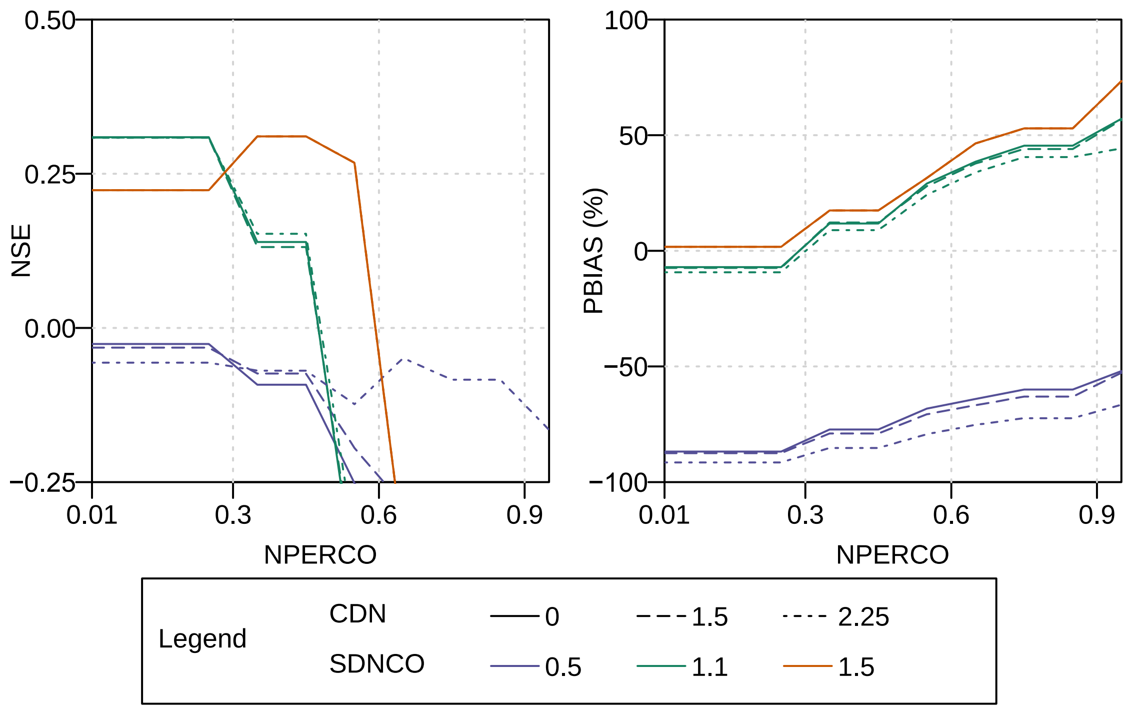

Figure 3.10 Sensitivity Curves for NPERCO using the modified SWAT streamflow

Overall, the SDNCO and NPERCO values showed much more sensitivity than the CDN values. These two variables were also very dependent on each other, similar to CN and LATKSATF's relationship with tile flow performance. The NPERCO value determines the amount of nitrate going into the soil profile and SDNCO determines when denitrification occurs in the soil profile. The two variables also had very small ranges of sensitivity, a potential drawback when calibrating, especially in automatic calibration, as the range could be potentially missed. Since CDN is not used in the SWAT subroutines unless the SDNCO threshold is reached and it only has an effect if there is enough nitrate in the soil from the NPERCO ratio, the small amount of sensitivity the variable itself had is understandable. While these combinations are insightful, a more thorough study would further show how sensitive these variables are for heavily tiled watersheds.

3.3.4 Final Calibration Parameters

The final calibrated parameters were different between the original and modified SWAT subroutines (Table 3.9). The selected curve number reduction was greater for the modified SWAT. LATKSATF values were lower for the modified subroutines with the exception of B3, the site with the most uncertainty in drainage area. Arnold et al. (2012) suggested LATKSATF values should be between 0.001 and 4, and, while the modified SWAT best values were not always within these bounds, they were closer to the recommended values than the original SWAT. The restrictive layer depth was raised more from the original estimated value for the modified SWAT than the original SWAT.

Table 3.9 Final Tile Flow Calibration Parameters for both versions of SWAT

Version	Subbasin	CN2	LATKSATF	DEP_IMP [mm]	KSAT_IMP [mm/hr]
Uncalibrated	(All)	-	1	2000	0
Original SWAT	B2	-10%	5	1900	
	B3	-5%	4	1700	
	B4	-10%	6	1500	
	B5	-30%	10	2000	
	B6	-25%	10	2000	
	B8	-25%	10	2000	
Modified SWAT	B2	-50%	4	2000	0.1
	B3	-45%	2	2000	0
	B4	-50%	3	1600	0.25
	B5	-50%	7	1500	0
	B6	-50%	5	1500	0
	B8	-50%	7	1500	0

The best combination of nitrate parameters for each subbasin is found in Table 3.10. The overall best combination was determined using the watershed nitrate values, as the calibration parameters were basin-wide (Table 3.11). For the original SWAT, NPERCO values between 0.01 and 0.25 made no difference so the lowest was chosen. For the modified SWAT, CDN made no difference for the final best calibration so the lowest was used as well.

Table 3.10 Subbasin Specific Calibration (2005-2006) Best Performance for Tile Nitrate

Version	Subbasin	NPERCO	SDNCO	CDN	NSE	PBIAS
Original SWAT	B2	0.95	1.0	0.5	0.08	1.3%
	B3	0.95	1.1	3.0	0.06	8.3%
	B4	0.01	1.1	0.5	0.14	-3.5%
	B5	0.01	0.9	0.25	0.17	-24.2%
	B6	0.95	0.5	0.5	0.07	13.3%
	B8	0.01	1.3	0.01	0.09	-3.2%
Modified SWAT	B2	0.01	1.3	0.01	0.11	-61.1%
	B3	0.35	1.0	0.5	0.12	-1.2%
	B4	0.01	1.3	0.01	0.10	-77.6%
	B5	0.01	1.3	0.01	-0.22	-1.0%
	B6	0.95	0.5	0.25	-0.00	0.2%
	B8	0.01	1.3	0.01	0.09	-3.2%

Table 3.11 Final Tile Nitrate Calibration Parameters for both versions of SWAT

Version	NPERCO	SDNCO	CDN
Uncalibrated Value	0.2	1.1	1.4
Original SWAT	0.01	1.0	3.0
Modified SWAT	0.35	1.2	0.75

3.4 Results

3.4.1 Hydrology

3.4.1.1 Subbasin Tile Flow

Calibration (2005-2008) and validation (2009-2012) for each subbasin had mixed results when comparing the modified and original subroutines, especially for PBIAS (Table 3.12). The original SWAT subroutines were not as consistent in performance between calibration and validation periods, with PBIAS magnitudes ranging from a 0.7% (B8) to a 46.3% (B5) increase, including two instances the PBIAS switched from over- to under-prediction (B3 & B6). The modified SWAT had a lower magnitude PBIAS than the original SWAT subroutines on average, and was more consistent between calibration and validation periods than original SWAT. In every calibration and validation set except for B3's calibration and B4's validation (where the drainage control structure had been installed), the modified SWAT subroutines performed better according the NSE.

Table 3.12 Calibration and Validation Tile Flow Performance Statistics

Subbasin	Time Period	Original SWAT		Modified SWAT	
		NSE	PBIAS	NSE	PBIAS
B2	Calibration (2005-2008)	0.37	23.7%	0.60	5.7%
	Validation (2009-2012)	0.25	15.4%	0.26	-0.4%
B3	Calibration (2005-2008)	0.27	37.7%	0.11	17.1%
	Validation (2009-2012)	0.34	-41.4%	0.34	-47.6%
B4	Calibration (2005-2008)	0.28	34.1%	0.40	7.8%
	Validation (2009-2012)*	0.15	26.9%	-0.05	1.4%
B5	Calibration (2005-2008)	0.31	-20.6%	0.42	-34.5%
	Validation (2009-2012)	0.25	-46.3%	0.38	-53.7%
B6	Calibration (2005-2008)	0.36	3.9%	0.39	-0.4%
	Validation (2009-2012)	0.34	-8.8%	0.40	-10.4%
B8	Calibration (2005-2008)	0.26	-0.7%	0.54	-7.7%
	Validation (2009-2012)	0.20	-40.7%	0.43	-43.6%

** Drainage Control Structure installed at B4 in 2009*

The original SWAT never achieved a NSE higher than 0.5 while the modified SWAT did in two calibration periods (B2 and B8). These values should still be considered satisfactory as it is daily tile flow and not monthly streamflow, the normal performance statistic used to determine overall acceptance of model accuracy (Moriasi et al., 2007b). Overall, the modified SWAT performed statistically better when compared to the original although the PBIAS magnitude tends to be greater. The large performance drop between calibration and validation periods for B4 is partially due to the drainage control structure installed as part of a study in 2009 (Williams et al., 2015b) which was not simulated. This control structure was lowered prior to fall or spring field management and raised again shortly afterwards.

SWAT performance was not just statistically improved, but the tile drainage hydrograph shape fits better with the measured data when the modifications were included (Figure 3.11). Improvements in performance with the modified SWAT included: better prediction in the number of peaks, peak magnitude, rate of decrease after flow peaks, and base flow magnitude, as discussed in the paragraphs below.

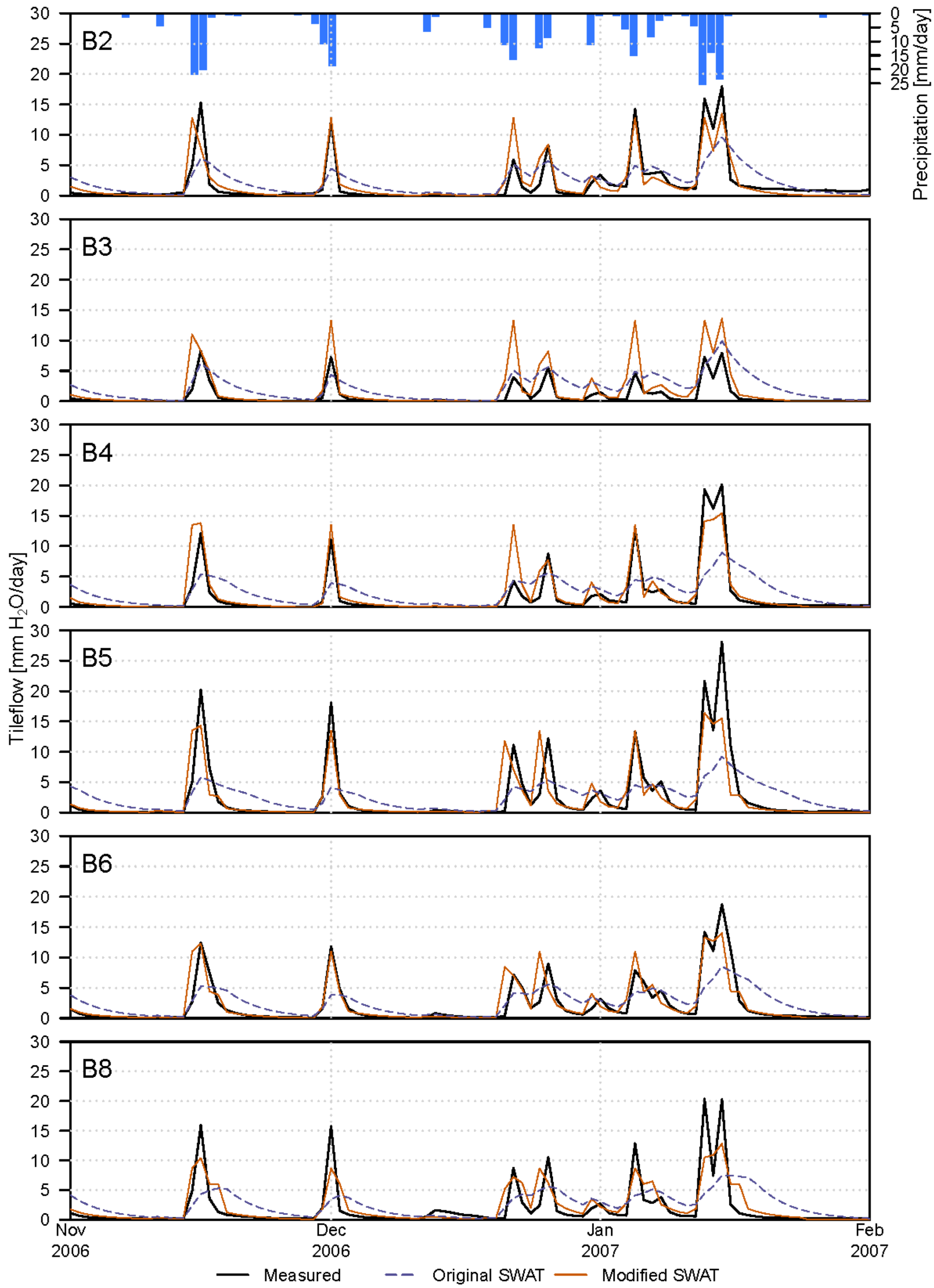

Figure 3.11 Subbasin B2-B8 measured and modeled tile flow

While most tile flow peaks were captured by both versions of SWAT, when there were two peaks close together the original subroutines only predicted one (for example in the last event shown in Figure 3.11). The original SWAT predicted a single peak at the same time as the second peak at a lower magnitude than both the measured peaks while the modified SWAT captured both peaks in many instances (ex. B2, B5, & B8). When both peaks were not captured (ex. B3, B4, & B6) the single peak started when the first peak was observed and lasted to the second observed peak.

In all subbasins, the modified SWAT better predicted the magnitude of peaks than the original SWAT, which under-predicted almost all peaks. This was partially due to the built in lag only allowing a portion of modeled flow to move in a single day. This under-prediction is evident in Figure 3.12. When the lag was removed in the modified SWAT, the full amount can flow through.

The original SWAT peaks not only were smaller, but did not decrease as quickly post-peak as was observed in the watershed. The modified SWAT improved the recession rate.

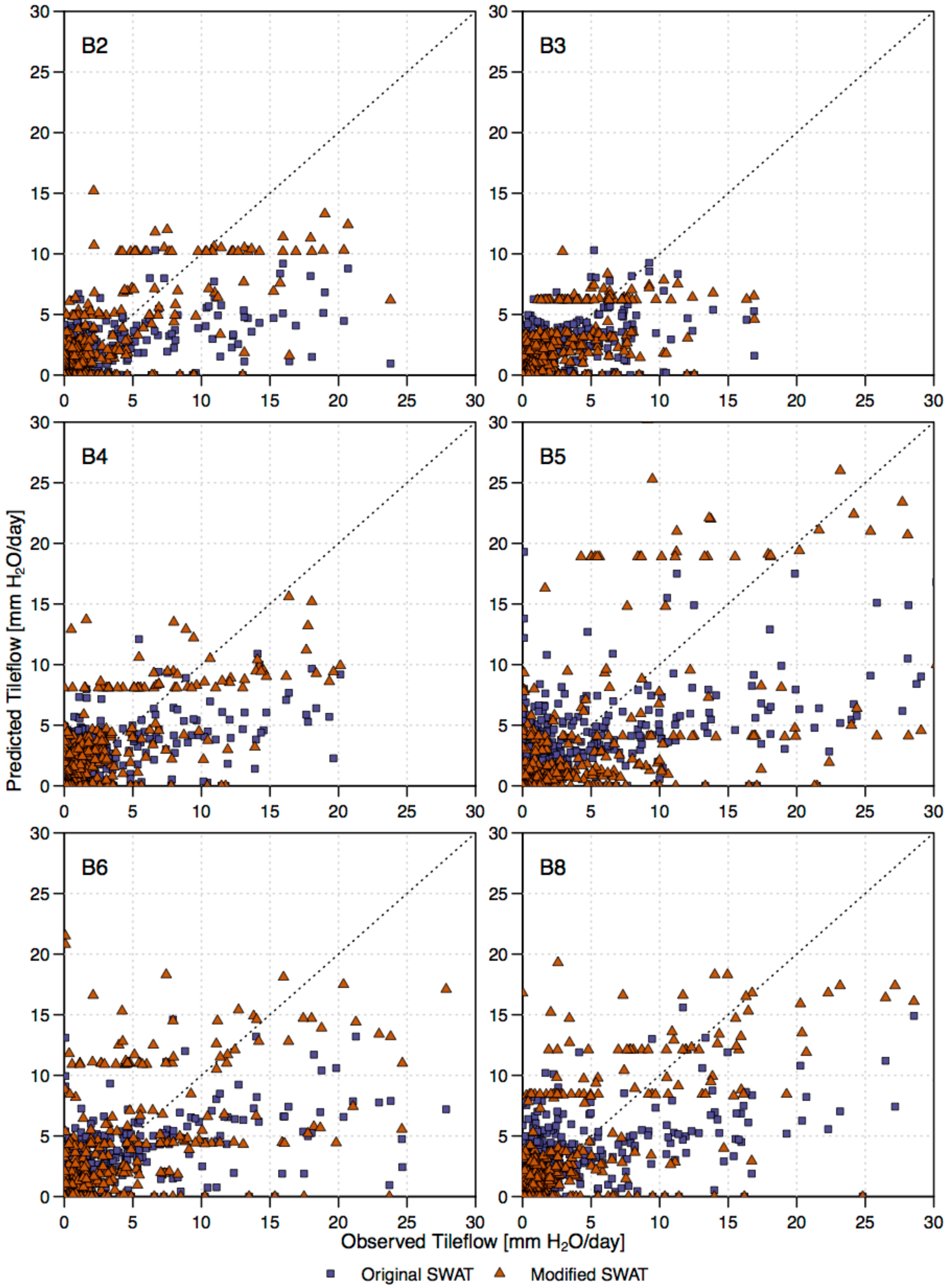

Figure 3.12 Subbasin B2-B8 Predicted vs Observed Tile Flow over Calibration Years

While most improvements primarily increased peak flow prediction performance, the modified subroutines had better base flow magnitude as well. Due to the slower rate of reduction after peaks in the original subroutines, the original SWAT consistently over-predicted the magnitude of flow during low-flow periods. Modified SWAT did have the same problem in B3, but in all other subbasins performed better during these periods. The original SWAT over predicted low flow periods partially due to the extended lag after drainage events. When only 20% of total flow is allowed every day it takes over 4 days for over 99% of the peak flow to go through the drains. As more flow occurs post-peak, the duration of drainage event's tail increases. The more stagnant and high water table, as shown in Chapter 2, also keeps the tile flowing for longer durations when the tile is not observed to have flow.

3.4.1.2 Watershed Stream flow

At the watershed outlet, the modified SWAT performed more consistently than original SWAT, although overall the performance was not as good (Table 3.13). The streamflow peaks were predicted higher with the modified algorithms than the original. In some cases this created an almost perfect peak magnitude match with the measured but in other cases the modified subroutines caused over-prediction in streamflow (Figure 3.13). The modified SWAT subroutines also consistently under-predicted the non-peak time periods, further explaining the lower NSE values.

Table 3.13 Watershed Outlet Streamflow Performance Statistics

Time Period	Original SWAT		Modified SWAT	
	NSE	PBIAS	NSE	PBIAS
Calibration (2005-2008)	0.65	-6.7%	0.48	-7.5%
Validation (2009-2012)	0.50	-26.8%	0.39	-26.5%

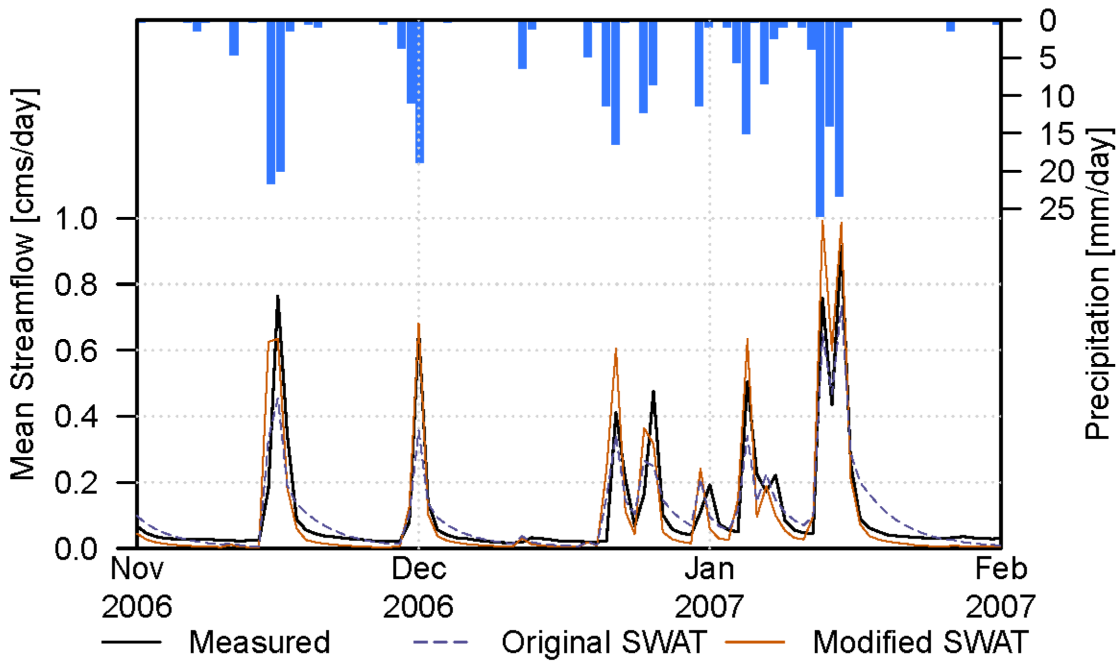

Figure 3.13 Watershed measured and modeled stream flow

Both the original and modified SWAT simulated similar water balances, including both on average predicting 72% of the measured annual total flow (Table 3.14). The under-prediction was primarily for 2009-2012, which corresponds to the validation period. The modified SWAT always under-predicted the proportion of tile drainage by a large range with the smallest under-prediction by 0.5% in 2006 and the largest by 54.5% in 2010. The original SWAT predicted the tile drainage portion of total flow closer but still had a 46.1% under-prediction in 2010. Groundwater additions to total flow were always zero for the original SWAT due to the placement of the restrictive layer.

Table 3.14 Annual flow partitioning for measured and predicted

Year	Precip. [mm H_2O]	Source	Total [mm H_2O]	% of Total Flow			
				Surface	Lateral	Ground	Tile
2005	1121	Measured	609				45.3%
		Orig. SWAT	552	48.5%	3.7%	0.0%	47.4%
		Mod. SWAT	554	54.4%	5.0%	0.4%	39.8%
2006	1064	Measured	467				48.8%
		Orig. SWAT	449	40.1%	4.1%	0.0%	55.9%
		Mod. SWAT	449	45.5%	5.7%	0.5%	48.3%
2007	1095	Measured	519				51.1%
		Orig. SWAT	479	48.1%	3.7%	0.0%	48.1%
		Mod. SWAT	471	52.1%	5.1%	0.4%	42.3%
2008	1006	Measured	611				75.6%
		Orig. SWAT	478	56.0%	4.0%	0.0%	40.0%
		Mod. SWAT	467	57.8%	5.5%	0.4%	36.3%
2009	938	Measured	441				66.9%
		Orig. SWAT	284	51.5%	3.1%	0.0%	45.3%
		Mod. SWAT	286	50.8%	5.3%	0.7%	43.2%
2010	773	Measured	340				90.3%
		Orig. SWAT	211	50.6%	5.2%	0.0%	44.2%
		Mod. SWAT	209	55.0%	8.2%	0.8%	35.8%
2011	1239	Measured	767				89.7%
		Orig. SWAT	566	43.1%	2.8%	0.0%	54.1%
		Mod. SWAT	567	47.0%	4.1%	0.4%	48.4%
2012	794	Measured	310				77.4%
		Orig. SWAT	229	46.3%	7.7%	0.0%	46.0%
		Mod. SWAT	230	47.7%	10.4%	0.6%	41.2%

While the annual total stream flow did not change significantly between the original and modified algorithms, there was a significant difference between the partitioned annual water yield. The tile flow predicted by modified SWAT was always lower than the original SWAT. This is primarily due to the extended lags seen in the tile flow images. The modified SWAT always under-predicted tile flow's contribution to total water yield, but modified SWAT had the smaller range of differences when compared with the original SWAT's performance compared to measured flow.

3.4.2 Nitrate

3.4.2.1 Subbasin Tile Nitrate

Neither the original nor modified SWAT successfully predicted daily nitrate loads from tile drains in either the calibration (2005-2006) or validation (2007-2008) periods (Table 3.15).

The NSE values for the modified subroutines were slightly better than for the original subroutines, but improvements were not consistent, and not within the “acceptable” range suggested by Moriasi et al. (2007b) for monthly stream nitrate. The PBIAS values for both versions of SWAT showed extreme under-prediction in most cases, and decreased still further when the modified SWAT subroutines were used.

Table 3.15 Calibration and Validation Tile Nitrate Performance Statistics

Subbasin	Time Period	Original SWAT		Modified SWAT	
		NSE	PBIAS	NSE	PBIAS
B2	Calibration (2005-2006)	0.08	-9.1%	0.09	-60.5%
	Validation (2007-2008)	-5.50	259.6%	-2.41	60.5%
B3	Calibration (2005-2006)	-4.32	275.0%	-2.16	75.6%
	Validation (2007-2008)	0.15	6.3%	0.12	-52.8%
B4	Calibration (2005-2006)	0.12	-33.8%	0.09	-72.2%
	Validation (2007-2008)	-0.65	56.0%	-0.15	-30.1%
B5	Calibration (2005-2006)	0.11	50.3%	0.16	-24.2%
	Validation (2007-2008)	0.28	-13.5%	0.39	-58.2%
B6	Calibration (2005-2006)	-2.59	402.2%	-1.89	134.0%
	Validation (2007-2008)	-0.80	110.6%	-0.98	-6.8%
B8	Calibration (2005-2006)	0.05	53.1%	0.31	-33.7%
	Validation (2007-2008)	0.10	-6.6%	0.23	-59.7%

Although both simulations were not statistically satisfactory, there were large changes in tile nitrate patterns (Figure 3.14). Throughout all four years, most peak magnitudes were not correctly predicted by either version of SWAT and in many cases, as seen in B3 and B6, there were consistent over predictions for months at a time in the original SWAT simulations. The modified SWAT predicted more peaks than the original SWAT, but the peak magnitudes were overestimated more than the original SWAT. In September 2005, a major storm event (precipitation of 57.89 mm in a single day) caused a large flow event that both versions of SWAT under-predicted, therefore the nitrate output was also very low. Additional images showing results for all four years (2005-2008) of data for nitrate are in Appendix D.

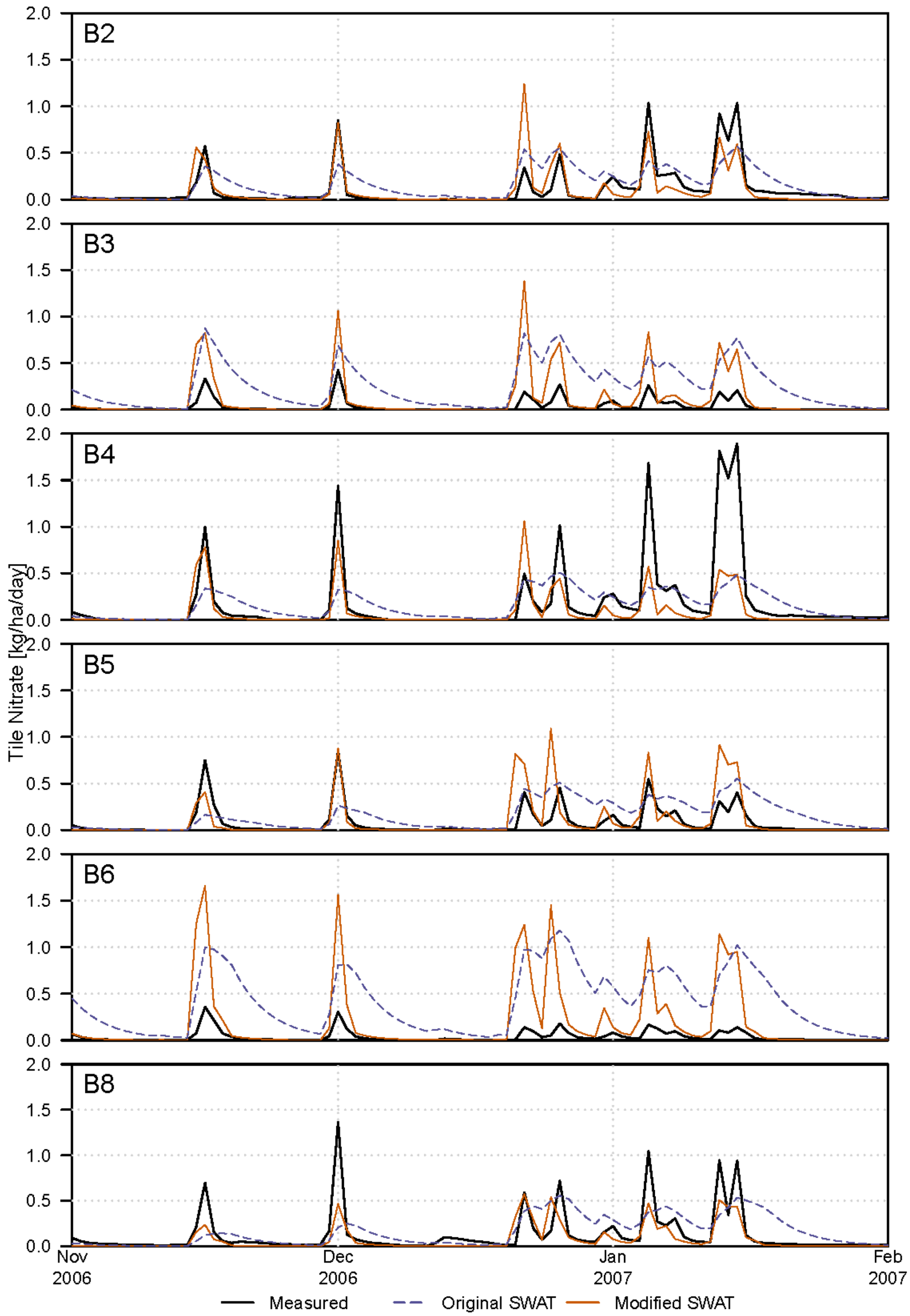

Figure 3.14 Subbasin B2-B8 measured and modeled tile nitrate

The original SWAT daily nitrate loads varied less than modified SWAT's. The shape of both versions of SWAT closely resembled the tile flow curves showing the high dependence nitrate loads have on tile flow and the small variation tile nitrate concentration varies. Despite the overall good tile flow hydrology, the nitrate results were unsatisfactory. The issue can then be traced back to the nitrate concentration in the tiles. The nitrogen cycle in SWAT consists of many calibration curves, and falls short in predicting tile flow loads accurately.

3.4.2.2 Watershed Stream Nitrate

At the watershed outlet, the modified SWAT consistently performed statistically worse than the original SWAT subroutines for NSE, but not PBIAS (Table 3.16). Both versions of SWAT performed better during the validation period, an unexpected phenomenon. The modified SWAT predicted a more sensitive nitrate load in the stream (Figure 3.15). The original SWAT did not have the capability to decrease nitrate loads fast enough in the stream to simulate the shape of the measured data although the magnitudes of the peaks did not have as consistent an over prediction. The higher PBIAS for original SWAT originated from the predicted slow decrease in nitrate load, effectively making up for the under-predicted periods occurring for most of the year.

Table 3.16 Watershed Outlet Stream Nitrate Performance Statistics

Time Period	Original SWAT		Modified SWAT	
	NSE	PBIAS	NSE	PBIAS
Calibration (2005-2006)	0.05	44.3%	-0.24	23.7%
Validation (2007-2008)	0.34	-9.6%	0.24	-22.4%

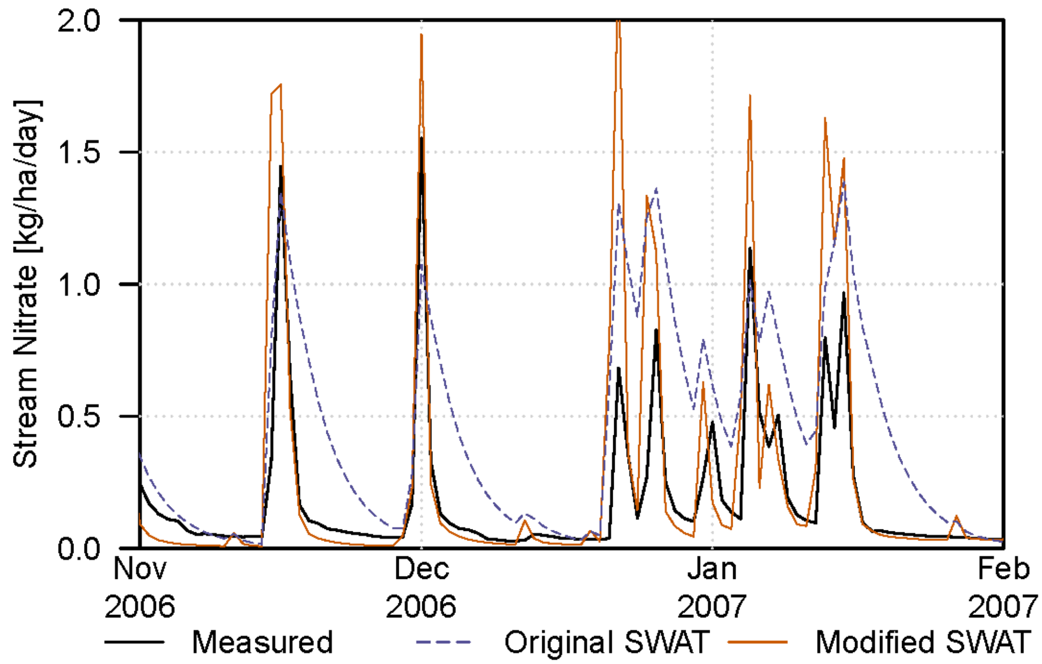

Figure 3.15 Watershed measured and modeled stream nitrate

For the original SWAT, auto-fertilization subroutines annually applied 337 kg N/ha and 303 kg N/ha for agricultural and residential land respectively on average. This is a gross over-estimation of what would be expected when compared to what is seen on the tiled lands. For the modified subroutines, the average annual rates lowered for both agricultural and residential land to 212 kg N/ha and 119 kg N/ha respectively. Despite a lower amount of nitrogen application for modified SWAT, the original SWAT modeled more nitrate load leaving the untiled agricultural land by tenfold when compared to the modified SWAT.

The auto-fertilization and the nitrate loss differences are due to the different calibration results in the nitrate calibration. The higher final NPERCO value for modified SWAT allowed to more nitrate to be released in surface runoff and less to percolate into the soil. With more nitrate in runoff, the areas with more surface runoff, in this case the untiled land, would have a higher nitrate contribution per acre to the final stream concentration. The original SWAT also had a higher CDN parameter. As CDN increases, the amount of nitrate in the soil profile lost to denitrification increases. This loss of nitrate in the soil would cause more nitrogen related stress to the crop and thus explains the larger amount of nitrogen applied to the untiled lands via auto-fertilization. The increase in nitrate also would reduce the amount of nitrate in lateral flow within the profile for the original SWAT routines.

3.4.3 Phosphorus in the Watershed Outlet

While phosphorus was not specifically calibrated for in this study, tile phosphorus was monitored for at the tiles and outlets. Currently, SWAT does not output tile phosphorus, so only the phosphorus at the watershed outlet is compared.

When comparing the measured soluble reactive phosphorus to the mineral phosphorus at the stream output, the performance statistics were reasonable and better than expected (Table 3.17). Both version of the SWAT model under-predicted at the higher peaks (mid-November 2006) but over-estimated the smaller peaks (Figure 3.16). The modified version of SWAT predicted higher peaks, which actually caused the PBIAS magnitude to lower, as both sets of subroutines consistently under-predicted the duration of the peak and the non-peak concentrations.

Table 3.17 Watershed Stream Statistics comparing measured soluble reactive phosphorus and modeled mineral phosphorus (2005-2008)

Version	NSE	PBIAS
Original SWAT	0.21	-27.0%
Modified SWAT	0.18	-21.0%

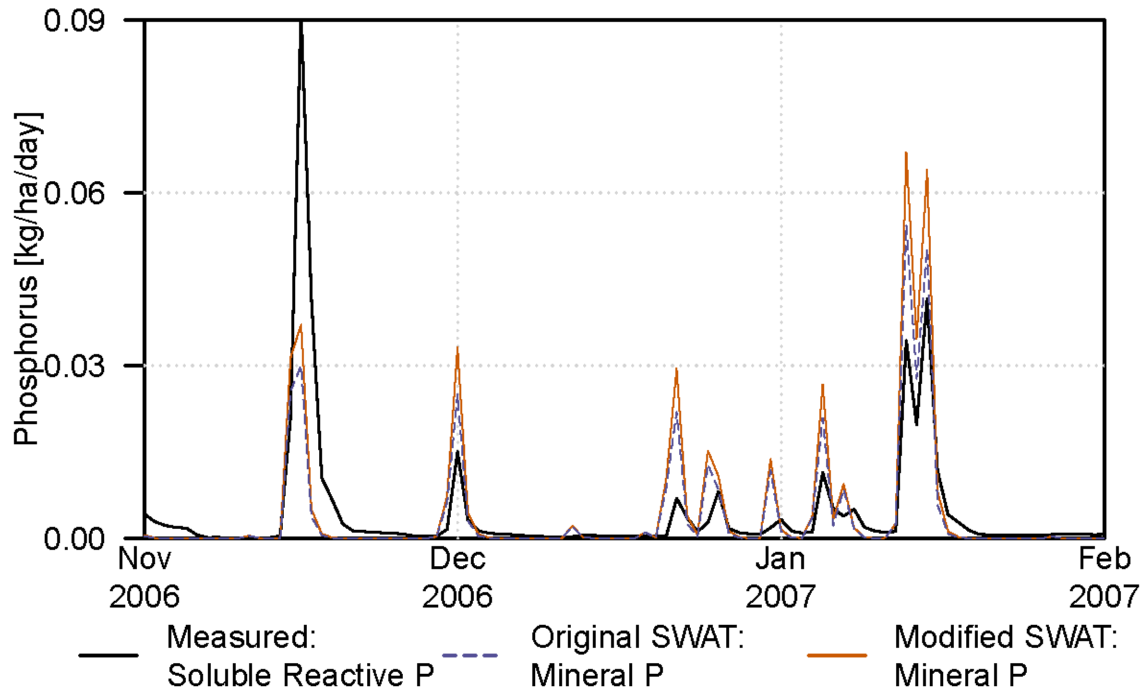

Figure 3.16 Watershed measured soluble reactive phosphorus and modeled mineral phosphorus

Unlike soluble reactive phosphorus and mineral phosphorus, the total phosphorus coming out of the stream performed extremely poorly for both versions of SWAT (Table 3.18). While the peak loads are temporally correct, the total phosphorus load is extremely over estimated at the peaks (Figure 3.17).

Table 3.18 Watershed Stream Total Phosphorous Performance Statistics (2005-2008)

Version	NSE	PBIAS
Original SWAT	-35.73	244.2%
Modified SWAT	-47.36	295.9%

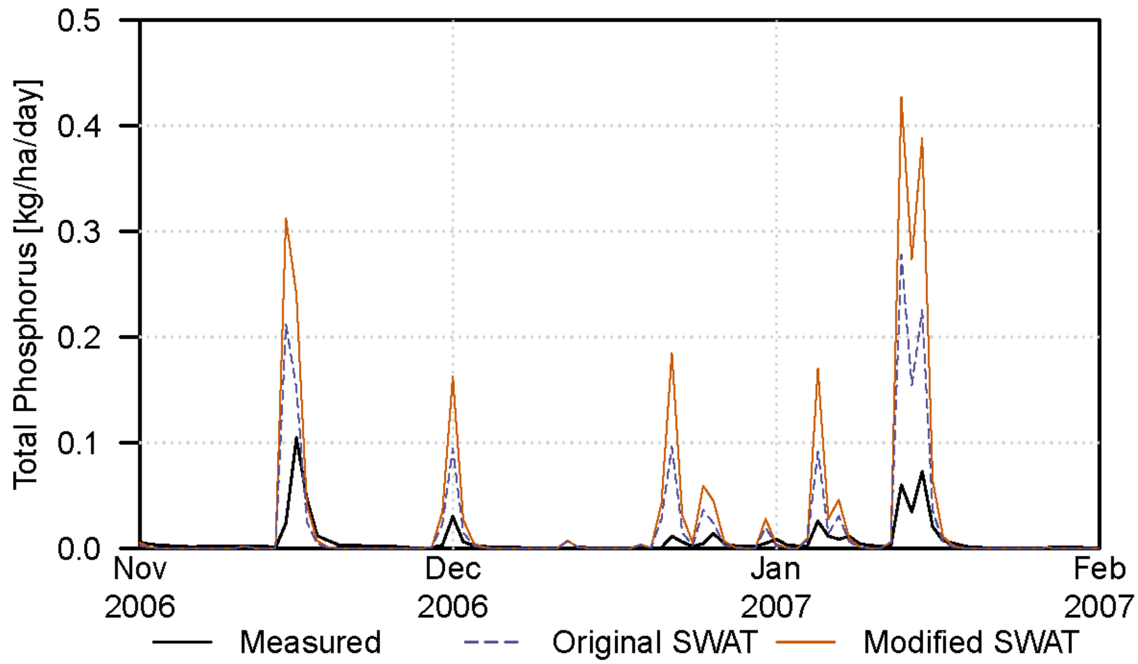

Figure 3.17 Watershed measured and modeled stream total phosphorus

SWAT's poor performance in predicting phosphorus is not surprising, especially since 40% of the total phosphorus this watershed output originated within the tile drains (King et al., 2015) and the primary route in SWAT for phosphorus is via sediment transport (Neitsch et al., 2011). The results show little change between the original and modified subroutines showing the little effect subsurface interactions have on phosphorus as most phosphorus is lost via erosion and sediment loss in surface runoff.

Radcliffe et al. (2015) showed that SWAT, like most other models, does not include macropore processes that produce most of the phosphorus loads in tile drains. The phosphorus processes in SWAT more generally have been recently improved by Collick et al. (2016) to better simulate management effects, but were not included in the version studied here.

3.5 Conclusions

This is the first study at a watershed scale that examined SWAT predictions at measured tile outlets on a daily scale beyond a single field. The drain flow performance was reasonably good after calibration of CN2 reduction and LATKSATF. However, it is clear more work needs to be done to improve nutrient outputs at the tiles.

The modified SWAT showed a very complex relationship between multiple parameters and each parameter's sensitivity. For tile flow, CN and LATKSATF are the most influential, with curve number requiring a large reduction and LATKSATF requiring a large increase. The modified SWAT was not sensitive to the redefined parameter DEP_IMP and the new parameter KSAT_IMP in this case, but more testing is needed. For nitrate predictions, SDNCO showed the largest sensitivity, but only once it had been increased to 0.9. A similar small range of sensitivity was observed for NPERCO as well. Denitrification is clearly a key process and the very high sensitivity of the model to small variations is a problem that needs to be addressed. More sensitivity studies should be done to further investigate these patterns and see the effect at multiple levels.

The modified SWAT tile flow values under-predicted flow by 13.9% on average compared to the original SWAT which under-predicted 1.4%. The modified SWAT also had an average NSE of 0.35 across all subbasin, higher than the original SWAT's 0.28 average. At the stream, the modified SWAT under-predicted streamflow by 17.0%, slightly more than the average 16.8% under-prediction by the original SWAT. The modified SWAT also improved the shape of the tile flow curves.

For nitrate, the modified SWAT tile flow predictions ranged from a -72.2% under-prediction (B4 calibration period) to a 134.0% over-prediction (B6 calibration period). The original SWAT saw an even more extreme range from a 33.8% under-prediction (B4 calibration) to a 402.2% over-prediction (B6 calibration period), including three other periods where the PBIAS was over-predicting by more than 100%. This is partially due to the nitrate calibration parameters being restricted at the watershed level. If the nitrate parameters could be calibrated at the subbasin level, the extreme prediction errors would have been reduced significantly, as shown in Table 3.10 At the watershed outlet, the modified SWAT over-predicted nitrate by 0.6% which was better than the 17.4% over-prediction by the original SWAT. These extreme changes in nitrate results show the need to further investigate how SWAT calculates nitrate that flows through tile drains. This problem can at least partially be attributed to the nitrate parameters being basin-wide and not subbasin specific.

Both the modified and original SWAT under-predicted mineral phosphorus to measured soluble reactive phosphorus by 21.0% and 27.0% respectively (as compared to measured soluble reactive phosphorus). The NSE values were reasonably similar with the modified SWAT at 0.18

and the original SWAT at 0.21. The original SWAT over-predicted total phosphorus by 244.2%, a slight improvement to the 295.9% over-prediction by the modified SWAT. Both NSE values for total phosphorus were below -30 further showing that phosphorus predictions were extremely poor. These results emphasize the need to update SWAT with the latest phosphorus knowledge, as proposed by Collick et al. (2016).

Although SWAT is a watershed model, it needs to be able to correctly predict processes that occur on a field scale and that SWAT is used to examine. Given the importance of tile drainage in the Western Lake Erie Basin and throughout the Midwest, studies like this are important for examining and continuing to improve and assess the tile drainage algorithms.

3.6 Bibliography

Arnold, J. G., Kiniry, J. R., Srinivasan, R., Williams, J. R., Haney, E. B., & Neitsch, S. L. (2012). *Soil & Water Assessment Tool: Input/Output documentation. version 2012*.

Arnold, J. G., Srinivasan, R., Muttiah, R. S., & Williams, J. R. (1998). Large Area Hydrologic Modeling and Assessment Part 1: Model Development. *Journal of the American Water Resources Association*, *34*(1), 73–89.

Boles, C. M. W., Frankenberger, J. R., & Moriasi, D. N. (2015). Tile Drainage Simulation in SWAT2012: Parameterization and Evaluation in an Indiana Watershed. *Transactions of the ASABE*, *58*(5), 1201–1213.

Collick, A. S., Veith, T. L., Fuka, D. R., Kleinman, P. J. A., Buda, A. R., Weld, J. L., … Easton, Z. M. (2016). Improved Simulation of Edaphic and Manure Phosphorus Loss in SWAT. *Journal of Environment Quality*.

Delaware Soil and Water Conservation District. (2009). Historic County Drainage [Online]. Delaware, OH: Delaware SWCD. Retrieved from http://www.delawareswcd.org/

Garen, D. C., & Moore, D. S. (2005). Curve number hydrology in water quality modeling: Uses, abuses, and future directions. *Journal of the American Water Resources Association*, *41*(2), 377–388.

Gesch, D. B. (2007). The National Elevation Dataset. In *Digital Elevation Model Technologies and Applications: The DEM User's Manual* (2nd ed., pp. 99–118). Bethesda, Maryland: American Society for Photogrammetry and Remote Sensing.

Gesch, D. B., Oimoen, M., Greenlee, S., Nelson, C., Steuck, M., & Tyler, D. (2002). The National Elevation Dataset: Photogrammetric Engineering and Remote Sensing.

Green, C. H., Tomer, M. D., Di Luzio, M., & Arnold, J. G. (2006). Hdrologic Evaluation of the Soil and Water Assessment Tool for a Large Tile-Drained Watershed in Iowa. *Transactions of the ASABE*, *49*(2), 413–422.

Kellogg, R. L., & Moffitt, D. C. (2011). Manure Loadings Used to Simulate Pastureland and Hay Land in CEAP HUMUS/SWAT Modeling.

King, K. W., Fausey, N. R., & Williams, M. R. (2014). Effect of subsurface drainage on streamflow in an agricultural headwater watershed. *Journal of Hydrology*, *519*, 438–445.

King, K. W., Smiley, P. C., Baker, B. J., & Fausey, N. R. (2008). Validation of paired watersheds for assessing conservation practices in the Upper Big Walnut Creek watershed, Ohio. *Journal of Soil and Water Conservation*, *63*(6), 380–395.

King, K. W., Williams, M. R., & Fausey, N. R. (2015). Contributions of Systematic Tile Drainage to Watershed-Scale Phosphorus Transport. *Journal of Environmental Quality*, *44*(2), 486.

King, K. W., Williams, M. R., & Fausey, N. R. (2016). Effect of crop type and season on nutrient leaching to tile drainage under a corn-soybean rotation. *Journal of Soil and Water Conservation*, *71*(1), 56–68.

Moriasi, D. N., Arnold, J. G., & Green, C. H. (2007a). Incorporation of Hooghoudt and Kirkham Tile Drain Equations into SWAT2005. In *4th Annual Interational SWAT Conference* (pp. 139–147).

Moriasi, D. N., Arnold, J. G., Van Liew, M. W., Binger, R. L., Harmel, R. D., & Veith, T. L. (2007b). Model evaluation guidelines for systematic quantification of accuracy in watershed simulations. *Transactions of the ASABE*, *50*(3), 885–900.

Neitsch, S. L., Arnold, J. G., Kiniry, J. R., & Williams, J. R. (2011). *Soil & Water Assessment Tool Theoretical Documentation*. College Station, TX: Texas Water Resources Institute.

NOAA National Climatic Data Center. (2015). National climatic data center gauge for COOP:338951 - Westerville, OH US [Online]. Washington, DC: NOAA-NCDC. Retrieved from http://www.ncdc.noaa.gov

Ohio Geographically Referenced Information Program. (2006). Ohio Statewide Imagery Program I [Online]. Columbus, OH: OGRIP. Retrieved from http://gis3.oit.ohio.gov/geodatadownload/osip.aspx

Radcliffe, D. E., Reid, D. K., Blombäck, K., Bolster, C. H., Collick, A. S., Easton, Z. M., … Smith, D. R. (2015). Applicability of models to predict phosphorus losses in drained fields: a review. *Journal of Environmental Quality*, *44*(2), 614–628.

Saha, S., Moorthi, S., Wu, X., Wang, J., Nadiga, S., Tripp, P., Behringer, D., Hou, Y., Chuang, H., Iredell, M., Ek, M., Meng, J. , Yang, R. , Mendez, M.P. , van den Dool, H. , Zhang, Q., Wang, W., Chen, M. , Becker, E. (2014). The NCEP Climate Forecast System Version 2. *Journal of Climate*, *27*, 2185–2208.

Skaggs, R. W. (1980). *DRAINMOD Reference Report*. Fort Worth, TX.

Skaggs, R. W., Brevé, M. A., & Gilliam, J. W. (1994). Hydrologic and water quality impacts of agricultural drainage. *Critical Reviews in Environmental Science and Technology*, *24*(1), 1–32.

USDA-NRCS Soil Survey Staff. (2014). Soil Survey Geographic (SSURGO) Database. Retrieved September 15, 2014, from http://sdmdataaccess.nrcs.usda.gov/

Williams, M. R., King, K. W., & Fausey, N. R. (2015a). Contribution of tile drains to basin discharge and nitrogen export in a headwater agricultural watershed. *Agricultural Water Management*, *158*(3), 42–50.

Williams, M. R., King, K. W., & Fausey, N. R. (2015b). Drainage water management effects on tile discharge and water quality. *Agricultural Water Management*, *148*, 43–51.

CHAPTER 4. CONCLUSIONS AND RECOMMENDATIONS

4.1 Conclusions

This study was among the first to examine tile flow and nitrate output from the SWAT model. This is important as tile drainage is a key source for downstream water quality problems as seen in the Gulf of Mexico (David et al., 2010; Skaggs et al., 1994). Computer modeling subsurface drainage is a key tool to assess the effect of different management practices that can influence flow and water quality. Currently SWAT tile drains have been tested for their effectiveness for tile flow at a watershed scale primarily on monthly and annual predications (Boles et al., 2015; Moriasi et al., 2012; Rahman et al., 2011) as well as for tile nitrate predictions (Moriasi et al., 2013a, 2013b; Sui and Frankenberger, 2008). None of these studies have had such rich data sets available for specific tile flow and field data in order to study drainage at a daily scale and the different processes that facilitate this practice.

This study addressed and uncovered multiple shortcomings with the SWAT model. First, the soil water algorithms not only were found to be problematic, but are based off of equations that often have little to no documented theory or physical basis behind them. This was partially addressed through the changes made to percolation, seepage, water table, and tile flow delay in the SWAT algorithms. In addition, many parts of the SWAT algorithms are not accurately represented in the documentation or in the research papers that introduce them. For example, the Moriasi et al. (2011) water table algorithms are not mentioned in the current documentation and are not the same as the equations presented in the journal article introducing the algorithm.

The changes to the SWAT model were implemented on a single tiled field in order to address the soil water balance issues. This is the first study to look at a single tile output with the SWAT model. Although this is not what SWAT was initially designed to do, it is essential for accurate small scale modeling in order to fully trust the large scale basins SWAT was designed to model. It was found the Moriasi et al. (2011) water table algorithms over-predicted water table extremely and the modified algorithms introduced here under-predicted the water table, but successfully predicted the key timing of when the water table moved from above to below the tile drains. Although there was no change to the nitrate subroutines, a decrease in tile nitrate performance was found when implementing the modified algorithms into SWAT.

The changes were expanded onto a small watershed in central Ohio to determine the effects at a larger scale. This is the first time SWAT modeled a watershed where every single tile field output was monitored as well as the watershed output. This allows for a holistic approach to analyze SWAT's ability to predict tile drainage on tiled fields as well as the effects of tiles at the watershed with measured data. It was found these modifications did cause some improvement to the tile drainage predictions from the subbasins. Through a sensitivity analysis on the calibration parameters it was found that the two restrictive layer variables were not extremely sensitive to these new algorithms. Concerns with the nitrate calibration parameters and the algorithms determining nitrate output were also uncovered during this analysis. Phosphorus was plotted and compared to find that the algorithms caused little change and much more work needs to be done to address phosphorus transport through the soil.

4.2 Recommendations for Future Work

In this study, the curve number method is used to determine the amount of water to infiltrate into the soil profile. Many issues have been brought up as the curve number method was not intended for this purpose, and might not be appropriate as it is currently used in modeling (Garen & Moore, 2005). The Green-Ampt infiltration model is more physically based and is available in SWAT. This method requires more detailed information such as hourly rainfall data that is freqently unavaiable across large watersheds. This study, despite hourly rainfall data availability, used the curve number method as it is the more frequently used method. The changes made should be tested with the Green-Ampt infiltration model. Bauwe et al. (2016) compared the Green-Ampt and curve number methods on the current tile drainage subroutines and found minimal changes after calibration. The addition of more physically based tile equations could cause the different methods to have statistically different results.

Although several improvements were proposed, a more comprehensive study is needed to understand and improve how the soil water balance and particularly the water table depth is determined within the soil profile. Improvements are particularly needed when it comes to poorly drained soils. The field capacity, porosity (and therefore saturation), and wilting point calculations are based on clay content, bulk density, and available water capacity. These calculations can be inaccurate for soils with tile drains as the amount of water that does drain from the profile is altered. A further look into the water table calculations is also needed. The changes made here were an improvement to both currently available algorithms, but more changes can be made to further enhance the theoretical basis of the algorithms.

One such change is to increase the value of field capacity, as tile drained fields tend to have a higher field capacity than undrained fields of the same soil type. The commonly used assumption of field capacity being 1/3 bar is not reasonable for poorly drained soils, especially those with tile drains. A more reasonable approximation would be closer to 0.1 bar. For example, Figure 4.1 shows the significant effect of multiplying available water content by 1.25 or 1.5 from the SSURGO database values. The multiplication of available water content effectively multiplies field capacity by the same multiplication factor, because SWAT currently calculates field capacity by adding available water content to the wilting point (also a calculated value in SWAT).

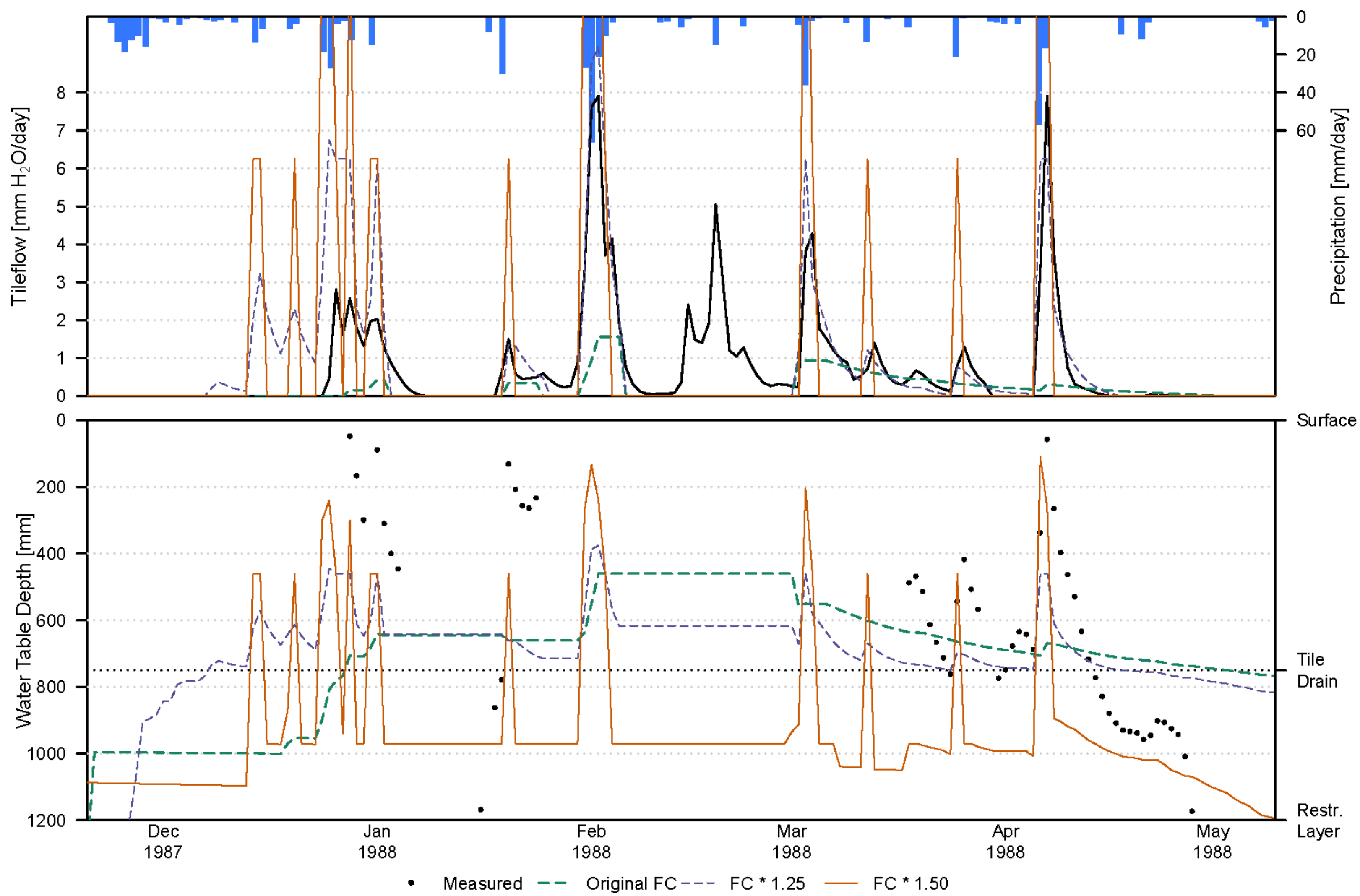

Figure 4.1 Effect of varying Field Capacity (FC) on water table and tile flow for the W20 tile model

Once the water table and drain flow are better predicted, more development is needed for nitrate transport, specifically within tile drains. The small watershed model clearly showed the extreme sensitivity of SDNCO at a small range, and the questionable effect of the other calibration parameters commonly used. In addition, adding subbasin specific nitrate parameters would further enhance the model. Especially when large, the different subbasins will need different calibration parameters in order to perform best, as was shown in the Ohio watershed.

There currently is not an output for tile phosphorus at the subbasin or watershed scale, making it difficult to determine how accurate phosphorus prediction are. Specifically reporting soluble reactive phosphorus, a commonly measured water quality parameter, would add additional usefulness to the model. Currently phosphorus tends to stay in the top soil layer and leaves the soil profile primarily by surface erosion. Determining subsurface phosphorus pathways on a physical basis is needed as phosphorus loading has become a more important issue.

In the future, the modified SWAT should be further tested on a larger variety of watersheds to determine how it simulates tile flow when compared to the original SWAT. The data sets as well as the two parameterized models developed here can be used when developing the model more as their data sets are extremely rich and complete.

The differences in algorithms between those described in the Theoretical Manual (Neitsch et al., 2011) or published papers and those actually in the code made it difficult to understand and then improve the model. These growing differences mean that SWAT users who have not studied the code cannot correctly understand the algorithms. While SWAT was originally very well documented, changes that have been made were not kept up to date. These changes also were not coded in the same manner, causing many redundancies within the program. In many instances, SWAT calculates the same parameter twice, calls the same variable using two different names, and uses the same variables in different subroutines to mean different things.

4.3 Bibliography

Bauwe, A., Kahle, P., & Lennartz, B. (2016). Hydrologic evaluation of the curve number and Green and Ampt infiltration methods by applying Hooghoudt and Kirkham tile drain equations using SWAT. *Journal of Hydrology*, *537*, 311–321.

Boles, C. M. W., Frankenberger, J. R., & Moriasi, D. N. (2015). Tile Drainage Simulation in SWAT2012: Parameterization and Evaluation in an Indiana Watershed. *Transactions of the ASABE*, *58*(5), 1201–1213.

David, M. B., Drinkwater, L. E., & McIsaac, G. F. (2010). Sources of nitrate yields in the Mississippi River Basin. *Journal of Environmental Quality*, *39*(5), 1657–1667.

Garen, D. C., & Moore, D. S. (2005). Curve number hydrology in water quality modeling: Uses, abuses, and future directions. *Journal of the American Water Resources Association*, *41*(2), 377–388.

Moriasi, D. N., Arnold, J. G., Vazquez-Amabile, G. G., & Engel, B. A. (2011). Shallow Water Table Depth Algorithm in SWAT: Recent Develpoments. *Transactions of the ASABE*, *54*(5), 1705–1711.

Moriasi, D. N., Gowda, P. H., Arnold, J. G., Mulla, D. J., Ale, S., & Steiner, J. L. (2013a). Modeling the impact of nitrogen fertilizer application and tile drain configuration on nitrate leaching using SWAT. *Agricultural Water Management*, *130*, 36–43.

Moriasi, D. N., Gowda, P. H., Arnold, J. G., Mulla, D. J., Ale, S., Steiner, J. L., & Tomer, M. D. (2013b). Evaluation of the Hooghoudt and Kirkham Tile Drain Equations in the Soil and Water Assessment Tool to Simulate Tile Flow and Nitrate-Nitrogen. *Journal of Environmental Quality*, *42*(6), 1699.

Moriasi, D. N., Rossi, C. G., Arnold, J. G., & Tomer, M. D. (2012). Evaluating hydrology of the Soil and Water Assessment Tool (SWAT) with new tile drain equations. *Journal of Soil and Water Conservation*, *67*(6), 513–524.

Neitsch, S. L., Arnold, J. G., Kiniry, J. R., & Williams, J. R. (2011). *Soil & Water Assessment Tool Theoretical Documentation*. College Station, TX: Texas Water Resources Institute.

Rahman, M. M., Lin, Z., & Moriasi, D. N. (2011). Applying SWAT for impact analysis of tile drainage on streamflow in a snow dominated watershed. Paper number 1110866. In *ASABE Annual International Meeting* (pp. 4934–4947). Louisville, KY.

Skaggs, R. W., Brevé, M. A., & Gilliam, J. W. (1994). Hydrologic and water quality impacts of agricultural drainage. *Critical Reviews in Environmental Science and Technology*, *24*(1), 1–32.

Sui, Y., & Frankenberger, J. R. (2008). Nitrate Loss From Subsurface Drains in an Agricultural Watershed Using Swat2005. *Transactions of the ASABE*, *51*(4), 1263–1272.

APPENDICES

Appendix A SWAT Algorithm Alterations

A.1 Additional Code in modparm.f

Additions were made in this subroutine to declare any additional variable added during the modifications and needed in multiple subroutines

Addition starting at line 908.

```
!!    Start CAM Adds
      integer :: iimp, iwdn, iwsl ! flags
      real, dimension(:), allocatable :: ksat_imp ! additional inputs
      real, dimension(:,:), allocatable :: sol_sep, sol_exw, sol_ule
          ! additional outputs
      real, dimension (:,:), allocatable :: bc_hb, bc_lam, bc_thr
          ! Brooks Corey Variables

!!    End CAM Adds
```

A.2 Additional Code in allocate_parms.f

Additions were made in this subroutine to define the size of any allocated variable added during the modifications.

Addition starting at line 1799:

```
!!    Start CAM Add
      allocate(ksat_imp(mhru))
      allocate(sol_sep(mlyr,mhru))
      allocate(sol_exw(mlyr,mhru))
      allocate(sol_ule(mlyr,mhru))
      allocate(bc_hb(mlyr,mhru))
      allocate(bc_lam(mlyr,mhru))
      allocate(bc_thr(mlyr,mhru))
!!    End CAM Add
```

A.3 Additional Code in zero2.f

Additions were made in this subroutine to define the initial value of any additional variables added in the modparm.f subroutine to be zero.

Addition starting at line 342:

```
!!    Start CAM Adds
      iimp = 0
      iwdn = 0
      iwsl = 0
      ksat_imp = 0
      sol_sep = 0
      sol_exw = 0
      sol_ule = 0
```

```
      bc_hb = 0
      bc_lam = 0
      bc_thr = 0
!!    End CAM Adds
```

A.4 Additional code in readbsn.f

Additions were made in this subroutine to read in the two new flags IIMP and IWDN from the basins.bsn input file.

Addition starting at line 568.

```
!!    Start CAM Add
      if (eof < 0) exit
      read (103,*,iostat=eof) iimp
      if (eof < 0) exit
      read (103,*,iostat=eof) iwdn
!!    End CAM Add
```

A.5 Additional code in readfile.f

Additions were made in this subroutine to read in the two new flag IWSL from the file.cio input file, create the output file soil_phys.out, and, if IWSL is greater than 0, open the output files sepday.out, satexcess.out, and ulexcess.out.

Addition starting at line 769.

```
!!    Start CAM Add
      read (101,5101) titldum
      read (101,*,iostat=eof) iwsl

      open (4444, file = 'soil_phys.out')
      write (4444,4445)
4445  format (t3,'SUB',t9,'HRU',t13,'LYR',t18,'SOLZmm',t29,'FCmm',
     &    t37,'SATmm',t49,'HK')
      if (iwsl > 0) then !! additional soil water files
          open (1290, file = 'sepday.out')
          write (1290,5002)
5002      format (t20,'Soil Seepage(mm)',/,t15,'Layer #',/,t3,'Day',
     &        t13,'HRU',t28,'1',t40,'2',t52,'3',t64,'4',t76,'5',
     &        t87,'6',t100,'7',t112,'8',t124,'9',t135,'10')
          open (1291, file = 'satexcess.out')
          write (1291,5003)
5003      format (t20,'Excess Water (mm)',/,t15,'Layer #',/,t3,'Day',
     &        t13,'HRU',t28,'1',t40,'2',t52,'3',t64,'4',t76,'5',
     &        t87,'6',t100,'7',t112,'8',t124,'9',t135,'10')
          open (1292, file = 'ulexcess.out')
          write (1292,5004)
5004      format (t20,'Excess Stored (mm)',/,t15,'Layer #',/,t3,'Day',
     &        t13,'HRU',t28,'1',t40,'2',t52,'3',t64,'4',t76,'5',
     &        t87,'6',t100,'7',t112,'8',t124,'9',t135,'10')
```

```
      end if
!!    End CAM Add
```

A.6 Alterations to readhru.f

Alterations were made in this subroutine to read in the new variable KSAT_IMP from all HRU input files.

From: (line 179) `read (108,5100,iostat=eof) titldum`

To: (line 179) `read (108,*,iostat=eof) ksat_imp(ihru)`

A.7 Additional Code in readsol.f

Additions were made in this subroutine to limit the soil profile to the restrictive layer if the new input IIMP was used.

Addition starting at line 180.

```
!!    Start CAM Add
      if (iimp == 1) then
          if (sol_z(nly,ihru) > dep_imp(ihru)) then
              do j = 1, nly
                  if (sol_z(j,ihru) > dep_imp(ihru)) then
                      if (sol_z(j-1,ihru) < dep_imp(ihru)) then
                          sol_nly(ihru) = j
                          nly = j
                          sol_z(j,ihru) = dep_imp(ihru)
                          exit
                      end if
                  end if
              end do
          end if
      end if
!!    End CAM Add
```

A.8 Additional Code in soil_phys.f

Additions were made to calculate the Brooks-Corey parameters for the new seepage algorithms in the percmain.f subroutine.

Addition starting at line 241:

```
!!    Start CAM Add
      if (iimp == 2 .or. iwdn == 1) then
          do ilyr = 1, sol_nly(i)
              bc_s = sol_sand(ilyr,i) / 100
              bc_c = sol_clay(ilyr,i) / 100
              bc_hb(ilyr,i) = Exp(5.3396738 + 0.1845038 * bc_c -
     &            2.48394546 * sol_por(ilyr,i) -
     &            0.00213853 * bc_c ** 2 -
     &            0.04356349 * bc_s * sol_por(ilyr,i) -
     &            0.61745089 * bc_c * sol_por(ilyr,i) +
     &            0.00143598 * bc_s ** 2 * sol_por(ilyr,i) ** 2 -
```

```
&             0.00855375 * bc_c ** 2 * sol_por(ilyr,i) ** 2 -
&             0.00001282 * bc_s ** 2 * bc_c +
&             0.00895359 * bc_c ** 2 * sol_por(ilyr,i) -
&             0.00072472 * bc_s ** 2 * sol_por(ilyr,i) +
&             0.0000054 * bc_c ** 2 * bc_s +
&             0.50028060 * sol_por(ilyr,i) ** 2 * bc_c)
          bc_hb(ilyr,i) = bc_hb(ilyr,i) * 10 ! calibrated eqn in cm
          bc_lam(ilyr,i) = Exp(-0.7842831 + 0.0177544 * bc_s -
&             1.062498 * sol_por(ilyr,i) -
&             0.00005304 * bc_s ** 2 -
&             0.00273493 * bc_c ** 2 +
&             1.11134946 * sol_por(ilyr,i) ** 2 -
&             0.03088295 * bc_s * sol_por(ilyr,i) +
&             0.00026587 * bc_s ** 2 * sol_por(ilyr,i) ** 2 -
&             0.00610522 * bc_c ** 2 * sol_por(ilyr,i) ** 2 -
&             0.00000235 * bc_s ** 2 * bc_c +
&             0.00798746 * bc_c ** 2 * sol_por(ilyr,i) -
&             0.00674491 * sol_por(ilyr,i) ** 2 * bc_c)
          bc_thr(ilyr,i) = -0.0182482 + 0.00087269 * bc_s +
&             0.00513488 * bc_c +
&             0.02939286 * sol_por(ilyr,i) -
&             0.00015395 * bc_c ** 2 -
&             0.0010827 * bc_s * sol_por(ilyr,i) -
&             0.00018233 * bc_c ** 2 * sol_por(ilyr,i) ** 2 +
&             0.00030703 * bc_c ** 2 * sol_por(ilyr,i) -
&             0.0023584 * sol_por(ilyr,i) ** 2 * bc_c
        end do
      end if
!!    End CAM Add
```

A.9 Alterations to hydroinit.f and schedule_ops.f

The same changes were made in both subroutines to remove the effect of the tile drain lag variable.

From: (hydroinit.f lines 139-143 & schedule_ops.f lines 74-78)

```
        if (ldrain(j) > 0 .and. gdrain(j) > 0.01) then
            tile_ttime(j) = 1. - Exp(-24. / gdrain(j))
        else
            tile_ttime(j) = 0.
        end if
```

To: (hydroinit.f lines 139-147 & schedule_ops.f lines 74-82)

```
      if (ldrain(j) > 0 .and. gdrain(j) > 0.01) then
          if (itdrn == 2) then
              tile_ttime = 1
          else
              tile_ttime(j) = 1. - Exp(-24. / gdrain(j))
          end if
      else
```

```
        tile_ttime(j) = 0.
    end if
```

A.10 Changes to percmain.f

Along with the additions mentioned below, the percmain.f subroutine was rewritten and cleaned up for easier reading

A.10.1 Alterations and Additions to add new Water Table Algorithm

The following alteration is to include a third algorithm to be dependent on IWTDN.

From: (Line 218)

```
      else
```

To: (Line 218)

```
        else if (iwtdn == 1) then ! wt_shall using Daniel's eqns
```

The following alteration is the algorithm for the new water table calculation.

Addition starting at line 242:

```
        else if (iwtdn == 2) then ! wt_shall using CAM's eqns
            wtlyr = sol_nly(ihru)
            do ilyr = sol_nly(ihru), 1, -1
                if (sol_st(ilyr,ihru) < 0.95*sol_ul(ilyr,ihru)) then
                    wtlyr = ilyr
                    exit
                end if
            end do
            if (wtlyr == 0) then
                wat_tbl(ihru) = 0
            else
                if(wtlyr == 1) lyrtop = 0
                if(wtlyr > 1)  lyrtop = sol_z(wtlyr-1,ihru)
                wat_tbl(ihru) = sol_z(wtlyr,ihru) -
     &              ((sol_st(wtlyr,ihru) - sol_fc(wtlyr,ihru)) /
     &              (sol_ul(wtlyr,ihru) - sol_fc(wtlyr,ihru))) *
     &              (sol_z(wtlyr,ihru) - lyrtop)
            end if
            wt_shall = dep_imp(ihru) - wat_tbl(ihru)
```

A.10.2 Additional Code

These additions were made to define variables for the additional files satexcess.out (line 151), sepday.out (line 157), and ulexcess.out (line 158)

Addition at line 151: `sol_exw(ilyr,ihru) = sw_excess`

Addition at line 157: `sol_sep(ilyr,ihru) = 0`

Addition at line 158: `sol_ule(ilyr,ihru) = 0`

A.11 Changes to percmicro.f

Along with the additions mentioned below, the percmicro.f subroutine was rewritten and cleaned up for easier reading. The line numbers referenced here are if no other changes were made to the subroutine other than the one referenced at the time.

A.11.1 Alterations to include Darcy and Buckingham Darcy Seepage Algorithm

From: (Lines 126-130)

```
sol_hk(ly1,j) = Max(2., sol_hk(ly1,j))

!! compute seepage to the next layer
sepday = 0.
sepday = sw_excess * (1. - Exp(-24. / sol_hk(ly1,j)))
```

To: (Lines 126-147)

```
if (iwdn == 0) then ! original calculation
    sol_hk(ilyr,ihru) = Max(2., sol_hk(ilyr,ihru))

!!  compute seepage to the next layer
    sepday = 0.
    sepday = sw_excess * (1. - Exp(-24. / sol_hk(ilyr,ihru)))
else if (iwdn == 1) then ! new seepage calculation
    if (ilyr == 1) z = sol_z(ilyr,ihru)
    if (ilyr > 1) z = sol_z(ilyr,ihru) - sol_z(ilyr-1,ihru)
    sepday = 0.
    if (sol_st(ilyr,ihru) > 0.95 * sol_ul(ilyr,ihru)) then
        sepday = sol_k(ilyr,ihru) * 24.
    else
        bc_th = sol_st(ilyr,ihru) / z + sol_wp(ilyr,ihru)
        se = (bc_th - bc_thr(ilyr,ihru)) /
&           (sol_por(ilyr,ihru) - bc_thr(ilyr,ihru))
        n = 3 + 2 / bc_lam(ilyr,ihru)
        sol_kun = sol_k(ilyr,ihru) * se ** n
        sepday = sol_st(ilyr,ihru) / z * sol_kun * 24.
   end if
    sepday = min(sw_excess, sepday)
end if
```

A.11.2 Alterations to include new Seepage Algorithm

From: (Lines 138-146)

```
!! restrict seepage if next layer is saturated
if (ly1 == sol_nly(j)) then
  xx = (dep_imp(j) - sol_z(ly1,j)) / 1000.
  if (xx < 1.e-4) then
    sepday = 0.
  else
    sepday = sepday * xx / (xx + Exp(8.833 - 2.598 * xx))
```

```
        end if
      end if
```

To: (Lines 138-150)

```
!!    restrict seepage if at bottom of profile
      if (ilyr == sol_nly(ihru)) then
          if (iimp == 1) then
              sepday = min(sepday, ksat_imp(ihru))
          else
              xx = (dep_imp(ihru) - sol_z(ilyr,ihru)) / 1000.
              if (xx < 1.e-4) then
                  sepday = 0.
              else
                  sepday = sepday * xx / (xx + Exp(8.833 - 2.598 * xx))
              end if
          end if
      end if
```

A.11.3 Additional Code

These additions were made to define variables for the additional file sepday.out.

Addition at line 163: `sol_sep(ilyr,ihru) = sepday`

A.12 Additional code in sat_excess.f

The sat_excess.f subroutine was rewritten and cleaned up for easier reading. Additions were made to define variables for the additional file ulexcess.out.

Addition at line 140: `sol_ule(ilyr,ihru) = sol_ule(ilyr,ihru) + ul_excess`

Addition starting at line 157:

```
                              sol_ule(ilyr,ihru) = sol_ule(ilyr,ihru)
     &                              + ul_excess
```

A.13 Additional Code in hruday.f90

Additions were made in this subroutine to write out the correct data to the new output files soil_phys.out.

Addition starting at line 540.

```
!!    Start CAM Add
    !! write out soil water properties
    ly2 = sol_nly(j)
    if ((iida == 1) .and. (curyr == nyskip + 1)) then
        write (4444, 4446) sb, j, 0, sol_z(ly2,j), sol_sumfc(j),
sol_sumul(j)
        do ly = 1, sol_nly(j)
            write (4444, 4447) sb, j, ly, sol_z(ly,j), sol_fc(ly,j),
sol_ul(ly,j), sol_hk(ly,j)
        end do
    end if
```

```
4446    format (i5,1x,i5,1x,i3,1x,f7.1,1x,f8.3,1x,f8.3)
4447    format (i5,1x,i5,1x,i3,1x,f7.1,1x,f8.3,1x,f8.3,1x,f8.3)
!!     End CAM Add
```

A.14 Additonal Code in writed.f

Additions were made in this subroutine to write out the correct data to the new output files sepday.out, satexcess.out, and ulexcess.out if IWSL is greater than 0.

Addition starting at line 176:

```
!!     Start CAM Add
       if (iwsl > 0) then !! additional soil water files
           do j = 1, nhru
               write (1290,5000) iida, j,
     &             (sol_sep(j1,j), j1 = 1, sol_nly(j))
               write (1291,5000) iida, j,
     &             (sol_exw(j1,j), j1 = 1, sol_nly(j))
               write (1292,5000) iida, j,
     &             (sol_ule(j1,j), j1 = 1, sol_nly(j))
           enddo
       end if
!!     End CAM Add
```

Appendix B R-Scripts Used in Processing

B.1 User Defined Functions

B.1.1 Read output.rch file

```
read.rch <- function(file.name){
      col.name <- c('V1','RCH','GIS','MO','DA','YR','AREA','FLOW_IN',
            'FLOW_OUT','EVAP','TLOSS','SED_IN','SED_OUT','SEDCONC',
            'ORGN_IN','ORGN_OUT','ORGP_IN','ORGP_OUT','NO3_IN',
            'NO3_OUT','NH4_IN','NH4_OUT','NO2_IN','NO2_OUT','MINP_IN',
            'MINP_OUT','CHLA_IN','CHLA_OUT','CBOD_IN','CBOD_OUT',
            'DISOX_IN','DISOX_OUT','SOLPST_IN','SOLPST_OUT',
            'SORPST_IN','SORPST_OUT','REACTPST','VOLPST','SETTLPST',
            'RESUSP_PST','DIFFUSEPST','REACBEDPST','BURYPST','BED_PST',
            'BACTP_OUT','BACTLP_OUT','CMETAL1','CMETAL2','CMETAL3',
            'TOT_N','TOT_P','NO3Conc','WTMPdegc')
      temp <- read.fwf(file = file.name, skip = 9, header = FALSE,
            widths = c(5,5,9,4,3,5,13,rep(12,46)),
            colClasses = c(rep('factor',3),rep('numeric',50)))
      colnames(temp) <- col.name
      temp$RCH <- gsub(" ", "", temp$RCH)
      temp$Date <- with(temp, as.Date(paste(YR,MO,DA,sep='-')))
      return(temp)
}
```

B.1.2 Read output.sub file

```
read.sub <- function(file.name){
      col.name <- c('V1','SUB','GIS','MO','DA','YR','AREA','PRECIP',
            'SNOMELT','PET','ET','SW','PERC','SURQ','GW_Q','WYLD',
            'SYLD','ORGN','ORGP','NSURQ','SOLP','SEDP','LATQ','LATNO3',
            'GWNO3','CHOLA','CBODU','DOXQ','QTILE','TNO3','TVAP')
      temp <- read.fwf(file = file.name, skip = 10, header = FALSE,
            widths = c(6,4,9,3,3,5,11,rep(10,18),11,rep(10,5)),
            colClasses = c(rep('factor',3),rep('numeric',28)))
      colnames(temp) <- col.name
      temp$SUB <- gsub(" ", "", temp$SUB)
      temp$Date <- with(temp, as.Date(paste(YR,MO,DA,sep='-')))
      return(temp)
}
```

B.1.3 Read output.swr, sepday.out, swexcess.out, or ulexcess.out

```
read.swr <- function(file.name, year.start){
      col.name <- c('Day','HRU',paste0('Lyr',1:10))
      temp <- read.fwf(file = file.name, skip = 3, header = FALSE,
            widths = c(5,6,13,rep(12,9)),
            colClasses = c('numeric','factor',rep('numeric',10)))
      colnames(temp) <- col.name
      temp <- temp[, !apply(is.na(temp), 2, all)]
```

```
	temp$HRU <- gsub(" ", "", temp$HRU)
	temp$Yr <- -1
	temp$Yr[1] <- year.start
	for (i in 2:nrow(temp)){
		temp$Yr[i] <- with(temp,
			ifelse(Day[i] > Day[i-1], Yr[i-1], Yr[i-1]+1))
	}
	temp$Date <- with(temp, as.Date(paste(Yr,Day,sep='-'),
		format = '%Y-%j'))
	return(temp)
}
```

B.1.4 Read soil_phys.out

```
read.slp <- function(file.name){
	temp <- read.table(file.name, header = TRUE, sep = '', fill = T)
	return(temp)
}
```

B.1.5 Run SWAT Executable

```
run.swat <- function(input.folder, exe.name = 'rev638_debug'){
	output.files <- c('output.hru','output.mgt','output.pst',
		'output.rch','output.rsv','output.sed','output.snu',
		'output.std','output.sub','output.swr','output.wql',
		'soil_phys.out','sepday.out','satexcess.out',
		'ulexcess.out')
	setwd(paste0(home.wd,'/', input.folder))
	file.remove(output.files[file.exists(output.files)])
	system(paste0(home.wd,'/SWATExecutables/',exe.name))
	output.folder <- paste0('Out_',exe.name)
	if (!file.exists(output.folder)){dir.create(output.folder)}
	file.copy(from = output.files[file.exists(output.files)],
		to = output.folder, overwrite = T)
	setwd(home.wd)
}
```

B.1.6 Alter SWAT Input (for algorithm flags)

```
alter.swat.flag <- function(input.folder, itdrn, iwtdn, iimp, iwdn,
	iwsl = NA){
	temp <- readLines(paste0(input.folder,'/basins.bsn'))
	if(!is.na(itdrn)){
		temp[123] <- gsub(substr(temp[123],16,16),itdrn,temp[123])
	}
	if(!is.na(iwtdn)){
		temp[124] <- gsub(substr(temp[124],16,16),iwtdn,temp[124])
	}
	if(!is.na(iimp)){
		temp[132] <- gsub(substr(temp[132],16,16),iimp,temp[132])
	}
	if(!is.na(iwdn)){
		temp[133] <- gsub(substr(temp[133],16,16),iwdn,temp[133])
```

```
      }
      writeLines(temp,paste0(input.folder,'/basins.bsn'))
      if(!is.na(iwsl)){
            temp <- readLines(paste0(input.folder,'/file.cio'))
            temp[87] <- gsub(substr(temp[87],16,16), iwsl, temp[87])
            writeLines(temp,paste0(input.folder,'/file.cio'))
      }
}
```

B.1.7 Alter SWAT Input (for calibration)

```
alter.swat.calib <- function(input.folder, calib.var, calib.type,
calib.chg){
      if(calib.var %in% c('DEP_IMP','KSAT_IMP')){
            type <- '.hru'
      } else if(calib.var %in% c('CN')){
            type <- '.mgt'
      } else if(calib.var %in% c('LATKSATF')){
            type <- '.sdr'
      } else if (calib.var %in% c('CMN','NPERCO','SDNCO')){
            type <- '.bsn'
      }
      calib.files <- list.files(input.folder, pattern = type)
      calib.files <- calib.files[calib.files != paste0('output', type)]
      for(file in calib.files){
            temp <- readLines(paste0(input.folder, '/', file ))
            line.old <- grep(calib.var, temp, value = TRUE)
            var.old <- gsub(' ', '', substr(line.old, 1, 16))
            if(calib.type == 'val'){
                  var.new <- calib.chg
            } else if(calib.type == 'pct'){
                  var.new <- as.numeric(var.old) * (1 + calib.chg/100)
            }
            decimal <- grep('.*\\.', var.old)
            if(length(decimal) > 0){
                  var.new <- sprintf(paste0('%.', nchar(decimal),'f'),
                        round(var.new, nchar(decimal)))
            } else {
                  var.new <- round(var.new, 0)
            }
            var.new <- paste0(paste0(rep(' ', 16 - nchar(var.new)),
                  collapse = ''), var.new)
            line.new <- gsub(substr(line.old,1,16), var.new, line.old)
            temp[grep(calib.var, temp)] <- line.new
            writeLines(temp, paste0(input.folder, '/', file ))
      }
}
```

B.2 Create a new set of inputs from another

```
## SCRIPT INPUTS
```

```
input.new <- 'SmallWatershed/B_Original/PostCalib_NO3_Orig'
input.old <- 'SmallWatershed/B_Original/PostCalib_TF_Orig'
# input changes (type is "pct" or "val")
NPERCO <- c('val', 0.85)
SDNCO <- c('val', 1)

## vars to edit
cal.var <- c('DEP_IMP','KSAT_IMP','CN','LATKSATF','NPERCO','SDNCO')

## Create new folder and copy old input over
if (!file.exists(input.new)){dir.create(input.new)}
for(file in list.files(input.old)){
	file.copy(paste0(input.old, '/', file),
		paste0(input.new, '/', file))
}

## Alter SWAT inputs
for(var in cal.var){
	if (exists(var)){
		alter.swat.calib(input.folder = input.new,
			calib.var = var, calib.type = get(var)[1],
			calib.chg = as.numeric(get(var)[2]))
	}
}

# write out meta data
meta <- c(paste('meta data for SWAT input files in folder:',input.new),
	paste('Source Files:', input.old), 'Value Changes:')
for(var in cal.var){
	if (exists(var)){
		meta <- c(meta, paste(var, 'changed to',
			get(var)[2], '(', get(var)[1], ')'))
	}
}
writeLines(meta, paste0(input.new, '/meta.txt'))
```

B.3 Extract SWAT executable and subroutines from FORTRAN Compiler and save in Repository

```
# name for new executable
store.name <- 'rev638_modified' # name of new executable

# source and store locations
source <- paste0(home.wd,'SWAT_Edited')
source.exe <- paste0(source,'/SWAT_Edited/x64/Debug/SWAT_Edited.exe')
source.folder <- paste0(source,'/rev638_code')
store.folder <- paste0(home.wd,'SWATExecutables')

# move executable to [store.folder] and rename
```

```
file.copy(from = source.exe, to =
paste0(store.folder,'/',store.name,'.exe'),
      overwrite = TRUE)

# move outputs to [store.name] folder in [store.folder]
dir.create(paste0(store.folder,'/',store.name))
file.copy(from = list.files(source.folder, full.names = TRUE),
      to = paste0(store.folder,'/',store.name), overwrite = TRUE)

# remove excess files
rm(store.name, source, source.exe, source.folder, store.folder)
```

B.4 Run SWAT and Save Outputs Based on Input Flags

```
## run executables
input.folders <- c('SmallWatershed/B_Original/PostCalib_NO3_Orig')

input.flags <- data.frame(c(1),c(1),c(0),c(0),c(1))
exe <- c('rev638_modified')

# SWAT output files to copy
output.files <- c('input.std','output.hru','output.mgt','output.pst',
      'output.rch','output.rsv','output.sed','output.snu','output.std',
      'output.sub','output.swr','output.wql', 'soil_phys.out',
      'sepday.out','satexcess.out','ulexcess.out')

# for each input.folder run each exe.names and copy outputs over
for (input in input.folders) {
      for (i in 1:nrow(input.flags)){
            alter.swat.flag(input.folder = input,
                  itdrn = input.flags[i,1], iwtdn = input.flags[i,2],
                  iimp = input.flags[i,3], iwdn = input.flags[i,4],
                  iwsl = input.flags[i,5])
            file.remove(output.files[file.exists(output.files)])
            run.swat(input.folder = input, exe.name = exe)
            output.folder <- paste0(input,'/Flag_',
                  paste0(input.flags[i,], collapse = '_'))
            file.rename(from = paste0(input,'/Out_',exe),
                  to = output.folder)
      }
}
rm(input, i, output.folder)

setwd(home.wd) # reset working directory
rm(input.folders, exe, output.files, input.flags) #remove leftover vars
```

B.5 Calibration Script for SEPAC Tile Flow

This script is representative of all the calibration scripts used in this study

```
## SCRIPT INPUTS
site <- 'W20'
```

```
base <- 'PostCalib_TF_Mod'

# input changes (type is "pct" or "val")
cal.var <- list('NPERCO', 'SDNCO', 'CMN')
cal.type <- list('val', 'val', 'val')
cal.chg <- list(seq(0.055,0.1,0.005),c(2),c(0.0003))
cal.yrs <- 1988:1989
cal.combo <- do.call(expand.grid, cal.chg)

exe <- 'rev638_modified'
inp.flags <- data.frame(c(2),c(2),c(1),c(1),c(0))

inp.old <- paste0('SingleTile/', site, '_Original/', base)
inp.new <- paste0(inp.old, '/Calib_Out')
if (!file.exists(inp.new)){dir.create(inp.new)}

## Set Up Observed
data.base <- in.measured[,c('Date',site)]
names(data.base)[names(data.base) == site] <- 'QTILEObs'
data.base$QTILEObs <- data.base$QTILEObs * 10 # convert to mm

## list files
inp.ls <- list.files(inp.old)[!(list.files(inp.old) == 'Thumbs.db' |
      list.files(inp.old) %in% list.dirs(inp.old, full.names = F))]

for (i in 1:nrow(inp.flags)){ ## for each model version

      # set up stats table
      cal.stat <- data.frame(matrix(nrow = 0,
            ncol = (length(cal.var) + 2)))
      colnames(cal.stat) <- c(cal.var, 'NSE', 'PBIAS')

      for(c in 1:nrow(cal.combo)){ ## for each variable combo

            # copy over files
            for(file in inp.ls){
                  file.copy(paste0(inp.old,'/',file),
                        paste0(inp.new,'/',file),overwrite = TRUE)
            }

            # set up flags
            alter.swat.flag(input.folder = inp.new,
                  itdrn = inp.flags[i,1], iwtdn = inp.flags[i,2],
                  iimp = inp.flags[i,3], iwdn = inp.flags[i,4],
                  iwsl = inp.flags[i,5])

            # set up variables
            for (v in 1:length(cal.var)){
```

```
                alter.swat.calib(input.folder = inp.new,
                      calib.var = cal.var[v],
                      calib.type = cal.type[v],
                      calib.chg = cal.combo[c,v])
          }

          run.swat(input.folder = inp.new, exe.name = exe)

          ## set up data
          data.chng <- read.sub(paste0(inp.new,
                '/Out_',exe,'/output.sub'))
          data <- merge(data.base, data.chng, by = 'Date')
          data <- data[format(data$Date,'%Y') %in% cal.yrs,]

          ## compare
          cal.nse <- NSE(sim = data$QTILE, obs = data$QTILEObs)
          cal.pbias <- pbias(sim = data$QTILE, obs = data$QTILEObs)
          cal.stat[c,] <- c(cal.combo[c,], cal.nse, cal.pbias)
    }
    write.csv(cal.stat, paste0(inp.new, '/Flag_',
          paste(inp.flags[i,], collapse = '_'),'.csv'))
}
```

Appendix C Additional Sensitivity Graphs for Watershed B

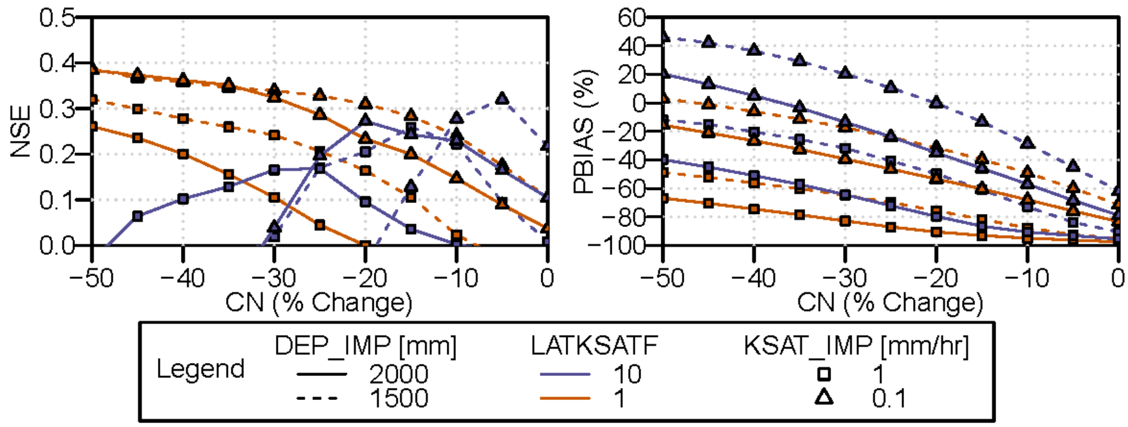

Figure C.1 Modified SWAT tile flow sensitivity curves for CN in subbasin B3

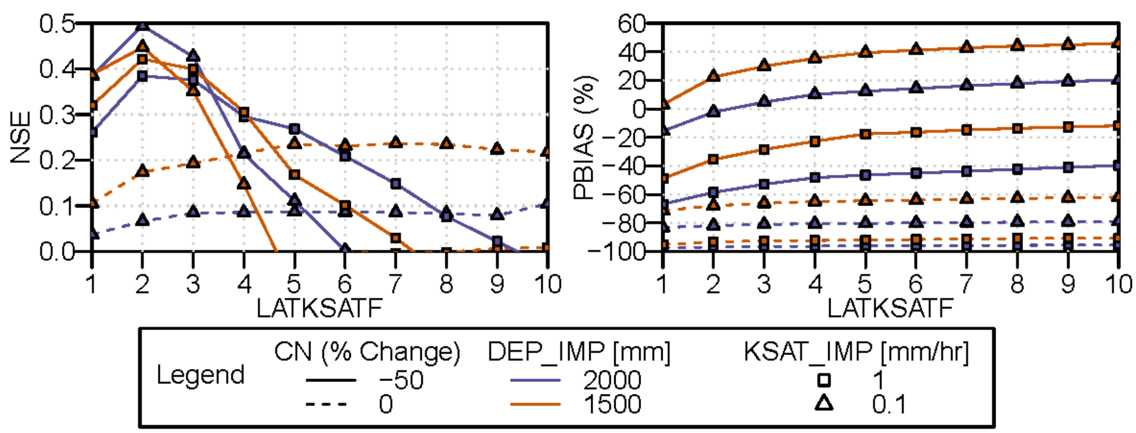

Figure C.2 Modified SWAT tile flow sensitivity curves for LATKSATF in subbasin B3

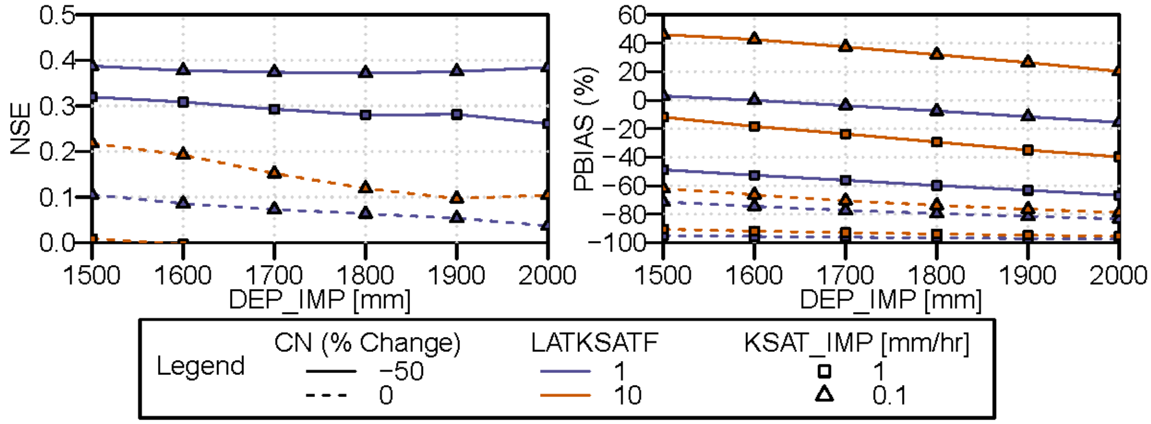

Figure C.3 Modified SWAT tile flow sensitivity curves for DEP_IMP in subbasin B3

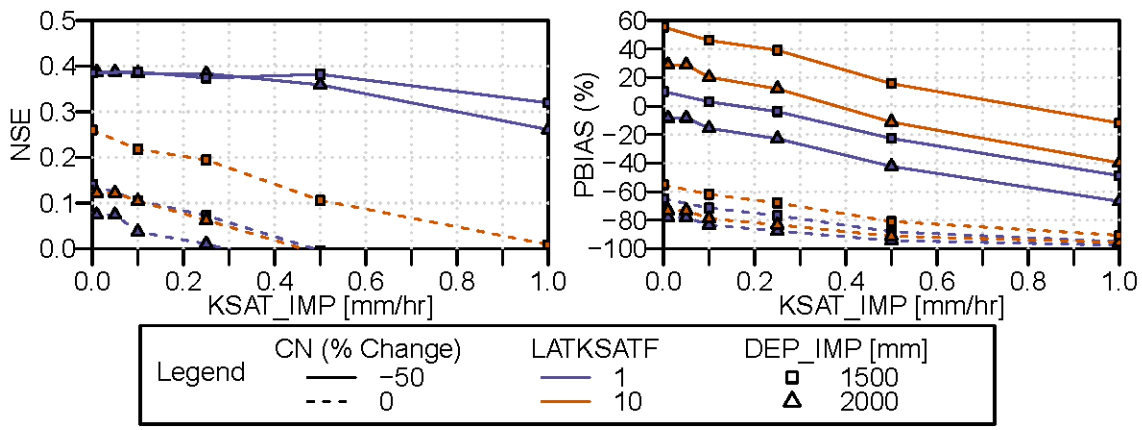

Figure C.4 Modified SWAT tile flow sensitivity curves for KSAT_IMP in subbasin B3

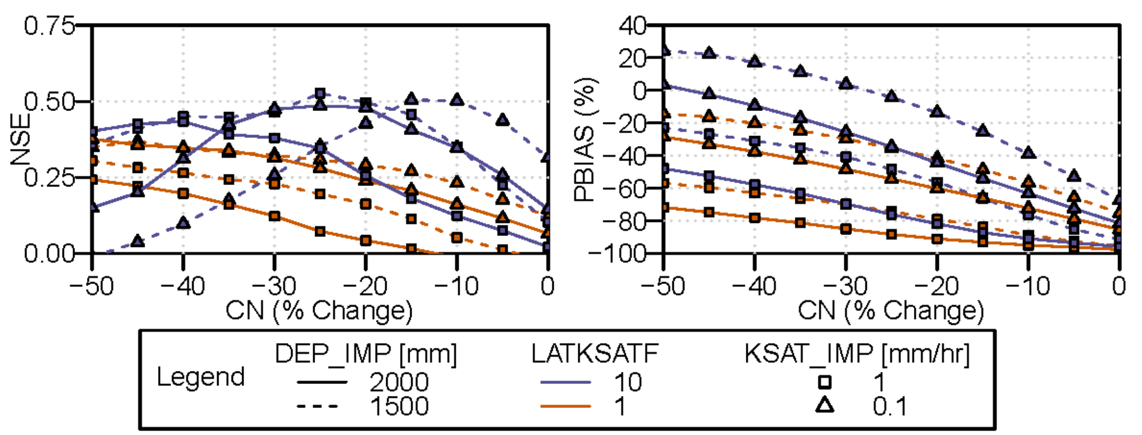

Figure C.5 Modified SWAT tile flow sensitivity curves for CN in subbasin B4

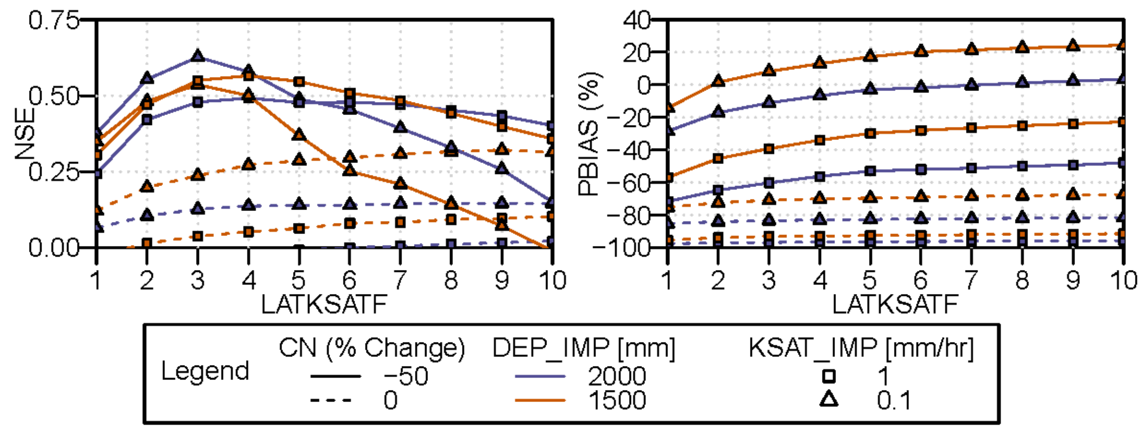

Figure C.6 Modified SWAT tile flow sensitivity curves for LATKSATF in subbasin B4

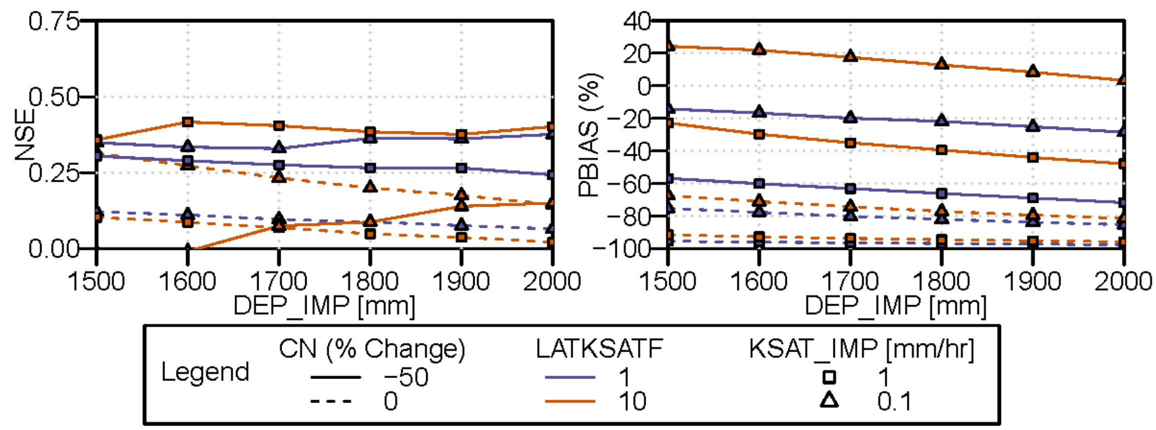

Figure C.7 Modified SWAT tile flow sensitivity curves for DEP_IMP in subbasin B4

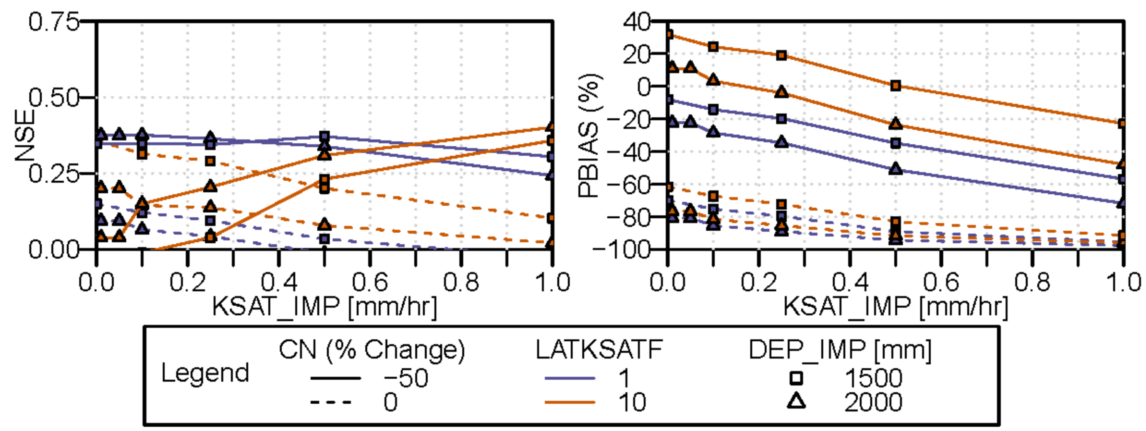

Figure C.8 Modified SWAT tile flow sensitivity curves for KSAT_IMP in subbasin B4

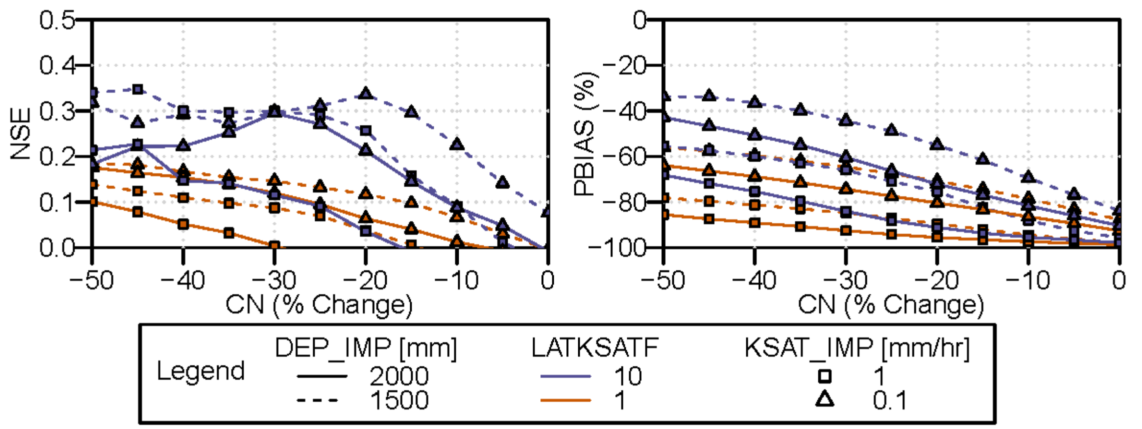

Figure C.9 Modified SWAT tile flow sensitivity curves for CN in subbasin B5

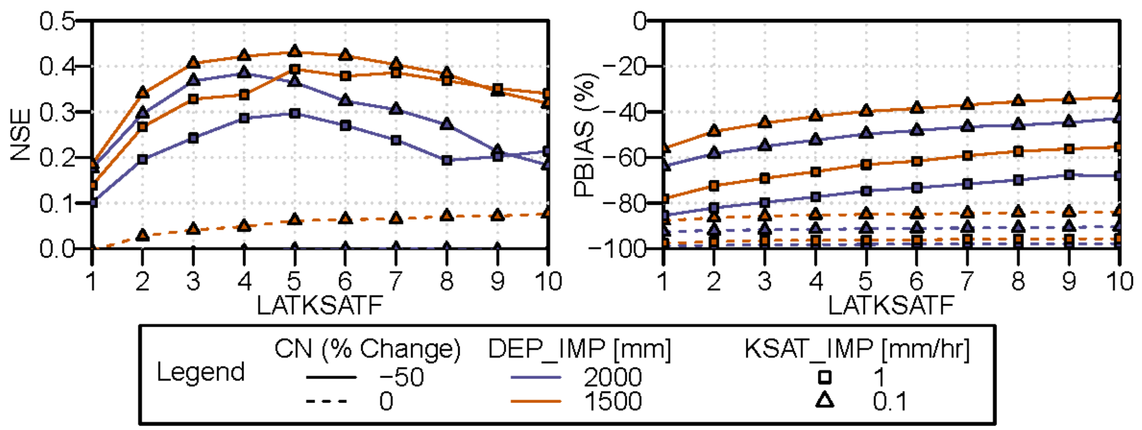

Figure C.10 Modified SWAT tile flow sensitivity curves for LATKSATF in subbasin B5

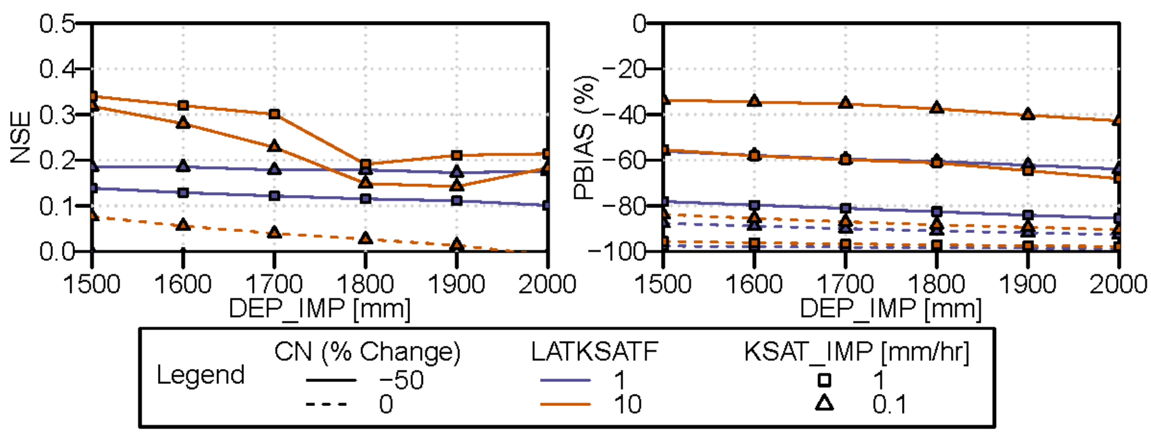

Figure C.11 Modified SWAT tile flow sensitivity curves for DEP_IMP in subbasin B5

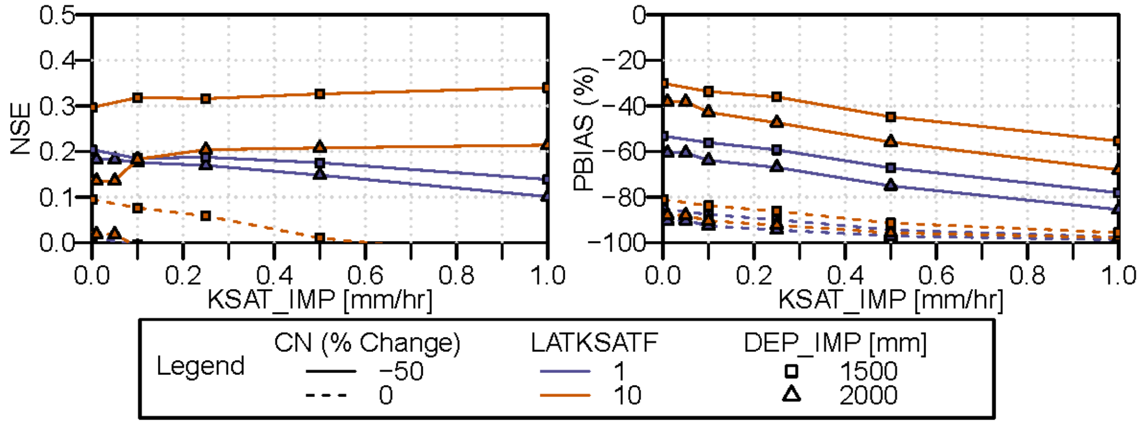

Figure C.12 Modified SWAT tile flow sensitivity curves for KSAT_IMP in subbasin B5

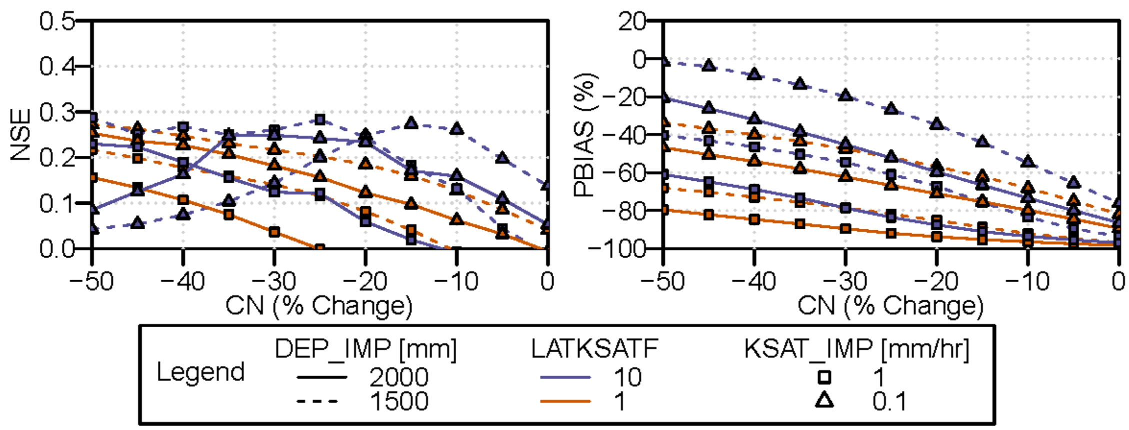

Figure C.13 Modified SWAT tile flow sensitivity curves for CN in subbasin B6

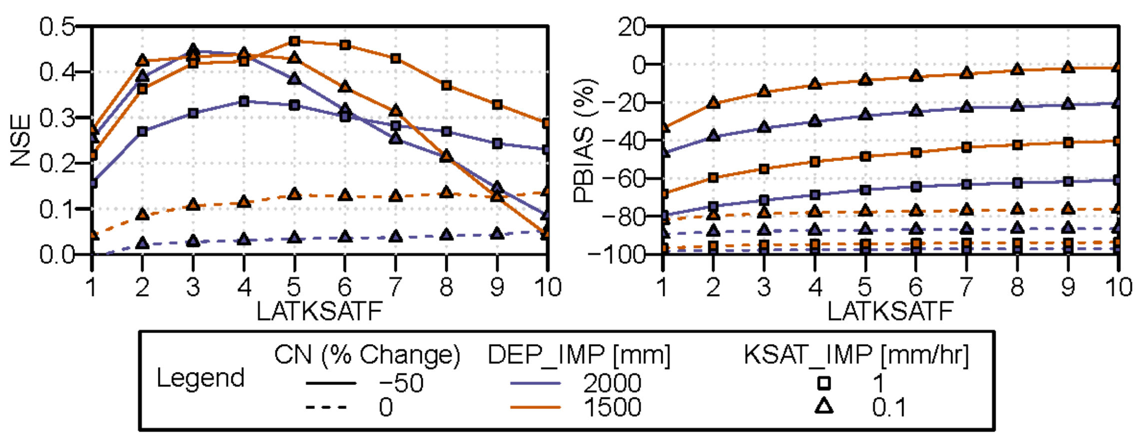

Figure C.14 Modified SWAT tile flow sensitivity curves for LATKSATF in subbasin B6

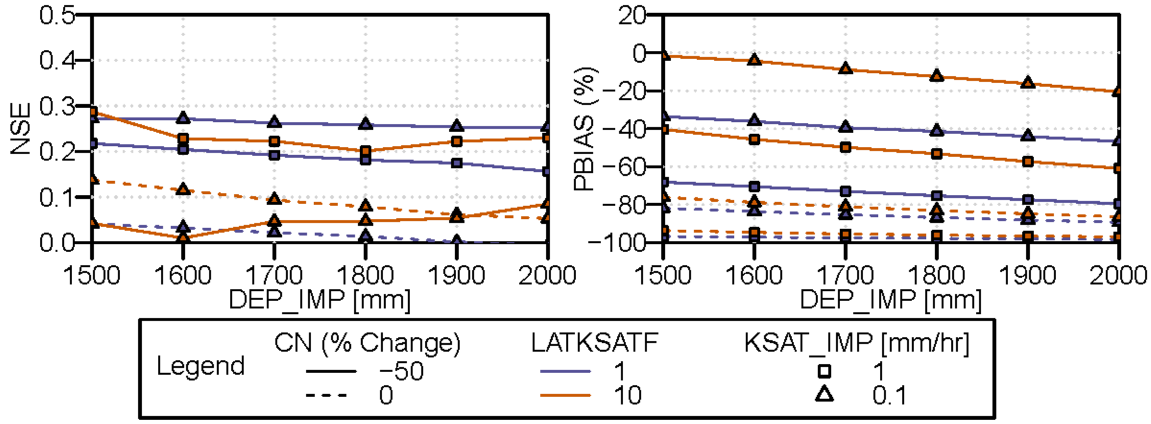

Figure C.15 Modified SWAT tile flow sensitivity curves for DEP_IMP in subbasin B6

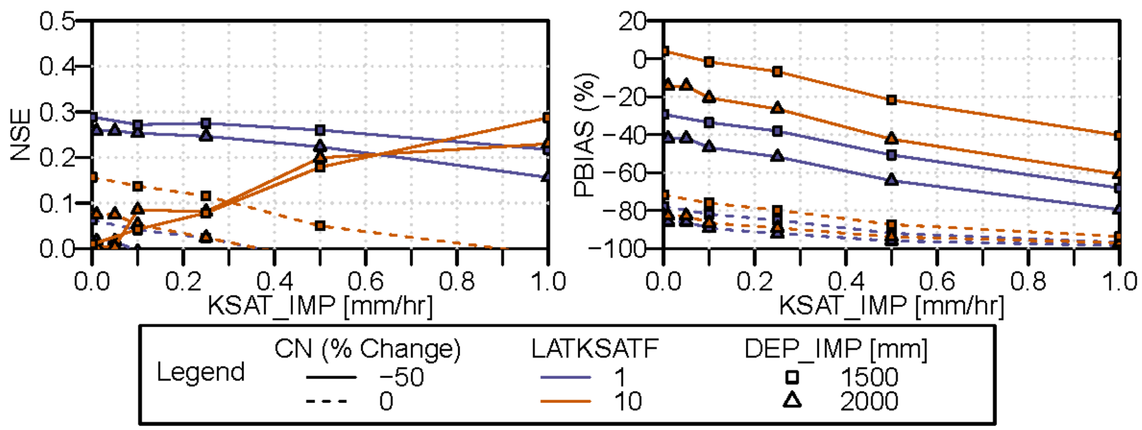

Figure C.16 Modified SWAT tile flow sensitivity curves for KSAT_IMP in subbasin B6

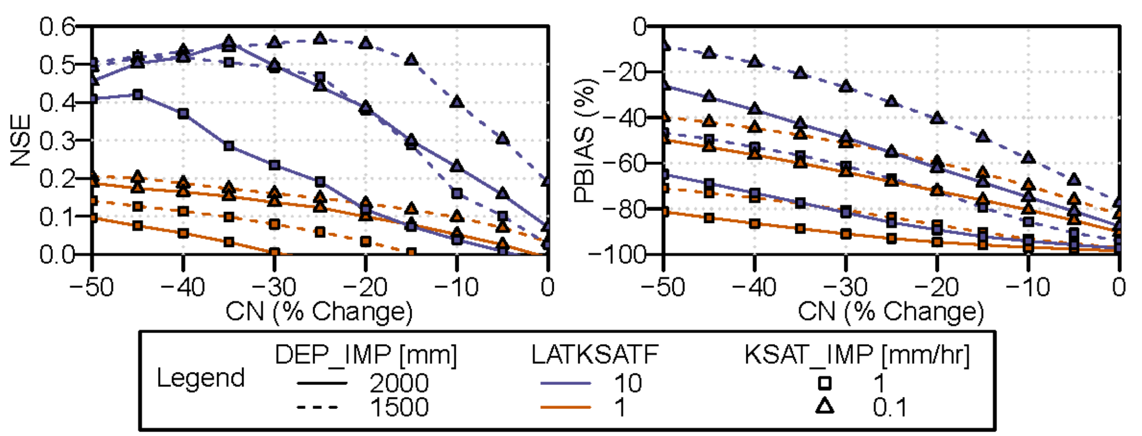

Figure C.17 Modified SWAT tile flow sensitivity curves for CN in subbasin B8

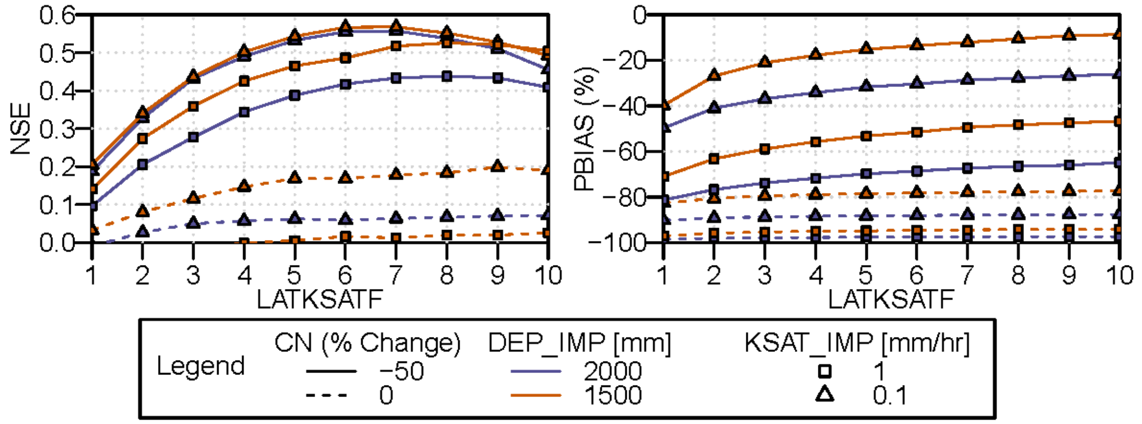

Figure C.18 Modified SWAT tile flow sensitivity curves for LATKSATF in subbasin B8

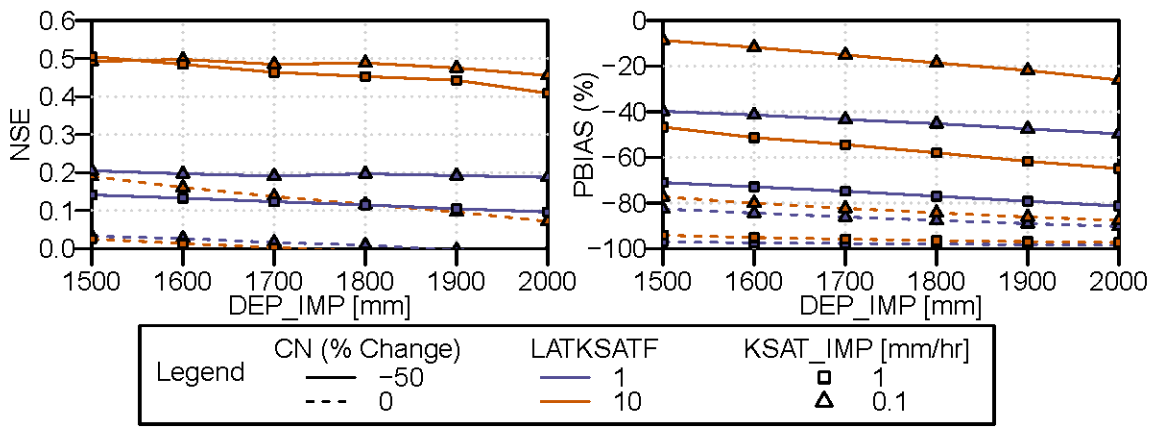

Figure C.19 Modified SWAT tile flow sensitivity curves for DEP_IMP in subbasin B8

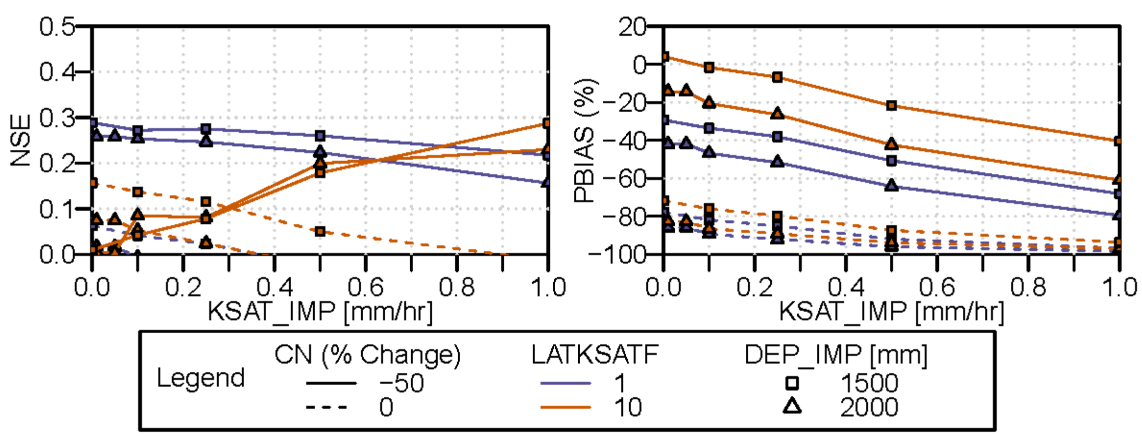

Figure C.20 Modified SWAT tile flow sensitivity curves for KSAT_IMP in subbasin B8

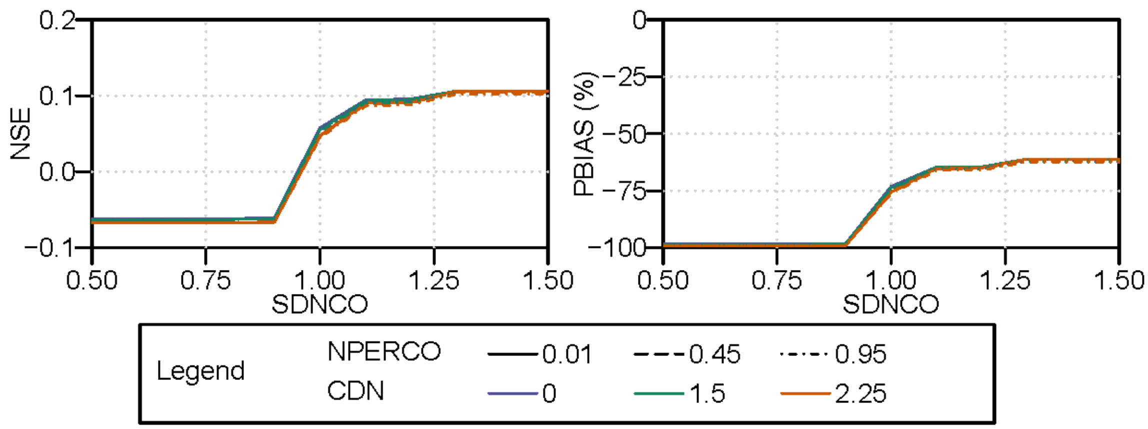

Figure C.21 Modified SWAT tile nitrate sensitivity curves for SDNCO in subbasin B2

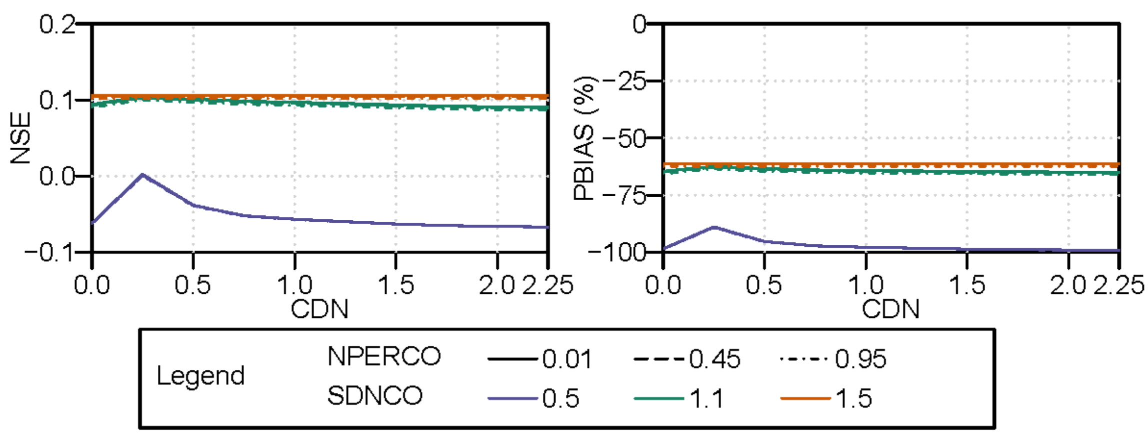

Figure C.22 Modified SWAT tile nitrate sensitivity curves for CDN in subbasin B2

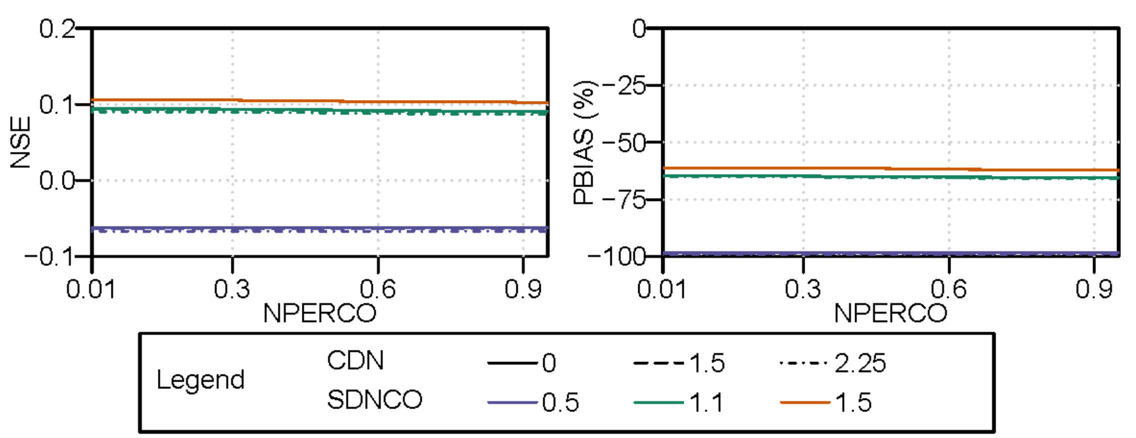

Figure C.23 Modified SWAT tile nitrate sensitivity curves for NPERCO in subbasin B2

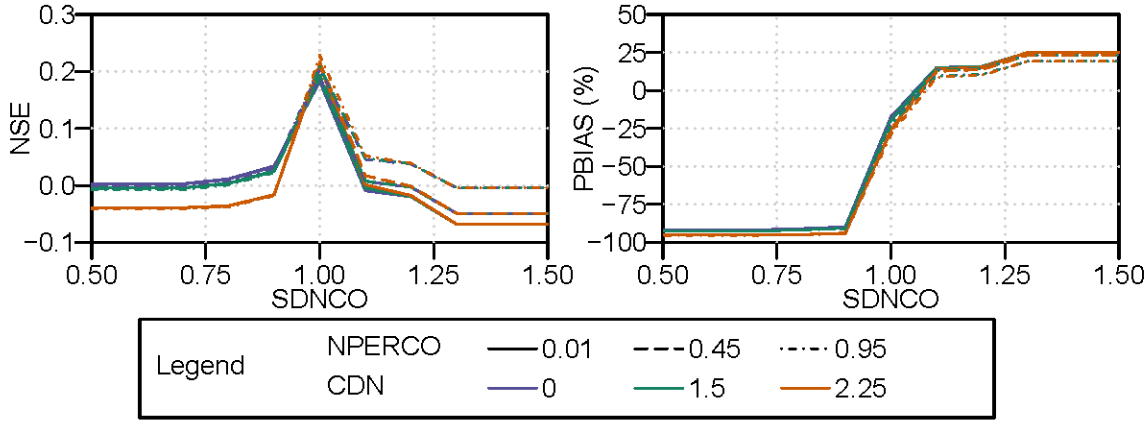

Figure C.24 Modified SWAT tile nitrate sensitivity curves for SDNCO in subbasin B3

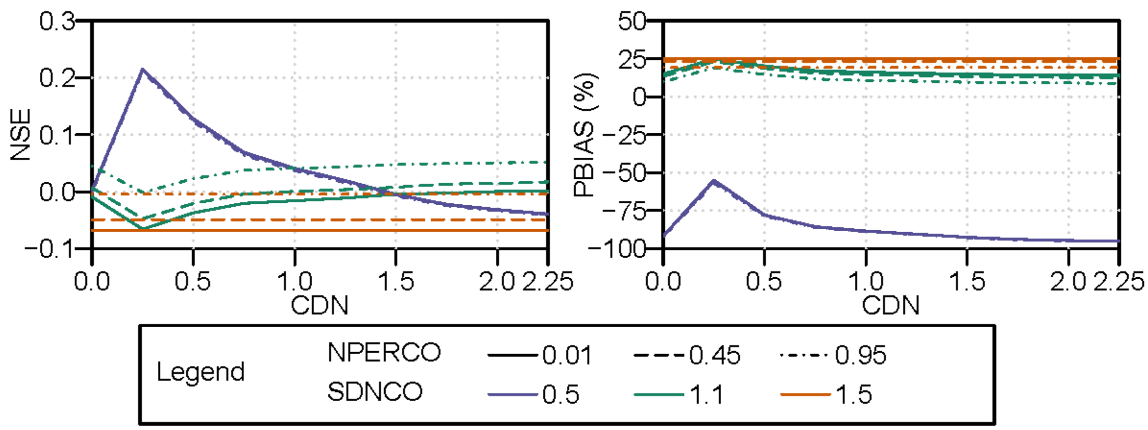

Figure C.25 Modified SWAT tile nitrate sensitivity curves for CDN in subbasin B3

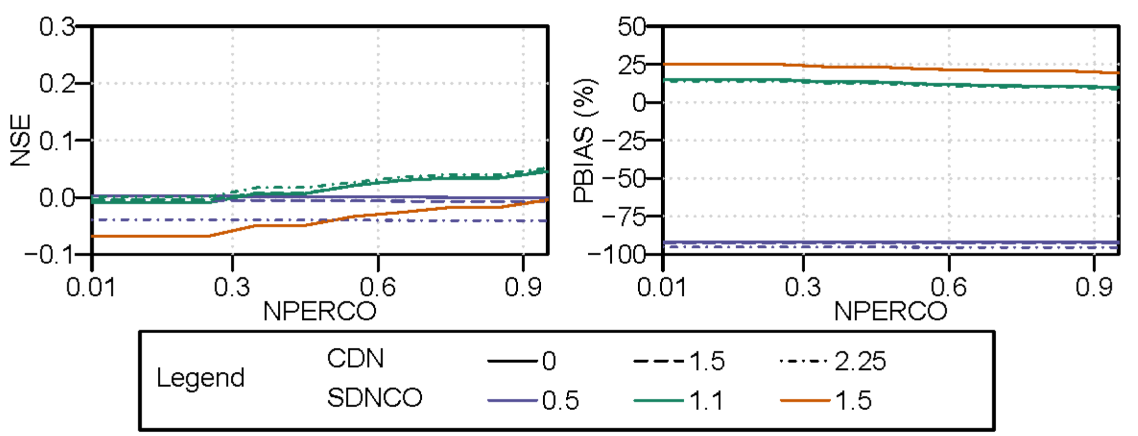

Figure C.26 Modified SWAT tile nitrate sensitivity curves for NPERCO in subbasin B3

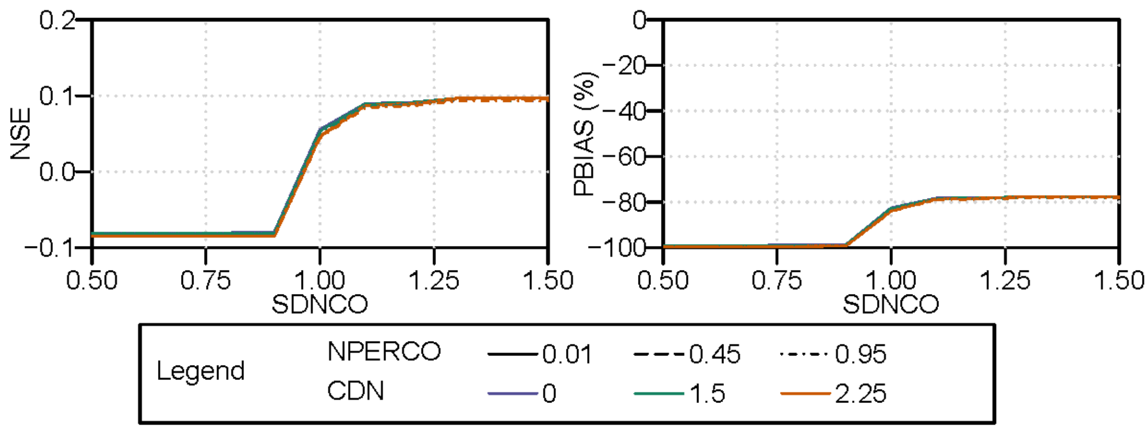

Figure C.27 Modified SWAT tile nitrate sensitivity curves for SDNCO in subbasin B4

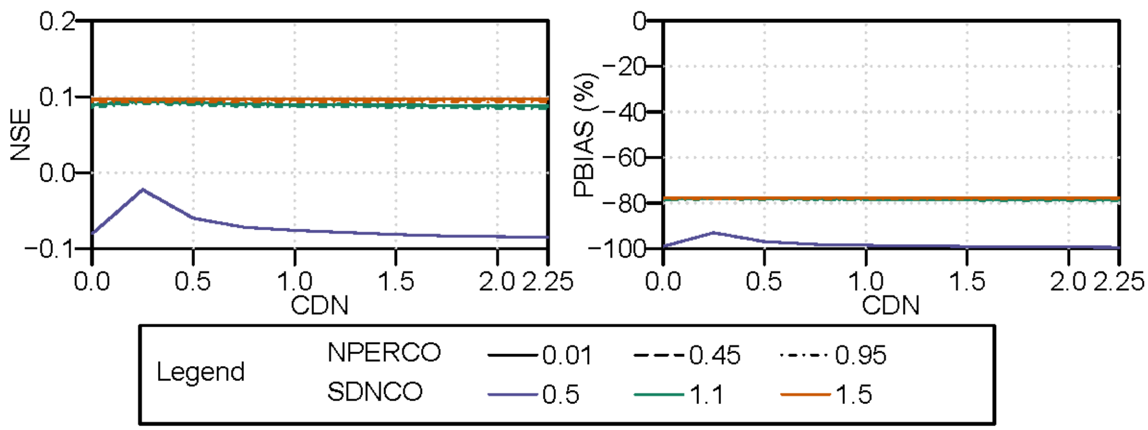

Figure C.28 Modified SWAT tile nitrate sensitivity curves for CDN in subbasin B4

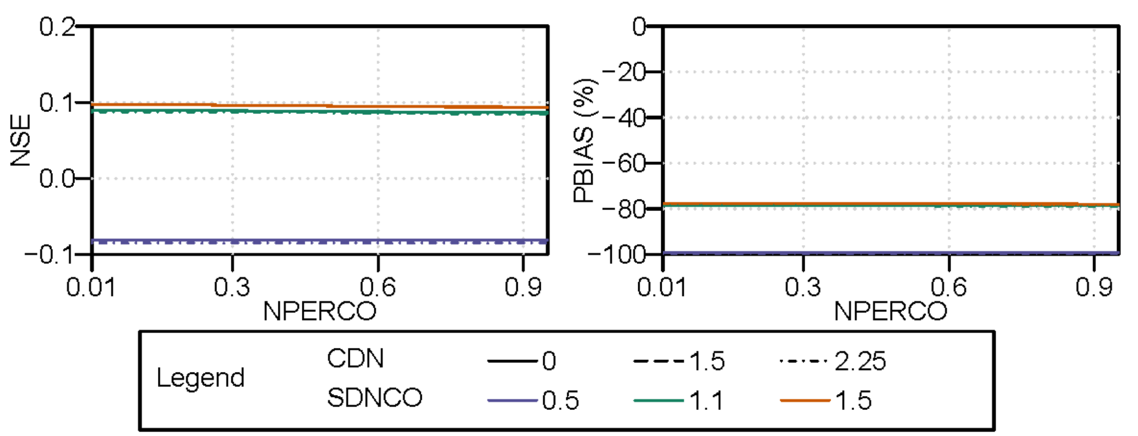

Figure C.29 Modified SWAT tile nitrate sensitivity curves for NPERCO in subbasin B4

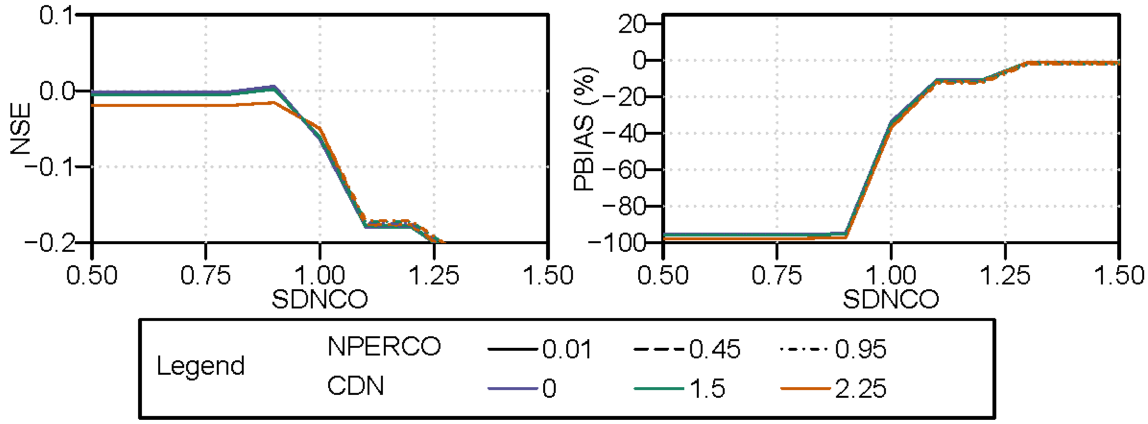

Figure C.30 Modified SWAT tile nitrate sensitivity curves for SDNCO in subbasin B5

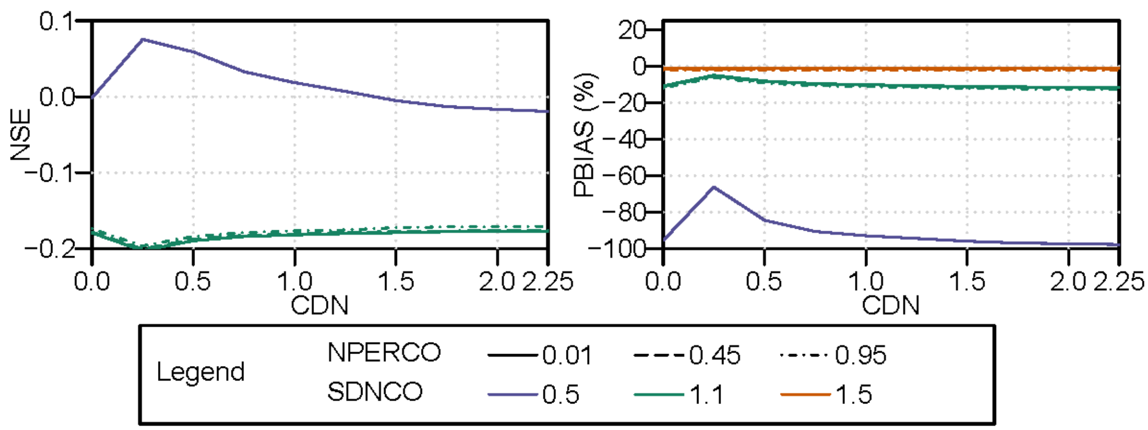

Figure C.31 Modified SWAT tile nitrate sensitivity curves for CDN in subbasin B5

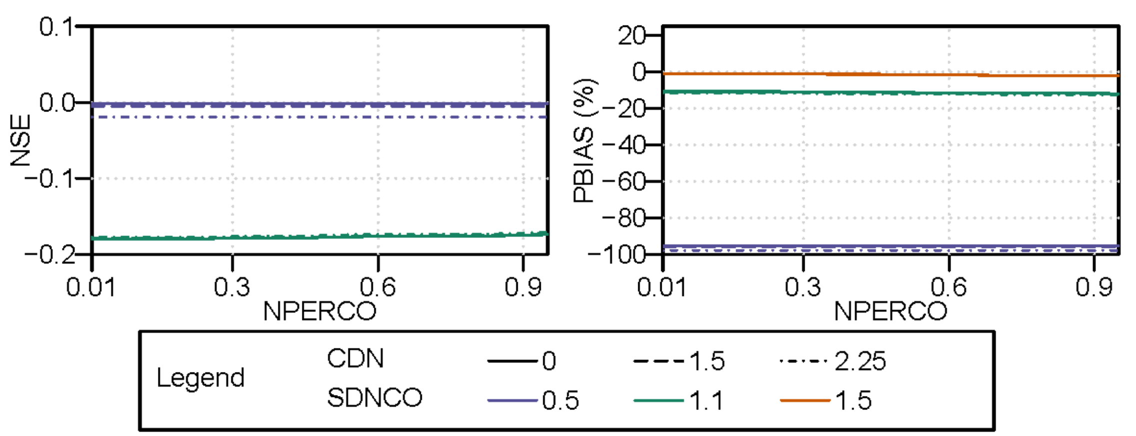

Figure C.32 Modified SWAT tile nitrate sensitivity curves for NPERCO in subbasin B5

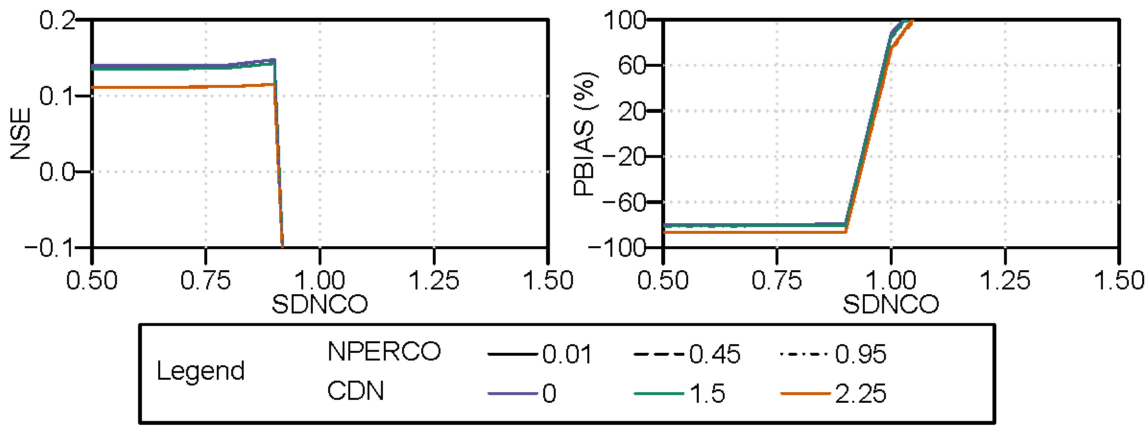

Figure C.33 Modified SWAT tile nitrate sensitivity curves for SDNCO in subbasin B6

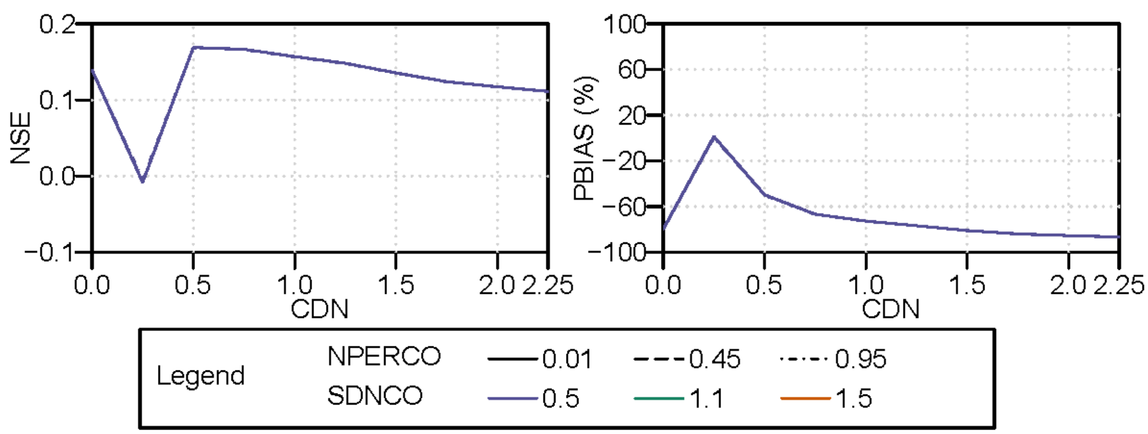

Figure C.34 Modified SWAT tile nitrate sensitivity curves for CDN in subbasin B6

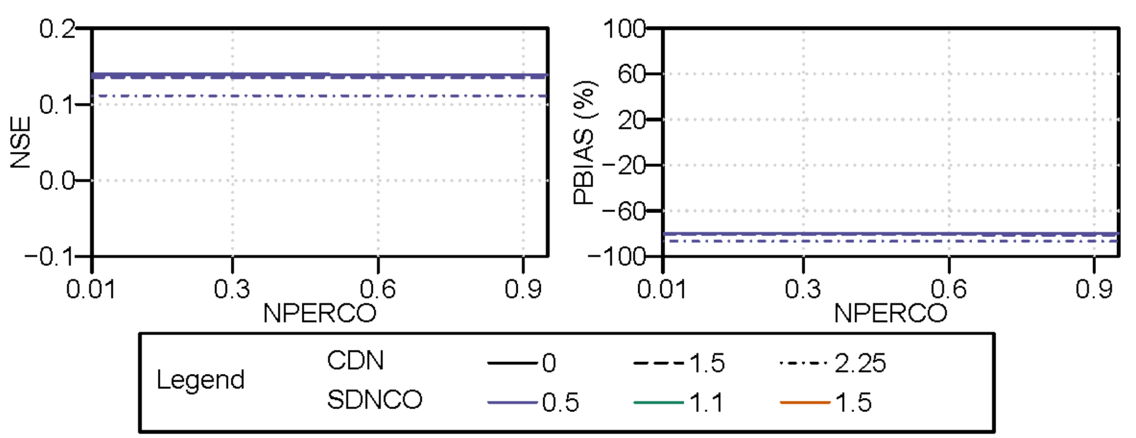

Figure C.35 Modified SWAT tile nitrate sensitivity curves for NPERCO in subbasin B6

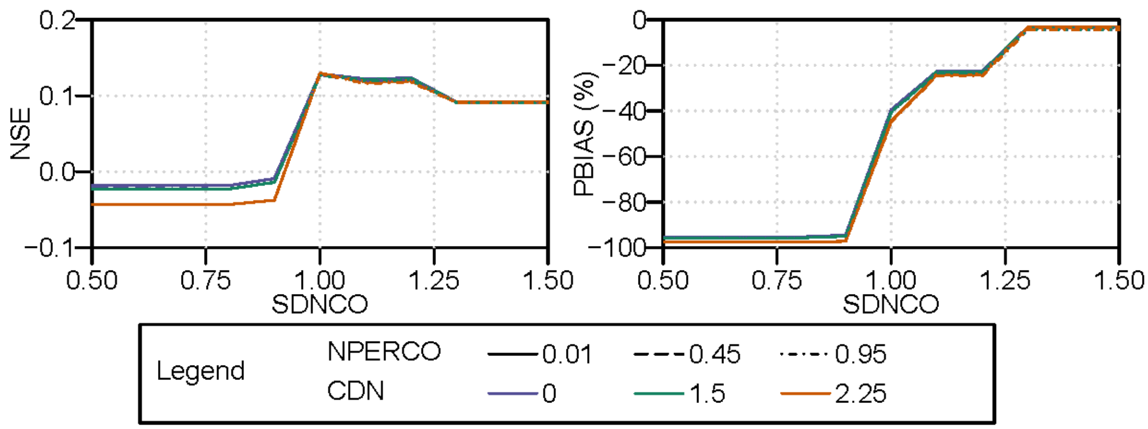

Figure C.36 Modified SWAT tile nitrate sensitivity curves for SDNCO in subbasin B8

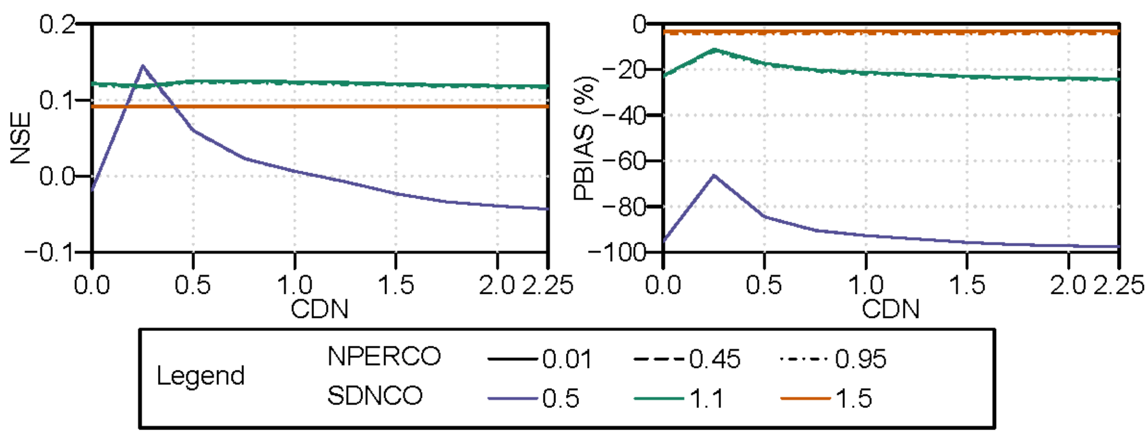

Figure C.37 Modified SWAT tile nitrate sensitivity curves for CDN in subbasin B8

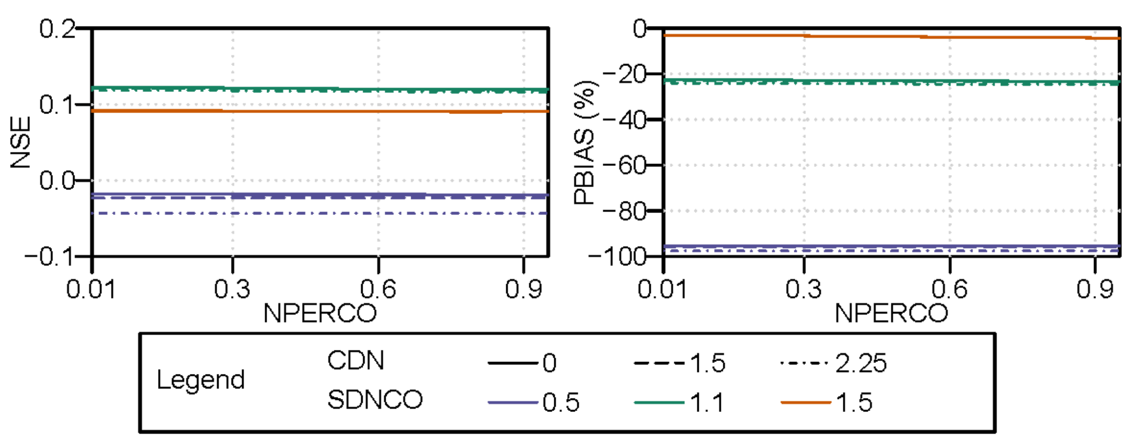

Figure C.38 Modified SWAT tile nitrate sensitivity curves for NPERCO in subbasin B8

Appendix D Additional Tile Nitrate Images for Watershed B

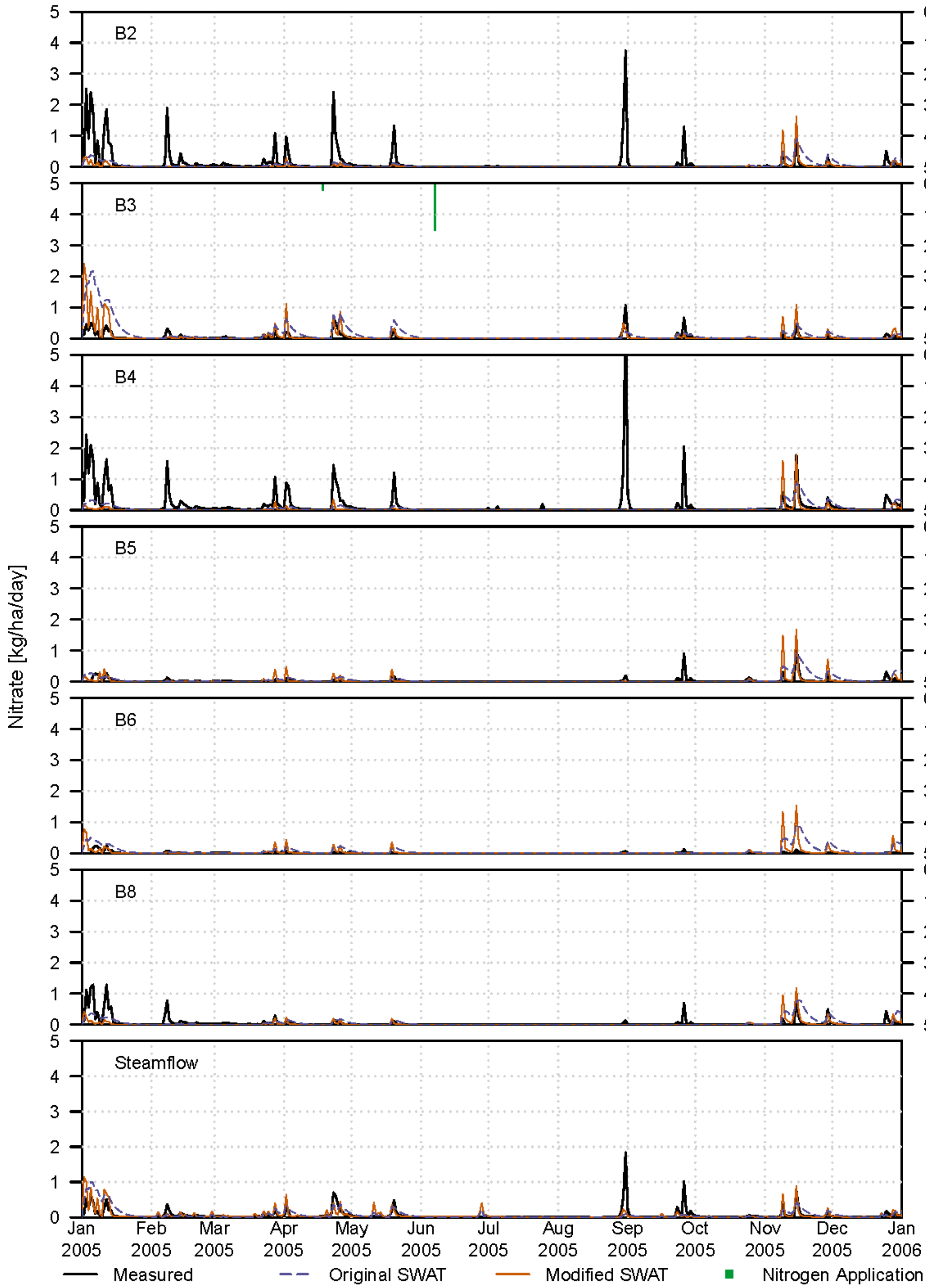

Figure D.1 Watershed B tile and stream nitrate and nitrogen applications in 2005

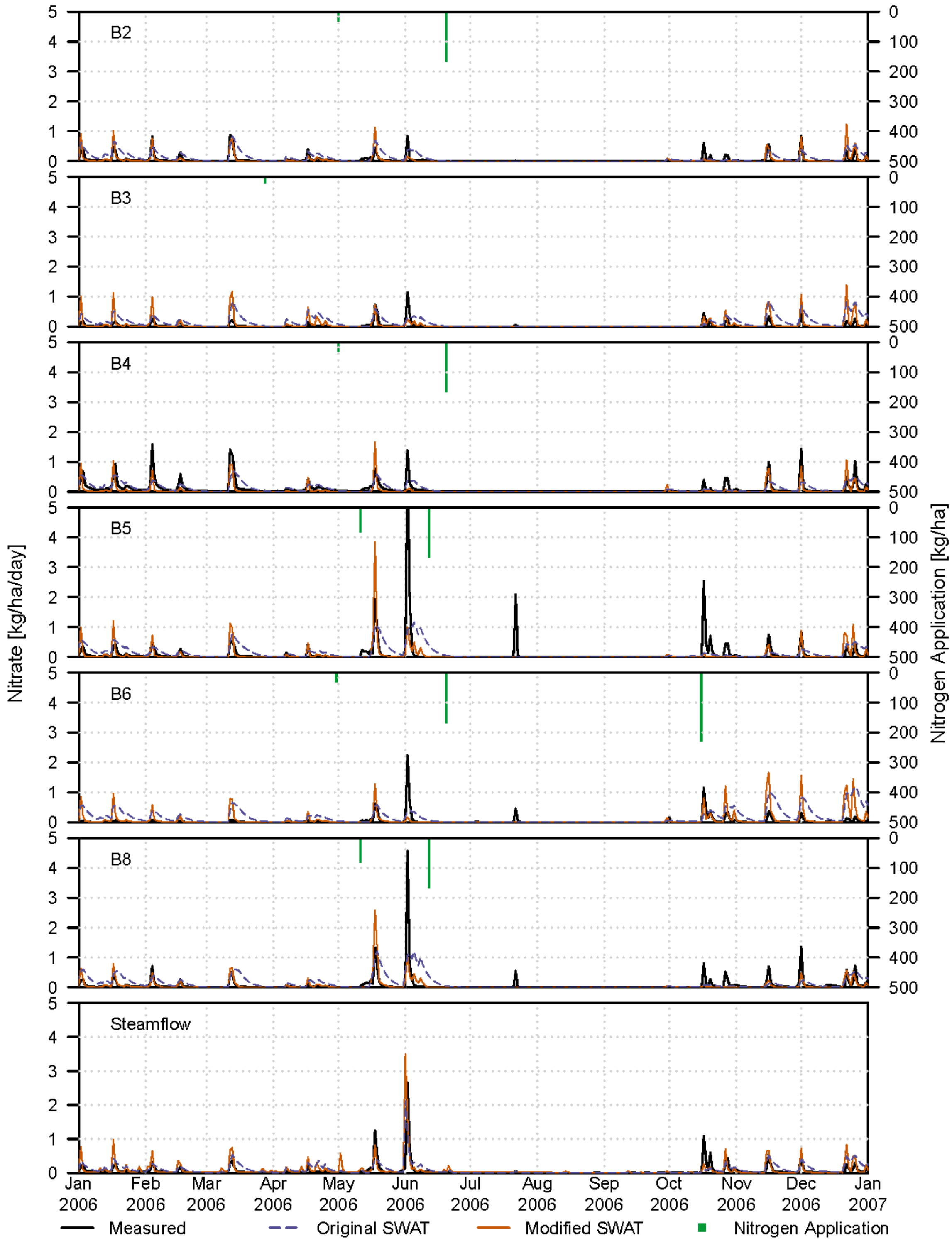

Figure D.2 Watershed B tile and stream nitrate and nitrogen applications in 2006

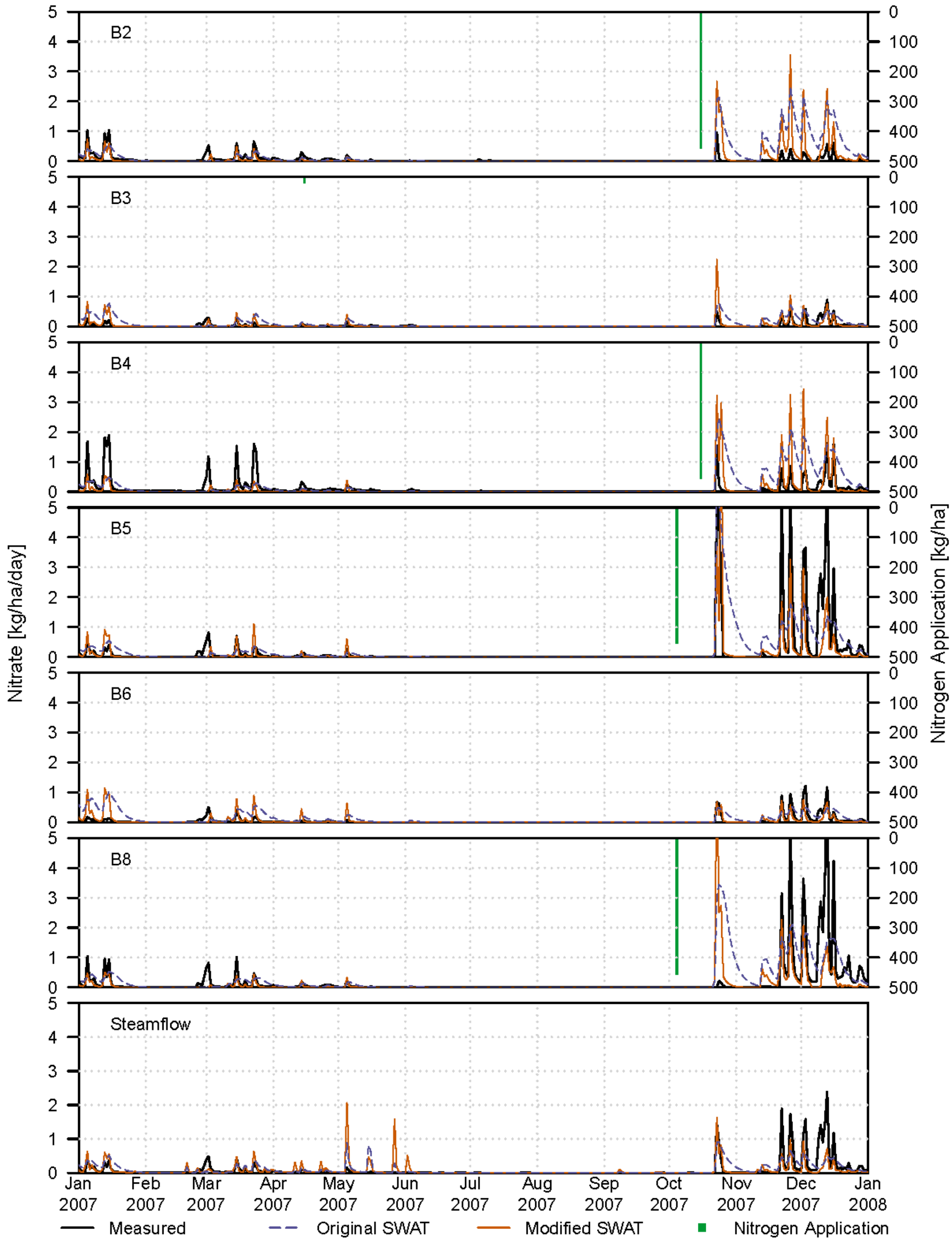

Figure D.3 Watershed B tile and stream nitrate and nitrogen applications in 2007

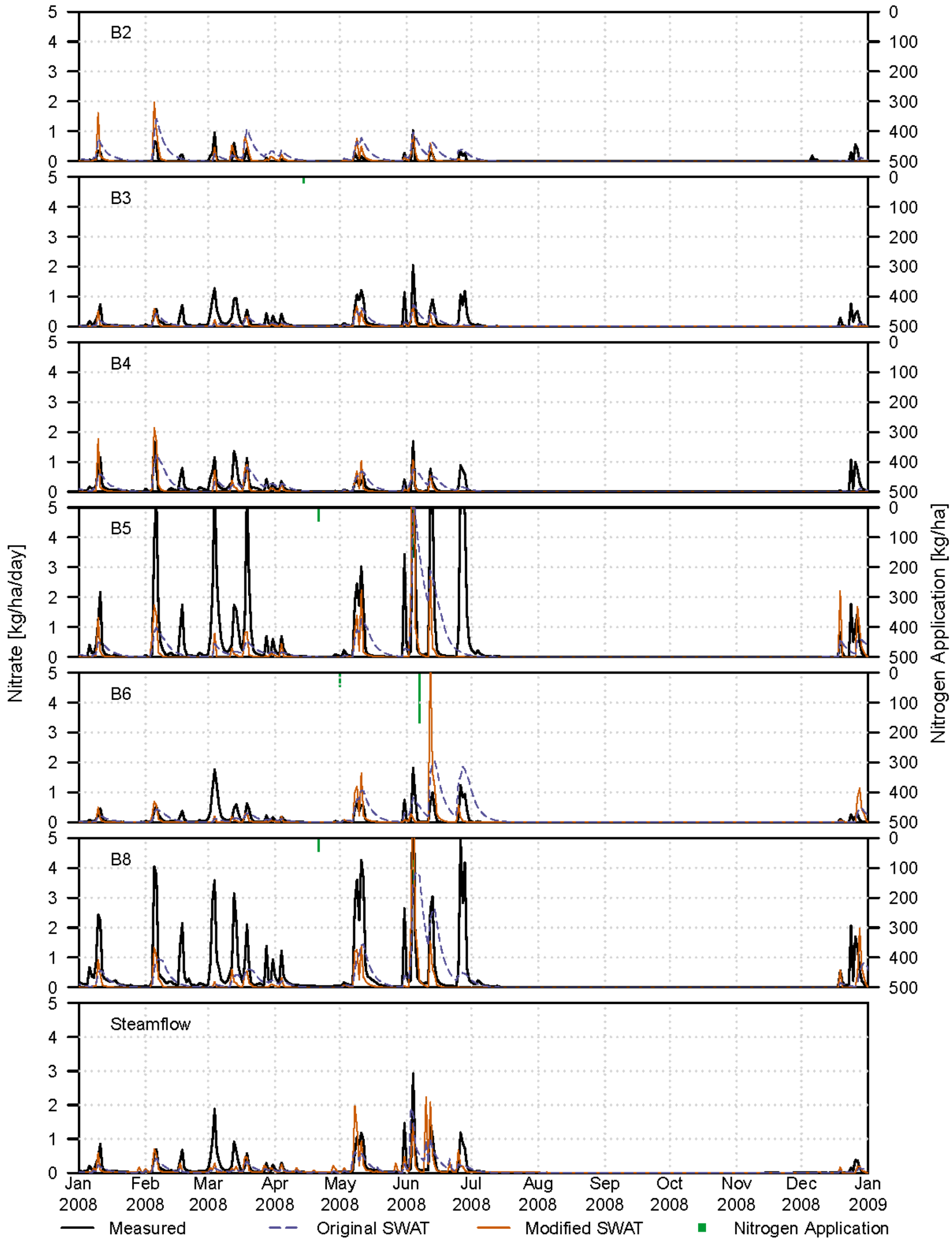

Figure D.4 Watershed B tile and stream nitrate and nitrogen applications in 2008